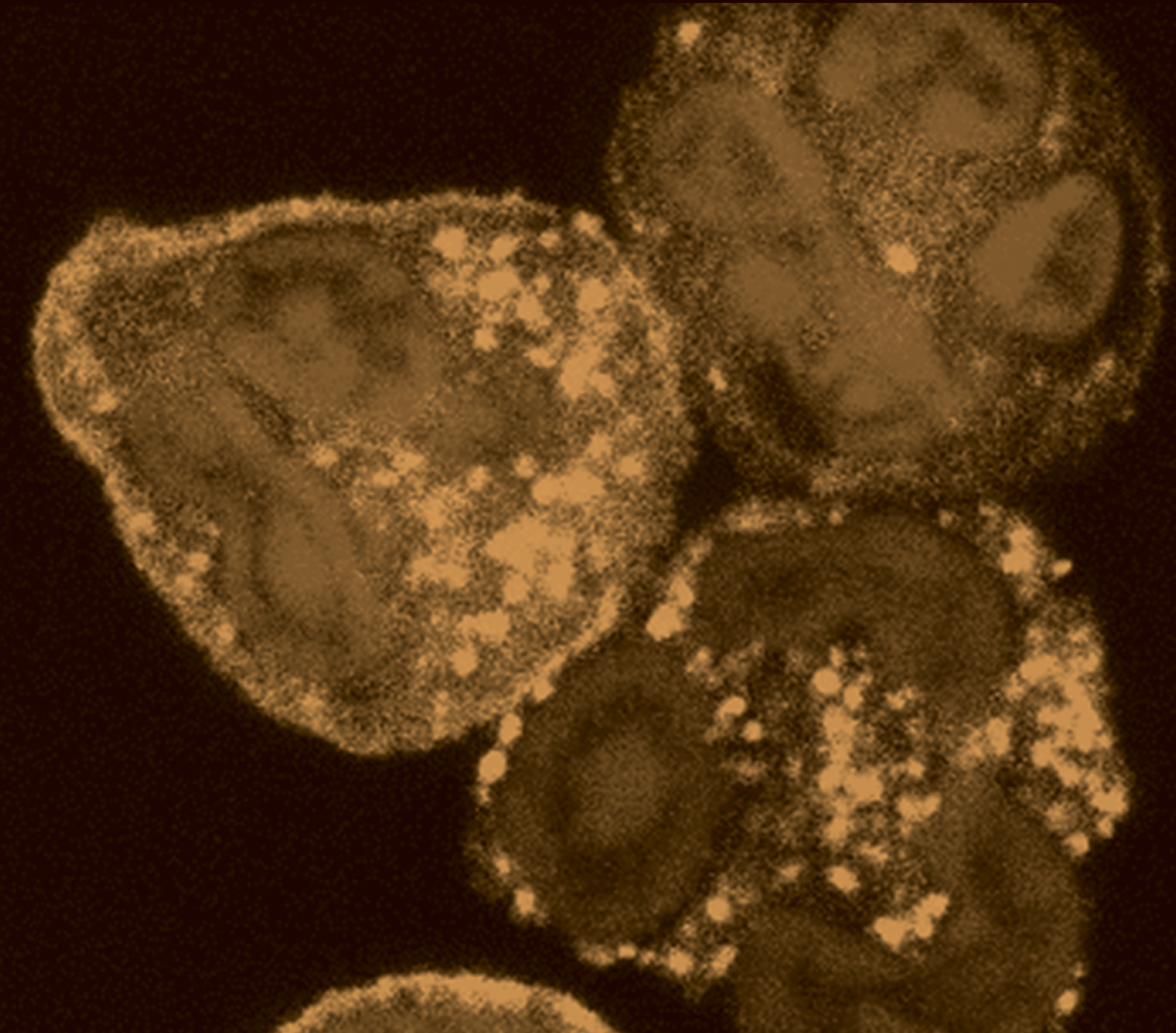


Mediators of Inflammation

Nutrition, Inflammation, and Infectious Disease

Guest Editors: Sung-Ling Yeh, Helieh S. Oz, and Rwei-Fen S. Huang





Nutrition, Inflammation, and Infectious Disease

Mediators of Inflammation

Nutrition, Inflammation, and Infectious Disease

Guest Editors: Sung-Ling Yeh, Helieh S. Oz,
and Rwei-Fen S. Huang



Copyright © 2012 Hindawi Publishing Corporation. All rights reserved.

This is a special issue published in “Mediators of Inflammation.” All articles are open access articles distributed under the Creative Commons Attribution License, which permits unrestricted use, distribution, and reproduction in any medium, provided the original work is properly cited.

Editorial Board

Anshu Agrawal, USA
Muzamil Ahmad, India
Simi Ali, UK
Philip Bufler, Germany
Hidde Bult, Belgium
Elisabetta Buommino, Italy
Dianne Cooper, UK
Guanglin Cui, Norway
Fulvio D'Acquisto, UK
Pham My-Chan Dang, France
Beatriz De las Heras, Spain
Chiara De Luca, Italy
Yves Denizot, France
Clara Di Filippo, Italy
Bruno L. Diaz, Brazil
Maziar Divangahi, Canada
Amos Douvdevani, Israel
Giamila Fantuzzi, USA
Stefanie B. Flohé, Germany
Tânia Silvia Fröde, Brazil
Julio Galvez, Spain
Christoph Garlich, Germany
Ronald Gladue, USA
Hermann Gram, Switzerland
Oreste Gualillo, Spain
Elaine Hatanaka, Brazil

Nina Ivanovska, Bulgaria
Yona Keisari, Israel
Alex Kleinjan, The Netherlands
Magdalena Klink, Poland
Elzbieta Kolaczowska, Poland
Dmitri V. Krysko, Belgium
Joan Kwakkel, The Netherlands
Philipp M. Lepper, Germany
Changlin Li, USA
Eduardo López-Collazo, Spain
Antonio Macciò, Italy
A. Malamitsi-Puchner, Greece
Sunil Kumar Manna, India
Francesco Marotta, Italy
Donna-Marie McCafferty, Canada
Céline Méhats, France
Barbro Melgert, The Netherlands
Vinod K. Mishra, USA
E. Moilanen, Finland
Eric F. Morand, Australia
Jonas Mudter, Germany
Marja Ojaniemi, Finland
Sandra H. P. Oliveira, Brazil
Kristen Page, USA
Andrew Parker, Switzerland
Jonathan Peake, Austria

Vera L. Petricevich, Mexico
Peter Plomgaard, Denmark
Marc Pouliot, Canada
Michal Amit Rahat, Israel
Jean-Marie Reimund, France
Alexander Riad, Germany
Huub Savelkoul, The Netherlands
Natalie J. Serkova, USA
Sunit Kumar Singh, India
Dirk E. Smith, USA
Helen C. Steel, South Africa
Dennis Daniel Taub, USA
Kathy Triantafyllou, UK
Fumio Tsuji, Japan
Peter Uciechowski, Germany
Giuseppe Valacchi, Italy
Luc Vallières, Canada
Jan van Amsterdam, The Netherlands
Elena Voronov, Israel
Jyoti J. Watters, USA
Soh Yamazaki, Japan
Satoru Yui, Japan
Teresa Zelante, Singapore
Dezheng Zhao, USA
Freek J. Zijlstra, The Netherlands

Contents

Nutrition, Inflammation, and Infectious Disease, Sung-Ling Yeh, Helieh S. Oz, and Rwei-Fen S. Huang
Volume 2012, Article ID 601283, 2 pages

L-Arginine and Asymmetric Dimethylarginine Are Early Predictors for Survival in Septic Patients with Acute Liver Failure, Thorsten Brenner, Thomas H. Fleming, Claudia Rosenhagen, Ute Krauser, Markus Mieth, Thomas Bruckner, Eike Martin, Peter P. Nawroth, Markus A. Weigand, Angelika Bierhaus, and Stefan Hofer
Volume 2012, Article ID 210454, 11 pages

Lactoferrin Levels in the Gastric Tissue of *Helicobacter pylori*-Positive and -Negative Patients and Its Effect on Anemia, Yaşar Doğan, Tülay Erkan, Zerrin Önal, Merve Usta, Gülen Doğusoy, Fügen Çullu Çokuğras, and Tufan Kutlu
Volume 2012, Article ID 214581, 5 pages

Zerumbone Attenuates the Severity of Acute Necrotizing Pancreatitis and Pancreatitis-Induced Hepatic Injury, Deng Wenhong, Yu Jia, Wang Weixing, Chen Xiaoyan, Chen Chen, Xu Sheng, and Jin Hao
Volume 2012, Article ID 156507, 12 pages

Effect of Magnolol on the Function of Osteoblastic MC3T3-E1 Cells, Eun Jung Kwak, Young Soon Lee, and Eun Mi Choi
Volume 2012, Article ID 829650, 7 pages

Pegylated Arginine Deiminase Downregulates Colitis in Murine Models, Helieh S. Oz, Jian Zhong, and Willem J. S. de Villiers
Volume 2012, Article ID 813892, 7 pages

Editorial

Nutrition, Inflammation, and Infectious Disease

Helieh S. Oz¹ and Sung-Ling Yeh²

¹ Departments of Physiology and Internal Medicine, College of Medicine, University of Kentucky Medical Center, KY, USA

² School of Nutrition and Health Sciences, Taipei Medical University, Taipei 110, Taiwan

Correspondence should be addressed to Helieh S. Oz, hoz2@email.uky.edu

Received 22 March 2012; Accepted 22 March 2012

Copyright © 2012 H. S. Oz and S.-L. Yeh. This is an open access article distributed under the Creative Commons Attribution License, which permits unrestricted use, distribution, and reproduction in any medium, provided the original work is properly cited.

Pathogens and their related toxins can stimulate the production of endogenous mediators leading to dysregulated reactive oxidative stress, inflammatory responses, and alterations of organ functions. Nutrition support is necessary to protect against infectious and inflammatory conditions, but the optimal nutritional formulation is still under investigation.

This special issue focuses on 5 distinct papers to deal with the pathogens and their products (i.e., *H. pylori*, LPS), specific nutrients (i.e., arginine, iron, plant extracts, antioxidants), and intervention and mechanism of interaction between various biological modifiers (i.e., superfamily of cytokines, inflammatory markers, adhesion molecules) involved in regulating the immune responses.

***H. pylori* and Iron Loss.** *H. pylori* is an important pathogen in the etiology of chronic gastritis and intestinal metaplasia. Studies suggest a link between iron deficiency anemia and *H. pylori* infection. However, the mechanism of action by which *H. pylori* causes anemia is yet to be defined. One possible mechanism is that lactoferrin captures the iron from transferrin mediated by the bacterial outer layer receptor to initiate iron loss in the feces. In a pilot clinical trial, Y. Doğan and his colleagues seek to determine the lactoferrin levels as a marker of anemia in *H. pylori* patients by means of immunohistochemical staining.

***Magnolia* to Preserve Bones.** Skeletal structure turnover is organized by multifactorial regulators including cytokines and chemokines. In this process, osteoblasts release the osteoclastogenetic molecules such as RANKL and TNF- α and IL-6. Here, Magnolol isolated from *Magnolia officinalis* is reported to significantly block the osteoclastic differentiation

in osteoblast MC3T3-E1 cultures. Therefore, E. J. Kwak et al. propose that Magnolol to preserve osteoblasts and possibly to prevent bone resorption and osteoporosis.

Zerumbone and Pancreatitis. D. Wenhong et al. investigate the effects of zerumbone pretreatment on acute necrotizing pancreatitis. They suggest zerumbone to attenuate the severity of pancreatitis as well as pancreatitis-induced hepatic injury through NF- κ B activation inhibition and downregulation of the ICAM-1 and IL-1 β .

Arginine Deiminase and IBD. Arginine, a conditional amino acid, is synthesized in the normal cells and tissues. Arginine deiminase (ADI) is a key enzyme player in the cell signaling pathways, apoptosis, differentiation, and transcriptional regulation. ADI function is dysregulated in multiple human inflammatory diseases and cancer. Since certain tumor cells and pathogens require arginine for growth, selective elimination of arginine may act as a cancer therapy and is being investigated in human trials. While ADI is very immunogenic with a short lifespan, when covalently modified by polyethylene glycol (ADI-PEG), it becomes more stable and less antigenic. H. S. Oz et al. challenge 2 diverse murine models representing Crohn's disease and ulcerative colitis to demonstrate the protective action of this novel microbial enzyme in attenuating inflammatory responses by suppressing macrophage infiltration and iNOS expression.

Prediction of Survival in Sepsis. Finally, septic shock and multiple-organ dysfunction syndrome (MODS) are associated with 40–70% mortality rate in the intensive care units.

T. Brenner et al. study the dysfunction of the arginine/nitric-oxide pathway in the pathogenesis of MODS and septic shock patients using an ELISA diagnostic technique. This simple technique may serve as a tool to predict the survival specifically in the severe sepsis patients with acute hepatic failure.

Helieh S. Oz
Sung-Ling Yeh

Clinical Study

L-Arginine and Asymmetric Dimethylarginine Are Early Predictors for Survival in Septic Patients with Acute Liver Failure

Thorsten Brenner,¹ Thomas H. Fleming,² Claudia Rosenhagen,¹ Ute Krauser,¹ Markus Mieth,³ Thomas Bruckner,⁴ Eike Martin,¹ Peter P. Nawroth,² Markus A. Weigand,⁵ Angelika Bierhaus,² and Stefan Hofer¹

¹ Department of Anesthesiology, University of Heidelberg, Im Neuenheimer Feld 110, 69120 Heidelberg, Germany

² Department of Medicine I and Clinical Chemistry, University of Heidelberg, Im Neuenheimer Feld 410, 69120 Heidelberg, Germany

³ Department of General and Transplant Surgery, University of Heidelberg, Im Neuenheimer Feld 110, 69120 Heidelberg, Germany

⁴ Institute of Medical Biometry and Informatics, University of Heidelberg, Im Neuenheimer Feld 305, 69120 Heidelberg, Germany

⁵ Department of Anesthesiology and Intensive Care Medicine, University of Gießen, Rudolf-Buchheim-Strasse 7, 35392 Gießen, Germany

Correspondence should be addressed to Thorsten Brenner, thorsten.brenner@med.uni-heidelberg.de

Received 31 October 2011; Revised 27 December 2011; Accepted 13 February 2012

Academic Editor: Helieh S. Oz

Copyright © 2012 Thorsten Brenner et al. This is an open access article distributed under the Creative Commons Attribution License, which permits unrestricted use, distribution, and reproduction in any medium, provided the original work is properly cited.

Dysfunctions of the L-arginine (L-arg)/nitric-oxide (NO) pathway are suspected to be important for the pathogenesis of multiple organ dysfunction syndrome (MODS) in septic shock. Therefore plasma concentrations of L-arg and asymmetric dimethylarginine (ADMA) were measured in 60 patients with septic shock, 30 surgical patients and 30 healthy volunteers using enzyme linked immunosorbent assay (ELISA) kits. Plasma samples from patients with septic shock were collected at sepsis onset, and 24 h, 4 d, 7 d, 14 d and 28 d later. Samples from surgical patients were collected prior to surgery, immediately after the end of the surgical procedure as well as 24 h later and from healthy volunteers once. In comparison to healthy volunteers and surgical patients, individuals with septic shock showed significantly increased levels of ADMA, as well as a decrease in the ratio of L-arg and ADMA at all timepoints. In septic patients with an acute liver failure (ALF), plasma levels of ADMA and L-arg were significantly increased in comparison to septic patients with an intact hepatic function. In summary it can be stated, that bioavailability of NO is reduced in septic shock. Moreover, measurements of ADMA and L-arg appear to be early predictors for survival in patients with sepsis-associated ALF.

1. Introduction

Septic shock as well as the resulting MODS represent an ongoing challenge in intensive care units [1]. The pathogenesis of MODS in patients with septic shock is a multifactorial process. Recent studies have provided evidence that an impaired NO homeostasis might play an important role [2–4]. Dysfunctions of the L-arg/NO pathway have been reported to be a reason for the deleterious vascular effects of diabetes mellitus, hypercholesterolemia, hypertension, smoking, and others [5]. Moreover, reduced endothelial NO bioavailability has suspected to be crucial in patients with

sepsis, since microcirculatory blood flow is disrupted and key bacterial functions in the host might be compromised [2, 4].

NO is synthesized from the conditionally essential amino acid L-arg by the action of NO-synthases (NOS) [6]. However, earlier published articles dealing with plasma levels of L-arg in septic patients revealed conflicting results [7–18]. ADMA represents one further main component of the NO homeostasis, due to its ability to serve as an endogenous NOS-inhibitor. The accumulation of ADMA was suspected to play an important role in the development of MODS and was independently associated with mortality in unselected critically ill patients [19, 20]. Competitive leveling of L-arg

and ADMA with regard to NOS activity was entitled L-arginine-paradox, describing an ADMA-induced right-shift of the NOS concentration-response curve for L-arg. Only small changes in L-arg plasma concentrations may, therefore, cause marked changes in NOS activity in order to avoid a relevant lack of NO [21].

The aims of this study were, therefore, threefold: (1) to determine plasma concentrations of L-arg and ADMA as well as the resulting ratio of both in patients with septic shock, surgical patients undergoing major abdominal surgery, as well as healthy volunteers, (2) to investigate the prognostic role of each parameter in patients with septic shock, and (3) to assess the applicability of newly developed ELISA-based measurements of L-arg and ADMA.

2. Materials and Methods

This observational clinical study was approved by the local ethics committee (Trial-Code-Nr.: S123-2009) and was conducted in the surgical intensive care unit of the University Hospital of Heidelberg, Germany. Study and control patients or their legal designees signed written informed consent. In total, 120 patients in 3 groups were enrolled in the study. The 3 groups included 60 patients with septic shock (referred to as the septic group), 30 patients after major abdominal surgery due to a tumorous disease (the surgical group), and 30 healthy volunteers (the healthy group, Table 1). The 60 patients were classified as having septic shock based on the criteria of the International Sepsis Definitions Conference [22]. Since patients with septic shock were recruited on a surgical intensive care unit, all of them underwent a surgical procedure in varying degrees of time prior to sepsis onset. Patients were eligible for enrollment with an onset of sepsis syndrome ≤ 24 hours. The initial blood draw was also performed within this period. In contrast, patients with an onset of sepsis syndrome > 24 hours were excluded from the study. The management of patients with septic shock in the intensive care unit included early goal-directed therapy (according to Rivers and colleagues [23]), elimination of the septic focus, and broad-spectrum antibiotics [24, 25]. Patients with renal disorders (as indicated by a serum-creatinine ≥ 1.2 mg/dL or $20.5 \mu\text{mol/L}$, according to sequential organ failure assessment (SOFA)-score) as well as liver diseases (as indicated by a serum-bilirubin ≥ 1.2 mg/dL or $20.5 \mu\text{mol/L}$, according to SOFA-score) prior to the onset of sepsis were excluded from the study. Blood samples from patients with septic shock were collected at sepsis onset (Onset), and 24 hours (24 h), 4 days (4 d), 7 days (7 d), 14 days (14 d), and 28 days (28 d) later. Relevant baseline data (demographic data, primary site of infection, outcome) and clinical data (disease severity scoring, hemodynamic data, need for catecholaminergic support, ventilator settings, etc.) were collected. Patients with septic shock were reevaluated for survival 28 days after enrollment in the study. These evaluations were performed using available hospital records. In case of the patient's discharge from the hospital, the family doctor was contacted. If necessary, direct contact was also made with the patient. Blood samples from the surgical group were collected prior to surgery (Pre), immediately after the end of the surgical

TABLE 1: Baseline data of 60 patients in the septic group, 30 patients in the surgical group and 30 individuals in the healthy group.

Septic Group ($n = 60$)	
<i>Demographic Data</i>	
Age, y	69 ± 12 ; 70; 64–76
Male sex	46 (76.7%)
ASA-Status: I; II; III; IV; V	1 (1.7%); 11 (18.3%); 29 (48.3%); 15 (25.0%); 1 (1.7%)
<i>Primary site of infection/septic focus (Double naming feasible)</i>	
Lung	12 (20.0%)
Gastrointestinal tract	32 (53.3%)
Genitourinary tract	6 (10.0%)
Surgical site	16 (26.7%)
Others	2 (3.3%)
<i>Septic complications/organ failures [Sepsis Onset—28 d]</i>	
Acute renal failure (ARF)	35 (58.3%)
Acute respiratory distress syndrome (ARDS)	49 (81.2%)
Acute liver failure (ALF)	15 (25.0%)
Surgical Group ($n = 30$)	
<i>Demographic Data</i>	
Age, y	61 ± 12 ; 62; 57–70
Male sex	16 (53.3%)
ASA-Status: I; II; III; IV; V	0 (0.0%); 9 (30.0%); 20 (66.7%); 1 (3.3%); 0 (0.0%)
<i>Site of surgery (Double naming feasible)</i>	
Liver	7 (23.3%)
Pancreas	11 (36.7%)
Gastro-intestinal	27 (90.0%)
Healthy Group ($n = 30$)	
<i>Demographic Data</i>	
Age	27 ± 6 ; 26; 24–28
Male sex	19 (63.3%)
ASA-Status: I; II; III; IV; V	21 (70.0%); 9 (30.0%); 0 (0.0%); 0 (0.0%); 0 (0.0%)

Data are presented by number (%) or by mean \pm standard deviation, median and interquartile range (Q1–Q3). Abbreviations: ASA-Status, physical status classification system according to the American Society of Anesthesiologists; ARF, acute renal failure; ARDS, acute respiratory distress syndrome; ALF, acute liver failure.

procedure (Onset), and 24 hours afterwards (24 h). No later blood draws were performed in the surgical group, since peak plasma levels of proinflammatory and anti-inflammatory cytokines are reported to appear on the 1st postoperative day in surgery-induced inflammation and the investigation associated burden of the individual study patient was demanded to be as minimal as possible [26]. Blood samples from the healthy group were collected once. In order to avoid diet-related affections of L-arg or ADMA plasma levels, neither patients in the septic group, nor surgical patients received immune-enhancing nutrition.

After blood collection, plasma of all study participants was immediately obtained by centrifugation, transferred into

cryotubes, and stored at -80°C until further processing. Serum tests for routine laboratory parameters (creatinine, urea, bilirubin, leukocytes, C-reactive protein, etc.) were performed at the same time.

Measurements of ADMA as well as L-arg were performed using ELISA-kits (Immundiagnostik, Bensheim, Germany) according to the manufacturer's instructions.

The resulting study data was evaluated using SPSS (statistical product and services solutions) software (Version 19.0, SPSS Inc, Chicago, USA). Categorical data were summarized by means of absolute and relative frequencies (counts and percentages). Quantitative data were summarized using the number of observations, mean, and standard deviation, as well as median with quartiles. Wherever appropriate, data were visualized using line charts or Box-and-Whisker plots. The Kolmogorov-Smirnov test was applied to check for normal distribution. Due to nonnormally distributed data, non-parametric methods for evaluation were used (chi-square test for categorical data, Mann-Whitney test for continuous data). A receiver operating characteristic (ROC) curve was established with suitable parameters, in order to create cut-off values to determine the prognostic value of each parameter with regard to survival. Correlation analysis was performed calculating Pearson's correlation coefficient (r). A P -value <0.05 was considered statistically significant. Concerning symbolism and higher orders of significance: $P < 0.05$: *, $P < 0.01$: **, $P < 0.001$: ***, n.s.: not statistically significant, Ø: no data available.

3. Results

Demographic data and baseline clinical data of all study groups are presented in detail in Table 1. The primary site of infection in the septic group (double naming feasible) was the gastrointestinal tract, followed by the surgical site, and the respiratory tract (Table 1). Surgical site infections (SSI) were described to be source deep or organ space SSIs (e.g., organ space abscesses, insufficiencies of anastomoses, etc.) in all cases. Hospital-acquired pneumonia (HAP) or ventilator-associated pneumonia (VAP) due to several triggers (e.g., aspiration, insufficient coughing with subsequent retention of secretion, etc.) are thought to represent the most important reasons for a pulmonary site of infection. Since all patients of the septic cohort underwent a surgical procedure and were, therefore, hospitalized for a certain time prior to sepsis onset, community-acquired pneumonia (CAP) can most probably be disregarded as a pulmonary focus. However, results of microbiological diagnostics in tracheal secretion have not been recorded, so that these reflections cannot be validated. All patients with septic shock revealed cardiovascular failure with the need for catecholaminergic support. The incidence of further sepsis-associated organ failures is presented in Table 1. In contrast, no patients in the surgical group developed any organ failure, such as acute renal failure (ARF), acute respiratory distress syndrome (ARDS), or ALF. In the septic group, 38 of 60 patients (63.3%) survived 28 days. Patients who survived or died showed no significant differences concerning their demographic data (data not

shown). None in the healthy or surgical groups died during the study.

In healthy volunteers, the following plasma levels could be observed: ADMA: $0.433\ \mu\text{mol/L}$; $0.369\text{--}0.506\ \mu\text{mol/L}$, L-arg: $112.6\ \mu\text{mol/L}$; $100.8\text{--}133.0\ \mu\text{mol/L}$, Ratio L-arg/ADMA: 273.5; 218.8–329.3 (Median; Q1–Q3). In surgical patients, plasma levels of ADMA were significantly elevated prior to the surgical procedure. Postsurgery, ADMA plasma levels decreased towards the levels observed for the healthy volunteers (Figure 1(a)). Plasma levels of L-arg were comparable in healthy volunteers and surgical patients prior to the surgical procedure. Within 24 hours postsurgery, plasma levels of L-arg decreased and showed significant differences in comparison to healthy volunteers (Figure 1(b)). The ratio of L-arg and ADMA was significantly reduced in surgical patients at all timepoints (Figure 1(c)). When comparing subgroups of patients in the surgical group who did ($n = 7$) or did not ($n = 23$) receive a liver resection, no significant differences were observed in the plasma levels of L-arg, ADMA as well as the resulting ratio of both (data not shown).

In patients with septic shock, plasma levels of ADMA and L-arg showed comparable trends within the 28-day observation period with significantly increasing levels until 4 days after the onset of sepsis, followed by a sudden decrease until day 7 (Figures 1(a) and 1(b)). When septic patients were compared with healthy volunteers, plasma levels of ADMA were significantly elevated at all time points (Figure 1(a)). Analogous to the peak concentrations of ADMA, plasma levels of L-arg were also significantly elevated 4 days after sepsis onset in comparison to healthy volunteers. In contrast to ADMA, plasma levels of L-arg tended to be decreased at sepsis onset ($P = 0.062$) and showed no significant differences at the other timepoints within the 28-day observation period (Figure 1(b)). The resulting ratio of L-arg and ADMA in septic patients was significantly reduced in comparison to healthy volunteers as well as surgical patients at all time points (Figure 1(c)).

When comparing subgroups of patients in the septic group who did or did not survive, plasma levels of ADMA tended to be increased at sepsis onset in the nonsurviving subgroup ($P = 0.059$). Afterwards, ADMA plasma levels were comparable between survivors and nonsurvivors. Plasma levels of L-arg were significantly elevated in the nonsurviving subgroup 24 hours as well as 7 days after sepsis onset (Table 2). Results of subgroup analyses comparing septic patients with an ARDS versus non-ARDS or ARF versus non-ARF are further described in Table 2. Measurements of ADMA and L-arg plasma levels in patients with sepsis who did or did not develop sepsis-induced ALF (serum-bilirubin $>/<4.0\ \text{mg/dL}$ or $70.0\ \text{mmol/L}$ [22]) are shown in Figures 2(a) and 2(b). ADMA was significantly elevated at all time points in the subgroup of ALF patients (Figure 2(a)). L-arg plasma levels were also significantly increased at sepsis onset and 24 hours later (Figure 2(b)), but not at later times. When comparing septic patients with an ALF who did ($n = 8$) or did not survive ($n = 7$) 28 days, plasma levels of ADMA showed a considerable trend towards higher levels in nonsurvivors at sepsis onset ($P = 0.072$). Afterwards ADMA plasma levels were comparable between the surviving and

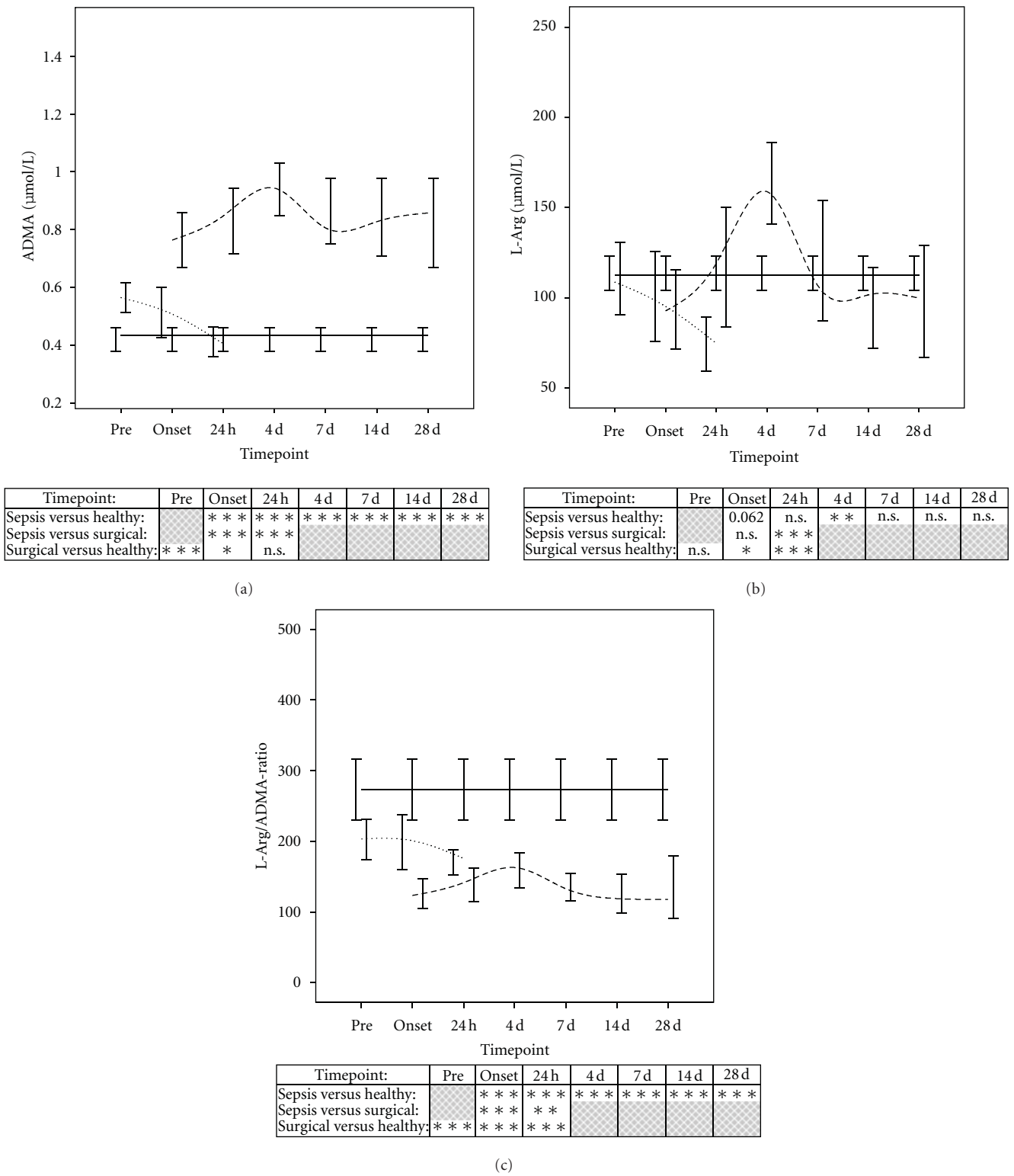


FIGURE 1: Comparison of ADMA (a) and L-arg (b) measurements as well as the resulting ratio of both (c) in healthy volunteers ($n = 30$, black continuous line), patients following major abdominal surgery ($n = 30$, short dashed line) and patients with septic shock ($n = 60$, long dashed line). Data in line charts are given as medians and the 95% CI. Concerning symbolism and higher orders of significance: $P < 0.05$: *, $P < 0.01$: **, $P < 0.001$: ***, n.s.: not statistically significant.

TABLE 2: L-arg and ADMA measurements in different subgroups of patients with septic shock.

Parameters	Timepoints	Units	Onset	24 h	L-arg and ADMA measurements in different subgroups of patients with septic shock								
Survival:					4 d	7 d	14 d	28 d					
Survivors at Day 28 (italic parts <i>n</i> = 38) versus Non-Survivors at Day 28 (bold parts, <i>n</i> = 22)													
L-arg		[μmol/L]	77.9; 62.1–115.3	n.s.	107.1; 65.9–150.1	* 154.2; 113.4–228.8	n.s.	97.0; 76.5–154.8	*	98.4; 67.7–125.0	n.s.	99.8; 66.4–138.3	Ø
			123.7; 66.1–175.4		158.4; 88.2–201.5	197.5; 149.7–240.0		172.2; 161.8–195.9		112.1; 102.1–145.3		Ø	
ADMA		[μmol/L]	0.74; 0.52–0.92	n.s.	0.84; 0.67–1.08	0.95; 0.72–1.11	n.s.	0.80; 0.63–1.05	n.s.	0.83; 0.70–1.04	n.s.	0.86; 0.67–0.99	Ø
			0.83; 0.61–1.21		0.87; 0.67–1.29	0.87; 0.71–1.27		0.83; 0.77–1.14		0.75; 0.60–0.91		Ø	
L-arg/ADMA-Ratio		[none]	126.5; 91.5–164.8	n.s.	135.0; 95.0–197.8	154.0; 123.0–191.5	n.s.	121.5; 97.5–160.5	*	111.0; 83.5–155.8	n.s.	118.0; 89.5–180.5	Ø
			118.5; 91.5–157.0		142.5; 105.0–186.5	196.0; 138.0–235.5		185.0; 143.5–240.0		191.0; 165.3–204.8		Ø	
Patients with ARDS (italic parts, <i>n</i> = 49) versus Non-ARDS (bold parts, <i>n</i> = 11)													
Pulmonary:													
L-arg		[μmol/L]	84.6; 61.4–145.9	n.s.	114.3; 72.9–161.0	167.5; 132.6–242.1	*	106.8; 84.7–172.2	n.s.	102.9; 69.2–128.8	n.s.	120.0; 66.7–149.3	n.s.
			94.6; 83.5–140.9		187.8; 152.2–228.0	76.0; 57.4–108.5		109.6; 91.2–168.5		150.8; 117.4–184.1		99.8; 99.8–99.8	n.s.
ADMA		[μmol/L]	0.81; 0.61–0.93	n.s.	0.85; 0.69–1.08	1.00; 0.72–1.19	n.s.	0.80; 0.68–1.05	n.s.	0.82; 0.68–1.03	n.s.	0.85; 0.67–1.00	n.s.
			0.55; 0.53–1.67		0.74; 0.67–1.62	0.78; 0.68–0.89		0.83; 0.71–1.03		0.84; 0.78–0.91		0.90; 0.90–0.90	n.s.
L-arg/ADMA-Ratio		[none]	124.0; 90.0–162.0	n.s.	141.0; 97.5–183.5	172.5; 129.0–215.5	n.s.	137.0; 102.0–171.0	n.s.	120.0; 93.0–162.0	n.s.	128.0; 90.3–179.8	n.s.
			109.0; 88.5–158.0		169.5; 107.5–324.5	111.0; 80.3–142.3		132.0; 127.0–158.5		170.0; 144.0–196.0		110.0; 110.0–110.0	n.s.
Patients with ARF (italic parts, <i>n</i> = 35) versus Non-ARF (grey boxes, <i>n</i> = 25)													
Renal:													
L-arg		[μmol/L]	95.8; 60.3–150.5	n.s.	114.3; 76.3–192.7	185.9; 140.7–246.7	*	147.8; 86.7–180.9	n.s.	101.6; 69.0–146.6	n.s.	120.8; 65.6–147.6	n.s.
			87.8; 67.0–142.7		134.7; 72.6–160.4	142.1; 105.3–162.9		99.1; 75.9–117.0		96.5; 68.1–111.6		81.6; 69.7–96.3	n.s.
ADMA		[μmol/L]	0.82; 0.59–1.09	n.s.	0.86; 0.66–1.10	1.02; 0.75–1.35	*	0.92; 0.75–1.26	*	0.85; 0.67–1.01	n.s.	0.85; 0.67–0.98	n.s.
			0.73; 0.51–0.86		0.83; 0.67–1.03	0.87; 0.68–1.01		0.79; 0.59–0.85		0.83; 0.70–1.06		0.91; 0.53–1.01	n.s.
L-arg/ADMA-Ratio		[none]	118.0; 95.0–160.5	n.s.	122.0; 98.0–179.0	172.0; 129.0–196.0	n.s.	141.0; 105.5–169.5	n.s.	123.5; 93.5–168.0	n.s.	138.0; 94.0–179.0	n.s.
			126.0; 88.3–169.8		146.5; 100.0–207.0	154.0; 109.0–230.0		120.5; 97.5–188.8		100.0; 75.5–125.5		96.0; 65.5–172.3	n.s.

Data are presented by median and interquartile range (Q1–Q3). Concerning symbolism and higher orders of significance: $P < 0.05$; *, $P < 0.01$; **, $P < 0.001$; ***, n.s.: not statistically significant; Ø: no data available. Abbreviations: L-arg, L-arginine; ADMA, asymmetric dimethylarginine; ARDS, acute respiratory distress syndrome; ARF, acute renal failure.

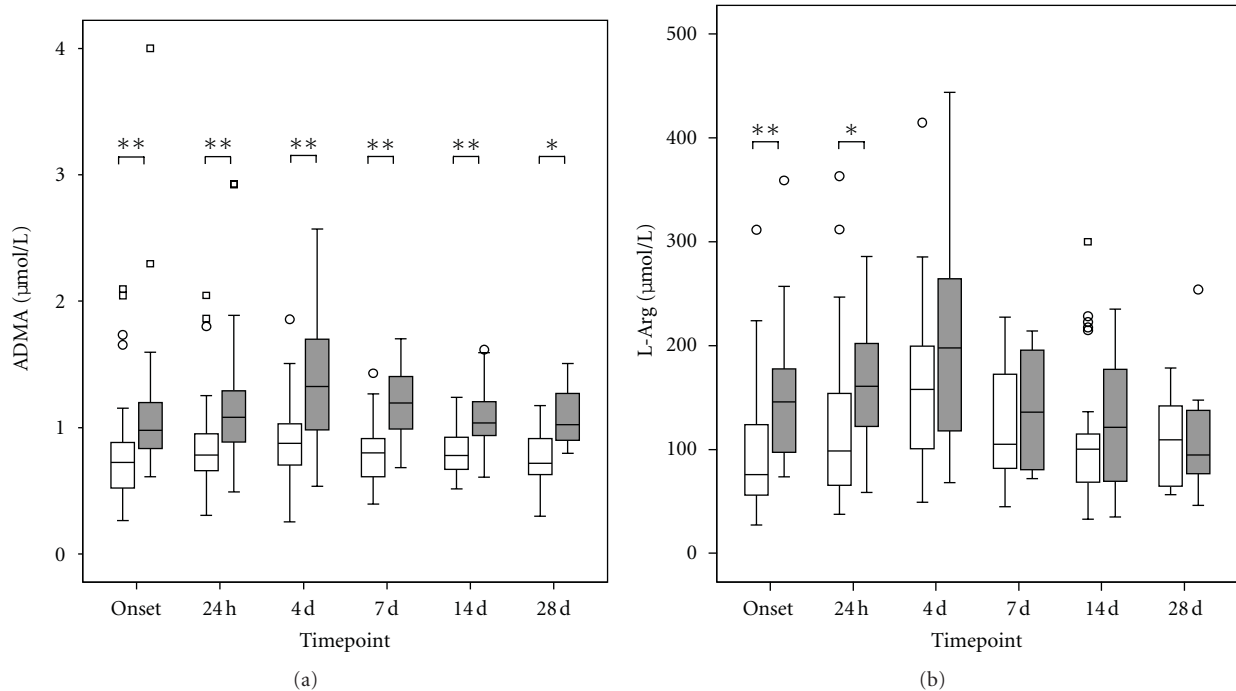


FIGURE 2: Comparison of ADMA (a) and L-arg (b) measurements in plasma samples of septic patients with an ALF ($n = 15$, grey box) in comparison to septic patients with a preserved liver function ($n = 45$, white box). Data in box plots are given as median, 25th percentile, 75th percentile, and the 1.5 interquartile range. Outliers are shown in form of circles (1.5–3 interquartile ranges above 75th percentile or below 25th percentile) or rectangles (>3 interquartile ranges above 75th percentile or below 25th percentile). Concerning symbolism and higher orders of significance: $P < 0.05$: *, $P < 0.01$: **, $P < 0.001$: ***, n.s.: not statistically significant.

nonsurviving subgroup. In contrast, plasma levels of L-arg were significantly elevated in the nonsurviving subgroup at sepsis onset ($P = 0.029^*$) but failed scarcely to show a significant difference 24 hours later ($P = 0.054$). At later time points, L-arg plasma levels were comparable between the surviving and nonsurviving subgroup. A comparable leveling could be observed for different routine markers for liver impairment. For example, plasma levels of lactate dehydrogenase (LDH) were significantly elevated in the nonsurviving subgroup at sepsis onset as well as 24 hours later. At later timepoints, LDH plasma levels were comparable between the surviving and nonsurviving subgroup. Substantially, similar results could be obtained for aspartat amino transferase (ASAT), alanine amino transferase (ALAT), as well as total bilirubine (Table 3).

In septic patients with an ALF, ROC curve analysis revealed a cut-off value for L-arg at sepsis onset (area under the curve/AUC = 0.839) of $143.41 \mu\text{mol/L}$ for early discrimination of survivors and nonsurvivors with a sensitivity of 0.857 and 1-specificity of 0.250 (Figure 3). Moreover, ROC analysis revealed a cut-off value for ADMA at the onset of sepsis syndrome (AUC = 0.786) of $0.853 \mu\text{mol/L}$ with a sensitivity of 0.857 and 1-specificity of 0.500 (Figure 3).

In order to assess the influence of packed red blood cell (PRBC) administration on plasma levels of L-arg and ADMA, septic patients receiving PRBC <24 h prior to the respective blood draw ($n = 39$) were compared with septic patients not receiving PRBC <24 h prior to the respective blood draw ($n = 21$). At early (Onset, 24 h) as well as late

stages of septic shock, L-arg and ADMA plasma levels did not differ significantly between the two subgroups (data not shown). Contrary to our expectations, in the interim phase (4 d) plasma levels of L-arginine and ADMA were significantly elevated in patients receiving PRBC (L-arg: $P = 0.032^*$ /ADMA: $P = 0.028^*$). At this timepoint (4 d), septic patients receiving PRBC were shown to be more severely injured as assessed by disease severity scoring (acute physiology and chronic health evaluation (APACHE) II-score: 0.007**/SOFA-score: 0.037*/simplified acute physiology score (SAPS): 0.007**). Moreover, the influence of body's own red blood cells (RBCs) on plasma levels of L-arg and ADMA was assessed. Therefore, the amount of red cell mass in each patient at the different timepoints was estimated with the accompanying hemoglobin (Hb) concentration. Hb concentrations were shown to be significantly reduced in patients with septic shock as well as surgical patients in comparison to healthy volunteers at all timepoints (data not shown). An ensuing correlation analysis including all studygroups revealed that L-arg plasma levels were not correlated with the accompanying Hb concentrations ($r = 0.090$). By analogy, ADMA plasma levels showed only a weak correlation with Hb concentrations ($r = 0.325$).

4. Discussion

As assessed by plasma levels of ADMA and L-arg, the present investigation describes decreased endothelial NO bioavailability in patients with septic shock in comparison to healthy

TABLE 3: Routine markers for liver impairment in surviving and nonsurviving septic patients with an ALF.

Parameters	Units	Onset	Routine markers for liver impairment in surviving and nonsurviving septic patients with an ALF.				
Timepoints			24 h	4 d	7 d	14 d	28 d
ALF: Survivors at Day 28 (italic parts, $n = 8$) versus nonsurvivors at Day 28 (bold parts, $n = 7$)							
ASAT	[U/L]		51.0; 25.5–164.0	62.0; 55.8–89.3	82.5; 47.8–115.3	52.0; 38.5–69.8	44.0; 39.5–99.5
		.072	438.0; 100.0–1653.0	n.s. 113.0; 71.0–621.0	n.s. 505.5; 267.8–743.3	n.s. 52.0; 43.0–61.0	Ø Ø
ALAT	[U/L]		20.0; 14.0–47.8	30.5; 19.8–39.5	23.5; 18.5–38.0	26.5; 18.5–45.0	31.0; 19.0–72.0
		*	266.0; 45.5–365.0	n.s. 125.0; 74.5–290.5	n.s. 211.0; 116.5–305.5	n.s. 49.5; 36.8–62.3	Ø
LDH	[U/L]		188.5; 179.5–230.5	229.0; 173.8–264.3	237.5; 187.5–327.8	216.0; 196.3–232.5	216.0; 184.0–262.5
		*	339.0; 300.0–1267.0	n.s. 315.0; 279.0–968.0	n.s. 664.0; 416.5–911.5	n.s. 236.0; 233.0–239.0	Ø
Total bilirubine	[mg/dL]		3.1; 2.1–4.7	3.8; 2.9–7.8	4.7; 2.9–10.0	5.8; 3.4–13.1	6.4; 4.2–14.7
		.054	9.0; 4.2–9.6	n.s. 2.4; 2.3–9.2	n.s. 2.3; 2.2–2.5	n.s. 4.8; 3.3–6.2	Ø

Data are presented by median and interquartile range (Q1–Q3). Concerning symbolism and higher orders of significance: $P < 0.05$; *, $P < 0.01$; **, $P < 0.001$; ***, n.s.: not statistically significant, Ø: no data available. Abbreviations: ALF, acute liver failure; ASAT, aspartat amino transferase; ALAT, alanine amino transferase; LDH, lactate dehydrogenase.

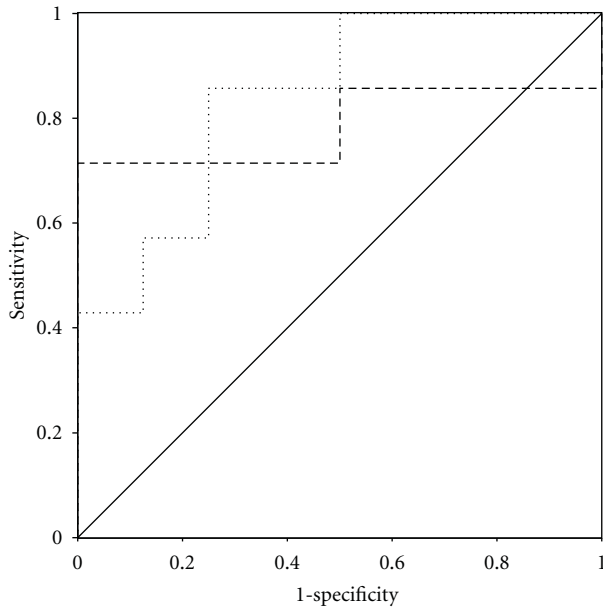


FIGURE 3: ROC curve for ADMA (long dashed line) and L-arg (short dashed line) plasma levels at sepsis onset in patients with septic shock and an accompanying ALF who ultimately did ($n = 8$) and did not ($n = 7$) survive within the 28 days observation period.

volunteers and patients following major abdominal surgery. Moreover, plasma levels of ADMA and L-arg were shown to be early predictors for survival in patients with septic shock and an accompanying ALF.

Concerning plasma levels of L-arg in septic patients, a recent review by Davis and Anstey failed to reveal conclusive results for patients with surgery-associated or trauma-associated sepsis [27]. In contrast, patients with sepsis not associated with trauma or surgery were observed to suffer from a hypoarginineamic state [27]. Since our study was performed with patients suffering from septic shock on a surgical intensive care unit, the pathogenesis of sepsis was at least surgery-associated in all cases. L-arg plasma levels tended to be decreased in the initial phase of NO depletion, probably due to a lower *de novo* L-arg production (e.g., decreased food intake and gut absorption) as well as an increased L-arg consumption (e.g., increased arginase and NO production and elevated protein need) [12, 16]. This consuming phase was followed by a secondary short-term restorative phase with increasing plasma levels of L-arg at day 4. Comparable plasma kinetics have already been described by Davis et al., showing lowest L-arg plasma levels at sepsis onset followed by an increase 2–4 days later [28]. We hypothesize that this excess supply of L-arg should counteract increasing plasma levels of nonselective endogenous inhibitors such as ADMA, which are able to reduce the activity of NOS. The NO-reducing effects of ADMA have been proven in animal as well as human models using experimental ADMA-infusion [29, 30]. ADMA can also compete with L-arg, symmetrical dimethylarginine (SDMA) and L-lysine for the cationic amino acid transporters-dependant transport across the cell membrane, especially in hepatocytes [31]. While the ADMA

uptake is performed for degradation, L-arg is used for NO-synthesis. Elevated plasma levels of ADMA have been reported for several disease states, which are known to be associated with an endothelial dysfunction such as hypertension, peripheral arterial disease, chronic renal disease, hypercholesterolemia, diabetes mellitus, and hyperhomocysteinemia [32–37]. Concerning patients with septic shock, ADMA plasma levels were also reported to be significantly elevated [2–4, 38, 39]. In contrast, in septic patients without shock, plasma ADMA concentrations did not differ compared to plasma levels in control patients [40]. As expected and in line with the literature, we were able to show significantly increased plasma levels of ADMA in the septic group of patients at all time points. Moreover, in analogy to the previously described results of L-arg measurements, a peak concentration for ADMA could be observed 4 days after sepsis onset. As described earlier, this comparable leveling of both, L-arg and ADMA may further support the hypothesis of the so-called L-arginine-paradox [21, 41]. Moreover, ADMA concentrations were shown to be elevated in patients of the surgical group prior to the surgical procedure in comparison to healthy volunteers. This effect might be due to several pre-existing conditions (e.g., hypertension, hypercholesterolemia) of the surgical cohort of patients, which are known to be associated with increased plasma levels of ADMA. Decreasing plasma levels of ADMA following the surgical procedure have most likely to be ascribed to simple dilution effects due to perioperative volume therapy.

With regard to the plasma levels of ADMA, the possible elimination pathways have to be taken into account, since MODS can frequently be observed in patients with septic shock [1]. ADMA is removed from the body by urinary excretion and therefore depends on kidney function [42]. On the other hand, ADMA is subject to enzymatic degradation into citrulline and dimethylamine by the enzyme dimethylarginine dimethylaminohydrolase (DDAH), which is highly expressed in the liver [43–45]. Accordingly, ADMA levels were shown to be significantly increased in patients with septic shock and an accompanying ARF. However, these results might have been underestimated since hemodialysis, peritonealdialysis and hemodiafiltration are known to be able to reduce ADMA plasma levels [46]. With respect to liver integrity, Nijfeldt et al. demonstrated in an animal model that the liver is a key player in the absorption and degradation of ADMA [42]. This observation was further supported by investigations in human patients suffering from either decompensated liver cirrhosis, ALF, or sepsis-associated hepatic dysfunction, showing a close correlation between ADMA plasma levels and the degree of hepatic dysfunction [2, 19, 47, 48]. Accordingly, we observed significantly elevated plasma levels of ADMA in patients with a sepsis-associated ALF. In terms of the “L-arginine-paradox,” L-arg plasma levels were also significantly elevated. Moreover, both biomarkers were shown to predict survival in this cohort of patients. However, the prognostic value of both biomarkers in septic patients with a sepsis-associated ALF seems to be most likely a reflection of poor hepatic function. Whether increased plasma levels of ADMA contribute causatively to the decrease in these patients cannot finally be concluded.

With regard to further influencing factors of L-arg and ADMA plasma levels, especially red blood cells came into the focus of interest. On the one hand, administration of PRBC is reported to be associated with L-arg consumption, since PRBCs contain relevant amounts of arginase [49, 50]. This enzyme is able to convert arginine to ornithine, resulting in a reduced bioavailability of this conditionally essential amino acid. Probably due to the vanishing low amount of PRBC administration in the presented patients with septic shock, PRBC-associated arginine consumption could not be observed. Instead, plasma levels of L-arg in patients receiving PRBCs were significantly elevated at 4 d. This might be probably attributable to significantly increased ADMA plasma levels in more severely injured septic patients receiving PRBCs especially at 4 d. Beside PRBCs, the body's own RBC might likewise be an influencing factor, since RBCs do also contain relevant amounts of L-arg metabolizing enzymes (e.g., arginase) as well as express amino acid transporters for the L-arg uptake [51, 52]. However, since hemoglobin concentrations in patients with septic shock did not reveal any significant changes within the 28 day observation period and L-arg plasma levels showed a sigmoidal leveling, red cell mass is unlikely to have affected L-arg plasma levels in a relevant manner. This hypothesis is further strengthened throughout the subsidiary performed correlation analysis, which was not able to show a correlation between hemoglobin concentrations and the accompanying L-arg plasma levels.

Notably, in the literature, normal plasma levels of L-arg in healthy persons are reported to be 70–80 $\mu\text{mol/L}$ as assessed by HPLC (*high performance liquid chromatography*) [53–55]. This is in contrast to our investigation, since baseline L-arg plasma levels in healthy volunteers were described to be 112.6 $\mu\text{mol/L}$ in median. Moreover, L-arg plasma levels of patients with septic shock within our investigation tended to be steadily increased in comparison to the available literature. However, the ELISA-based measurements of ADMA did not differ in a relevant manner in comparison to the traditional form of ADMA measurements using HPLC. To define whether an increased sensitivity of the newly developed ELISA-based method for L-arg determination in human plasma samples might explain the discrepancy is beyond the scope of this manuscript and needs to be studied in the future.

5. Conclusions

NO-bioavailability was demonstrated to be reduced in patients with septic shock. In comparison to healthy volunteers and patients following major abdominal surgery, patients with septic shock showed significantly increased levels of ADMA, as well as decreased levels of the ratio of L-arg and ADMA at all time points within the 28-day observation period. Moreover, plasma levels of ADMA and L-arg were significantly increased in septic patients with an ALF in comparison to those with an intact hepatic function. Most important, measurements of ADMA and L-arg at sepsis onset appeared to be early predictors for survival in septic patients with ALF.

Abbreviations

ADMA:	Asymmetric dimethylarginine
ALAT:	Alanine amino transferase
ALF:	Acute liver failure
APACHE II-score:	Acute physiology and chronic health evaluation II-score
ARF:	Acute renal failure
ARDS:	Acute respiratory distress syndrome
ASAT:	Aspartat amino transferase
AUC:	Area under the curve
CAP:	Community acquired pneumonia
DDAH:	Dimethylarginine dimethylaminohydrolase
ELISA:	Enzyme linked immunosorbent assay
HAP:	Hospital acquired pneumonia
Hb:	Hemoglobin
HPLC:	High performance liquid chromatography
L-arg:	L-arginine
LDH:	Lactate dehydrogenase
MODS:	Multiple organ dysfunction syndrome
NO:	Nitric oxide
NOS:	Nitric oxide synthases
PRBC:	Packed red blood cells
RBC:	Red blood cells
ROC:	Receiver operating characteristic
SAPS:	Simplified acute physiology score
SDMA:	Symmetrical dimethylarginine
SOFA-score:	Sequential organ failure assessment-score
SPSS:	Statistical product and services solutions
SSI:	Surgical site infection
VAP:	Ventilator associated pneumonia.

Competing Interests

The authors declare that they have no competing interests.

Acknowledgments

This investigation was carried out with financial resources of the Department of Anesthesiology (University of Heidelberg, Germany), the Department of Medicine I and Clinical Chemistry (University of Heidelberg, Germany), the Department of General and Transplant Surgery (University of Heidelberg, Germany), and the Institute of Medical Biometry and Informatics (University of Heidelberg, Germany). Moreover, this work was supported by the BMBF Program Bio-Chance PLUS to AB.

References

- [1] D. Annane, P. Aegerter, M. C. Jars-Guincestre, and B. Guidet, "Current epidemiology of septic shock: the CUB-Réa network," *American Journal of Respiratory and Critical Care Medicine*, vol. 168, no. 2, pp. 165–172, 2003.

- [2] J. S. Davis, C. J. Darcy, T. W. Yeo et al., "Asymmetric dimethylarginine, endothelial nitric oxide bioavailability and mortality in sepsis," *PLoS ONE*, vol. 6, no. 2, Article ID e17260, 2011.
- [3] M. S. Gough, M. A. M. Morgan, C. M. MacK et al., "The ratio of arginine to dimethylarginines is reduced and predicts outcomes in patients with severe sepsis," *Critical Care Medicine*, vol. 39, no. 6, pp. 1351–1358, 2011.
- [4] M. J. O'Dwyer, F. Dempsey, V. Crowley, D. P. Kelleher, R. McManus, and T. Ryan, "Septic shock is correlated with asymmetrical dimethyl arginine levels, which may be influenced by a polymorphism in the dimethylarginine dimethylaminohydrolase II gene: a prospective observational study," *Critical Care*, vol. 10, no. 5, article R139, 2006.
- [5] J. P. Cooke, "Asymmetrical Dimethylarginine: the Über Marker?" *Circulation*, vol. 109, no. 15, pp. 1813–1819, 2004.
- [6] U. Forstermann, H. H. H. W. Schmidt, J. S. Pollock et al., "Isoforms of nitric oxide synthase. Characterization and purification from different cell types," *Biochemical Pharmacology*, vol. 42, no. 10, pp. 1849–1857, 1991.
- [7] J. Askanazi, Y. A. Carpentier, and C. B. Michelsen, "Muscle and plasma amino acids following injury. Influence of intercurrent infection," *Annals of Surgery*, vol. 192, no. 1, pp. 78–85, 1980.
- [8] A. Barbul and A. Uliyargoli, "Use of exogenous arginine in multiple organ dysfunction syndrome and sepsis," *Critical Care Medicine*, vol. 35, no. 9, pp. S564–S567, 2007.
- [9] C. Chiarla, I. Giovannini, and J. H. Siegel, "Plasma arginine correlations in trauma and sepsis," *Amino Acids*, vol. 30, no. 1, pp. 81–86, 2006.
- [10] H. Freund, S. Atamian, J. Holroyde, and J. E. Fischer, "Plasma amino acids as predictors of the severity and outcome of sepsis," *Annals of Surgery*, vol. 190, no. 5, pp. 571–576, 1979.
- [11] A. C. Kalil and R. L. Danner, "L-Arginine supplementation in sepsis: beneficial or harmful?" *Current Opinion in Critical Care*, vol. 12, no. 4, pp. 303–308, 2006.
- [12] Y. C. Luiking, M. Poeze, C. H. Dejong, G. Ramsay, and N. E. Deutz, "Sepsis: an arginine deficiency state?" *Critical Care Medicine*, vol. 32, no. 10, pp. 2135–2145, 2004.
- [13] P. J. Milewski, C. J. Threlfall, and D. F. Heath, "Intracellular free amino acids in undernourished patients with or without sepsis," *Clinical Science*, vol. 62, no. 1, pp. 83–91, 1982.
- [14] J. B. Ochoa, V. Makarenkova, and V. Bansal, "A rational use of immune enhancing diets: when should we use dietary arginine supplementation?" *Nutrition in Clinical Practice*, vol. 19, no. 3, pp. 216–225, 2004.
- [15] J. B. Ochoa, A. O. Udekwu, T. R. Billiar et al., "Nitrogen oxide levels in patients after trauma and during sepsis," *Annals of Surgery*, vol. 214, no. 5, pp. 621–626, 1991.
- [16] P. J. Popovic, H. J. Zeh III, and J. B. Ochoa, "Arginine and immunity," *Journal of Nutrition*, vol. 137, no. 6, 2007.
- [17] L. R. B. Weitzel, W. J. Mayles, P. A. Sandoval, and P. E. Wischmeyer, "Effects of pharmacutrients on cellular dysfunction and the microcirculation in critical illness," *Current Opinion in Anaesthesiology*, vol. 22, no. 2, pp. 177–183, 2009.
- [18] G. Wu and S. M. Morris Jr., "Arginine metabolism: nitric oxide and beyond," *Biochemical Journal*, vol. 336, no. 1, pp. 1–17, 1998.
- [19] R. J. Nijveldt, T. Teerlink, B. van der Hoven et al., "Asymmetric dimethylarginine (ADMA) in critically ill patients: high plasma ADMA concentration is an independent risk factor of ICU mortality," *Clinical Nutrition*, vol. 22, no. 1, pp. 23–30, 2003.
- [20] M. P. C. Siroen, P. A. M. van Leeuwen, R. J. Nijveldt, T. Teerlink, P. J. Wouters, and G. van den Berghe, "Modulation of asymmetric dimethylarginine in critically ill patients receiving intensive insulin treatment: a possible explanation of reduced morbidity and mortality?" *Critical Care Medicine*, vol. 33, no. 3, pp. 504–510, 2005.
- [21] R. H. Böger, "Asymmetric dimethylarginine, an endogenous inhibitor of nitric oxide synthase, explains the "L-arginine paradox" and acts as a novel cardiovascular risk factor," *Journal of Nutrition*, vol. 134, no. 10, supplement, pp. 2842S–2847S, 2004, discussion 2853S.
- [22] M. M. Levy, M. P. Fink, J. C. Marshall et al., "2001 SCCM/ESICM/ACCP/ATS/SIS International Sepsis Definitions Conference," *Critical Care Medicine*, vol. 31, no. 4, pp. 1250–1256, 2003.
- [23] E. Rivers, B. Nguyen, S. Havstad et al., "Early goal-directed therapy in the treatment of severe sepsis and septic shock," *The New England Journal of Medicine*, vol. 345, no. 19, pp. 1368–1377, 2001.
- [24] J. A. Russell, "Management of sepsis," *The New England Journal of Medicine*, vol. 355, no. 16, pp. 1699–1713, 2006.
- [25] M. A. Weigand, H. J. Bardenheuer, and B. W. Böttiger, "Clinical management of patients with sepsis," *Anaesthesist*, vol. 52, no. 1, pp. 3–22, 2003.
- [26] K. Miyaoka, M. Iwase, R. Suzuki et al., "Clinical evaluation of circulating interleukin-6 and interleukin-10 levels after surgery-induced inflammation," *Journal of Surgical Research*, vol. 125, no. 2, pp. 144–150, 2005.
- [27] J. S. Davis and N. M. Anstey, "Is plasma arginine concentration decreased in patients with sepsis? A systematic review and meta-analysis," *Critical Care Medicine*, vol. 39, no. 2, pp. 380–385, 2010.
- [28] J. S. Davis, T. W. Yeo, J. H. Thomas et al., "Sepsis-associated microvascular dysfunction measured by peripheral arterial tonometry: an observational study," *Critical Care*, vol. 13, no. 5, p. R155, 2009.
- [29] V. De Gennaro Colonna, S. Bonomo, P. Ferrario et al., "Asymmetric dimethylarginine (ADMA) induces vascular endothelium impairment and aggravates post-ischemic ventricular dysfunction in rats," *European Journal of Pharmacology*, vol. 557, no. 2-3, pp. 178–185, 2007.
- [30] P. Vallance, A. Leone, A. Calver, J. Collier, and S. Moncada, "Accumulation of an endogenous inhibitor of nitric oxide synthesis in chronic renal failure," *The Lancet*, vol. 339, no. 8793, pp. 572–575, 1992.
- [31] E. I. Closs, F. Z. Basha, A. Habermeier, and U. Förstermann, "Interference of L-arginine analogues with L-arginine transport mediated by the y+ carrier hCAT-2B," *Nitric Oxide*, vol. 1, no. 1, pp. 65–73, 1997.
- [32] F. Abbasi, T. Asagmi, J. P. Cooke et al., "Plasma concentrations of asymmetric dimethylarginine are increased in patients with type 2 diabetes mellitus," *American Journal of Cardiology*, vol. 88, no. 10, pp. 1201–1203, 2001.
- [33] R. H. Böger, S. M. Bode-Böger, A. Szuba et al., "Asymmetric dimethylarginine (ADMA): a novel risk factor for endothelial dysfunction: its role in hypercholesterolemia," *Circulation*, vol. 98, no. 18, pp. 1842–1847, 1998.
- [34] S. Dayal and S. R. Lentz, "ADMA and hyperhomocysteinemia," *Vascular Medicine*, vol. 10, no. 1, pp. S27–S33, 2005.
- [35] J. T. Kielstein, R. H. Böger, S. M. Bode-Böger et al., "Marked increase of asymmetric dimethylarginine in patients with incipient primary chronic renal disease," *Journal of the American Society of Nephrology*, vol. 13, no. 1, pp. 170–176, 2002.
- [36] F. Mittermayer, K. Krzyzanowska, M. Exner et al., "Asymmetric dimethylarginine predicts major adverse cardiovascular events in patients with advanced peripheral artery disease,"

- Arteriosclerosis, Thrombosis, and Vascular Biology*, vol. 26, no. 11, pp. 2536–2540, 2006.
- [37] A. Surdacki, M. Nowicki, J. Sandmann et al., “Reduced urinary excretion of nitric oxide metabolites and increased plasma levels of asymmetric dimethylarginine in men with essential hypertension,” *Journal of Cardiovascular Pharmacology*, vol. 33, no. 4, pp. 652–658, 1999.
- [38] G. Iapichino, M. Umbrello, M. Albicini et al., “Time course of endogenous nitric oxide inhibitors in severe sepsis in humans,” *Minerva Anestesiologica*, vol. 76, no. 5, pp. 325–333, 2010.
- [39] T. Nakamura, E. Sato, N. Fujiwara et al., “Circulating levels of advanced glycation end products (AGE) and interleukin-6 (IL-6) are independent determinants of serum asymmetric dimethylarginine (ADMA) levels in patients with septic shock,” *Pharmacological Research*, vol. 60, no. 6, pp. 515–518, 2009.
- [40] C. Zoccali, R. Maas, S. Cutrupi et al., “Asymmetric dimethylarginine (ADMA) response to inflammation in acute infections,” *Nephrology Dialysis Transplantation*, vol. 22, no. 3, pp. 801–806, 2007.
- [41] D. Tsikas, R. H. Böger, J. Sandmann, S. M. Bode-Böger, and J. C. Frölich, “Endogenous nitric oxide synthase inhibitors are responsible for the L-arginine paradox,” *FEBS Letters*, vol. 478, no. 1–2, pp. 1–3, 2000.
- [42] R. J. Nijveldt, T. Teerlink, M. P. C. Siroen, A. A. van Lambalgen, J. A. Rauwerda, and P. A. M. van Leeuwen, “The liver is an important organ in the metabolism of asymmetrical dimethylarginine (ADMA),” *Clinical Nutrition*, vol. 22, no. 1, pp. 17–22, 2003.
- [43] M. Kimoto, H. Tsuji, T. Ogawa, and K. Sasaoka, “Detection of N(G),N(G)-dimethylarginine dimethylaminohydrolase in the nitric oxide-generating systems of rats using monoclonal antibody,” *Archives of Biochemistry and Biophysics*, vol. 300, no. 2, pp. 657–662, 1993.
- [44] T. Ogawa, M. Kimoto, and K. Sasaoka, “Purification and properties of a new enzyme, N(G),N(G)-dimethylarginine dimethylaminohydrolase, from rat kidney,” *Journal of Biological Chemistry*, vol. 264, no. 17, pp. 10205–10209, 1989.
- [45] T. Teerlink, “ADMA metabolism and clearance,” *Vascular Medicine*, vol. 10, no. 1, pp. S73–S81, 2005.
- [46] J. Eiselt, D. Rajdl, J. Racek, R. Šíroková, L. Trefil, and S. Opatrná, “Asymmetric dimethylarginine in hemodialysis, hemodiafiltration, and peritoneal dialysis,” *Artificial Organs*, vol. 34, no. 5, pp. 420–425, 2010.
- [47] P. Lluch, B. Torondel, P. Medina et al., “Plasma concentrations of nitric oxide and asymmetric dimethylarginine in human alcoholic cirrhosis,” *Journal of Hepatology*, vol. 41, no. 1, pp. 55–59, 2004.
- [48] R. P. Mookerjee, R. N. Dalton, N. A. Davies et al., “Inflammation is an important determinant of levels of the endogenous nitric oxide synthase inhibitor asymmetric dimethylarginine (ADMA) in acute liver failure,” *Liver Transplantation*, vol. 13, no. 3, pp. 400–405, 2007.
- [49] A. Bernard, M. Kasten, C. Meier et al., “Red blood cell arginase suppresses Jurkat (T cell) proliferation by depleting arginine,” *Surgery*, vol. 143, no. 2, pp. 286–291, 2008.
- [50] A. Bernard, C. Meier, N. Lopez et al., “Packed red blood cell-associated arginine depletion is mediated by arginase,” *Journal of Trauma*, vol. 63, no. 5, pp. 1108–1112, 2007, discussion 1112.
- [51] P. S. Kim, R. K. Iyer, K. V. Lu et al., “Expression of the liver form of arginase in erythrocytes,” *Molecular Genetics and Metabolism*, vol. 76, no. 2, pp. 100–110, 2002.
- [52] B. M. Rotoli, E. I. Closs, A. Barilli et al., “Arginine transport in human erythroid cells: discrimination of CAT1 and 4F2hc/y+LAT2 roles,” *Pflügers Archiv European Journal of Physiology*, vol. 458, no. 6, pp. 1163–1173, 2009.
- [53] R. H. Böger, S. M. Bode-Böger, W. Thiele, W. Junker, K. Alexander, and J. C. Frölich, “Biochemical evidence for impaired nitric oxide synthesis in patients with peripheral arterial occlusive disease,” *Circulation*, vol. 95, no. 8, pp. 2068–2074, 1997.
- [54] M. L. Selley, “Increased concentrations of homocysteine and asymmetric dimethylarginine and decreased concentrations of nitric oxide in the plasma of patients with Alzheimer’s disease,” *Neurobiology of Aging*, vol. 24, no. 7, pp. 903–907, 2003.
- [55] J. T. Kielstein, R. H. Böger, S. M. Bode-Böger et al., “Asymmetric dimethylarginine plasma concentrations differ in patients with end-stage renal disease: relationship to treatment method and atherosclerotic disease,” *Journal of the American Society of Nephrology*, vol. 10, no. 3, pp. 594–600, 1999.

Clinical Study

Lactoferrin Levels in the Gastric Tissue of *Helicobacter pylori*-Positive and -Negative Patients and Its Effect on Anemia

Yaşar Doğan,^{1,2} Tülay Erkan,¹ Zerrin Önal,¹ Merve Usta,¹ Gülen Doğusoy,³
Fügen Çullu Çokuğraş,¹ and Tufan Kutlu¹

¹ Division of Pediatric Gastroenterology Hepatology and Nutrition, Department of Pediatrics, Cerrahpaşa Medical Faculty, İstanbul University, İstanbul 23119, Turkey

² Fırat Üniversitesi Hastanesi Çocuk Sağ. ve Hast. Anabilim Dalı Elazığ, Turkey

³ Department of Medical Pathology, Cerrahpaşa Medical Faculty, İstanbul University, İstanbul 23119, Turkey

Correspondence should be addressed to Yaşar Doğan, yasardogan@ttmail.com

Received 12 August 2011; Accepted 10 January 2012

Academic Editor: Helieh S. Oz

Copyright © 2012 Yaşar Doğan et al. This is an open access article distributed under the Creative Commons Attribution License, which permits unrestricted use, distribution, and reproduction in any medium, provided the original work is properly cited.

Aim. To determine gastric tissue lactoferrin (Lf) levels of *Helicobacter pylori*- (Hp-) positive and -negative patients and its effect on anemia. **Methods.** Cases in which initial presentation was of abdominal pain and that were Hp-positive at endoscopy were included. Hp-positive cases and -negative controls were divided into two groups. **Results.** The study included 64 cases (average: 10.2 ± 0.4 years, 39 male and 25 female). Lf levels were subsequently studied on 61 cases. 45 (73.8%) of these were Hp-positive, while 16 (22.2%) were Hp-negative. In Hp-positive cases, mean staining percentages and density of glands in the antral mucosa were $45.5 \pm 4.7\%$ and 1.9 ± 0.1 , respectively. Hp-negative cases showed significantly different values of $17.8 \pm 4.5\%$ and 1.3 ± 0.2 , respectively. Hemoglobin and serum ferritin values of Hp-positive cases were 12.7 ± 0.2 g/dL and 32.5 ± 2 ng/mL, but these were comparable with Hp-negative cases (12.6 ± 0.1 g/dL and 30.7 ± 4.4 ng/mL). **Conclusions.** Tissue Lf was significantly higher in Hp-positive cases compared to Hp-negative cases, but no difference was observed between the two groups with regards to hemoglobin and ferritin level. As a result, it is difficult to say that this rise in Lf plays a role in the development of iron deficiency anemia in Hp-positive patients.

1. Introduction

Helicobacter pylori (Hp) is an important etiologic cause of diseases such as chronic gastritis, duodenal and gastric ulcers, atrophic gastritis, intestinal metaplasia, and gastric lymphoma (Mucosa-associated lymphoid tissue, MALT lymphoma type) [1, 2]. Many studies suggest a relationship between iron deficiency anemia (IDA) and Hp infection, but it is not clear the mechanism by which this occurs [3, 4]. One of the suggested mechanisms occurs through Hp-mediated Lf increase in gastric tissue via neutrophils. Lf captures iron from transferrin. The iron, thus, bound to Lf is in turn picked up by the bacterium, by means of its outer membrane receptors, for its own growth. As *H. pylori* turnover is very rapid, the bacterial iron stores are rapidly lost in the stools, together with the dead bacteria. This mechanism, or at least

its template, could explain why an iron supply is no longer available for hemopoiesis, which only enhances *H. pylori* proliferation [5, 6]. The proposed hypothesis is not able to answer why IDA does not develop in all infected subjects. It is possible that the presence of specific bacterium strains and the high needs for iron required by the host under particular conditions could both play a crucial role in the onset of IDA [7]. Therefore, the purpose of this study is to determine the Lf levels in the gastric tissue of Hp-positive and -negative patients and whether this has an effect on anemia.

2. Methods

Patients over 4 years of age with recurring abdominal pain of unknown cause who subsequently underwent endoscopy at our hospital's Pediatric Gastroenterology, Hepatology and

TABLE 1: Endoscopic findings of Hp-positive and -negative cases.

	Hp-positive cases		Hp-negative cases		Total cases	
	N	%	N	%	N	%
Number of subjects	48	75	16	25	64	100
Endoscopic findings						
Normal	6	12.5	8	50	14	21.9
Antral hyperemia	15	31.2	6	37.5	21	32.8
Antral nodularity*	27	56.2	2	12.5	29	45.3

* $P = 0.008$ 95%, confidence interval (CI): 0.006–0.01.

Nutrition Department have been included in the study. Approval was obtained from the hospital's ethical committee prior to this study. Before the patients were examined, their families were informed within the frame of the Helsinki report, and their signatures were taken on an informed consent form. Following record of age, gender, weight, height, and clinical details, all cases underwent an upper GIS endoscopy aimed at diagnosis. During the endoscopy, biopsy samples were taken from the gastric antrum for histological examination and tissue Lf measurement. A *Helicobacter pylori* gastritis diagnosis was only made after histological examination of biopsy samples. Blood was taken from all cases for full blood count, serum iron, iron binding capacity (IBC), total iron binding capacity (TIBC), and ferritin level. Patients with a digestive system or systemic disorder other than Hp gastritis, cases previously treated for Hp gastritis or peptic ulcer disease, and patients taking proton pump inhibitors or antibiotics were not included in the study.

Tissue Lf level was evaluated by a blinded pathology specialist, who was not informed about the patients' clinical progress or the gastric antral immunohistochemical study results from primary antibody assays (DakoCytomation, LSAB2 System-HRP, Denmark).

Lactoferrin was quantitated immunohistochemically by two methods: in the first method, all samples were evaluated from 0% to 100% according to the staining percentage of glands in the antrum; in the second method, all samples were evaluated based on no staining (0), light (1), medium (2), or dense (3) according to stain-holding densities of glands in the antrum. Biopsy samples of cases were also grouped as no neutrophils (0), light (1), medium (2), or dense (3) according to the density of Lf-secreting neutrophils.

Data from this study were analyzed using the SPSS statistics software package. Nonparametric MannWhitney U and Chi-square tests were used to compare the data. In all tests, $P < 0.05$ was taken as significant.

3. Results

The study consisted of 64 patients with ages ranging between 4 and 17 years (average: 10.2 ± 0.4 years). 39 (60.9%) of the cases were male, while 25 (39.1%) were female. As a result of histological examination of the gastric antrum biopsy samples, 48 (75%) out of 64 cases were found to

be Hp-positive, while 16 (25%) cases were Hp-negative. Endoscopic findings of Hp-positive and -negative cases are shown in Table 1. Antral nodularity in Hp-positive group was significantly higher compared to Hp-negative group ($P = 0.008$), (95% Confidence interval (CI) = 0.006–0.01).

The average age of positive cases was 10.9 ± 0.5 years, and the average age of negative cases was 8.1 ± 0.9 , which was statistically significant ($P = 0.009$). Positive Hp was seen in more male patients, but this difference was statistically insignificant ($P = 0.1$). (Table 2). Serum iron; IBC, TIBC, ferritin levels; full blood count and hemoglobin (Hb), hematocrit (Htc), leucocyte (WBC), thrombocyte (PLT), and erythrocyte count (RBC); average erythrocyte volume (MCV), average erythrocyte hemoglobin concentration (MCHC), erythrocyte distribution range (RDW), and average erythrocyte hemoglobin (MCH) values were also separately evaluated for Hp-positive and -negative cases, but no significant differences were observed. Results of power analyses for Mann-Whitney tests provided a wide range from very low to very high such as 0.051 for Hb, 0.386 for Htc, 0.421 for ferritin, and 0.948 for serum iron. These results can be interpreted as %39 power to detect a difference between Htc values of two groups with sample sizes of 16 and 48. (Table 3).

As three cases had insufficient tissue for assay, tissue Lf was only measured in the remaining 61 cases. 45 of these cases were Hp-positive, while 16 were Hp-negative. In Hp positive cases, staining percentages and density of glands in the antral mucosa were $45.5 \pm 4.7\%$ and 1.9 ± 0.1 , respectively, while these figures were $17.8 \pm 4.5\%$ and 1.3 ± 0.2 [$(P = 0.001, CI = 0.0–0.048)$, ($P = 0.016, CI = 0.0–0.048$)] in Hp-negative cases. (Figures 1 and 2). The neutrophil density in the Hp-positive group was also significantly higher compared to the Hp-negative group. ($P = 0.001, CI = 0.0–0.046$) (Figure 3).

4. Discussion

One of the most important clinical findings caused by Hp infection other than gastrointestinal diseases is anemia [8]. There are quite a number of studies in the literature demonstrating the relationship between Hp and anemia in both adults and infants [9–12]. For example, in a study of young patients in South Korea, IDA in individuals infected with Hp was reported as 2.9 times higher compared to uninfected cases [13]. It has been reported that this anemia did not improve despite iron treatment, but the hemoglobin,

TABLE 2: Details of cases included in the study.

Characteristics	Hp-positive cases		Hp-negative cases		Total Cases		P value
	N	Mean \pm SEM	N	Mean \pm SEM	N	Mean \pm SEM	
Mean (Age)	48	10.9 \pm 0.5	16	8.1 \pm 0.9	64	10.2 \pm 0.4	0.009*
Male	32	10.5 \pm 0.6	7	8.51.7	39	10.18 \pm 0.6	0.1 [†]
Female	16	11.8 \pm 0.8	9	7.8 \pm 0.9	25	10.43 \pm 0.7	
Weight (kg)	48	35.63 \pm 1.85	16	27.46 \pm 2.77	64	33.58 \pm 1.6	0.03*
Height (cm)	48	139.99 \pm 2.78	16	128.56 \pm 4.84	64	137.13 \pm 2.4	0.056 [†]

* $P < 0.05$.[†] $P > 0.05$.

SEM: Standard. error of mean.

TABLE 3: Full blood count, serum iron, TIBC, and ferritin values of cases.

	Hp-positive	Hp-negative	P value
Hb (gr/dL)	12.6 \pm 0.1	12.6 \pm 0.2	0.7
Htc (%)	37.3 \pm 0.4	37.0 \pm 0.8	0.7
WBC (mm ³)	7203 \pm 258	7836 \pm 690	0.2
PLT (mm ³)	303520 \pm 12048	282187 \pm 17604	0.3
RBC (mm ³)	4526479 \pm 47995	4565625 \pm 92812	0.6
MCV	82.0 \pm 0.7	80.6 \pm 1.4	0.3
MCHC	34.0 \pm 0.2	33.8 \pm 0.2	0.6
RDW	12.6 \pm 0.1	12.9 \pm 0.2	0.1
MCH	28.5 \pm 0.2	27.6 \pm 0.5	0.1
Serum Iron	72.9 \pm 5.3	57.5 \pm 5.7	0.1
IBC	274.1 \pm 8.8	274 \pm 7.5	0.9
TIBC	347 \pm 7.2	331.5 \pm 7.3	0.2
Ferritin	32.3 \pm 2.4	30.7 \pm 4.4	0.7

serum iron, and ferritin levels improved following treatment of Hp infection [14]. In a random, placebo-controlled study in 43 infants and adults, hemoglobin levels were also reported to be significantly improved following Hp treatment [15].

In addition to studies suggesting a relationship between Hp and anemia, there are also studies suggesting the opposite. Collet et al. [16], in a study conducted on 1060 cases, reported that there was no significant difference between serum ferritin level and HP in both males and females. In a review of the current data, Bini [17] tried to analyze whether Hp was really to blame for anemia in these cases or whether it is an innocent bystander. He tried to find the answers as to why Hp causes anemia in only a small percentage of infected patients, how this organism causes anemia if at all, and whether or not there is improvement in anemia after treatment. As a result of this evaluation, it was shown that Hp positively correlated with low levels of ferritin, though this may not play a direct role. Our results were contrary to other studies that reported a relationship between Hp and IDA, as there was no significant difference between the average hemoglobin, hematocrit, serum iron, and ferritin levels of Hp-positive and Hp-negative groups (Table 3).

Despite all these results, it is still unclear with which mechanism Hp causes IDA in these cases. Mechanisms proposed include loss of blood from the digestive system,

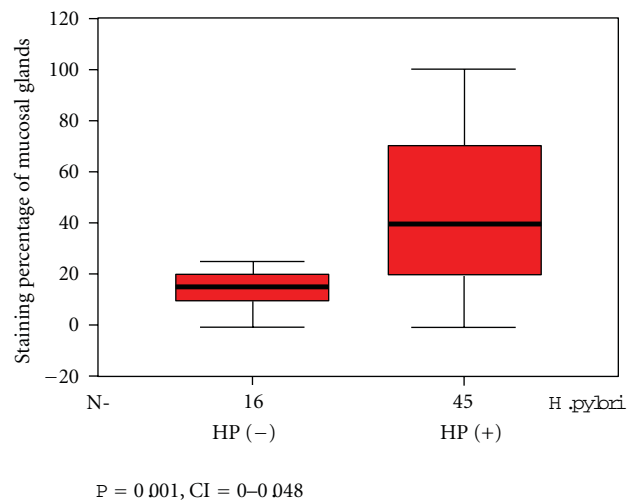


FIGURE 1: Staining percentage of antral mucosal glands by Hp-positive and -negative cases.

poor iron intake, iron absorption disorder, and use of iron in the reticuloendothelial system [11, 18, 19], and Hp is an etiological factor for gastric atrophy. Hypo- or achlorhydria may develop in individuals with atrophic gastritis, and iron

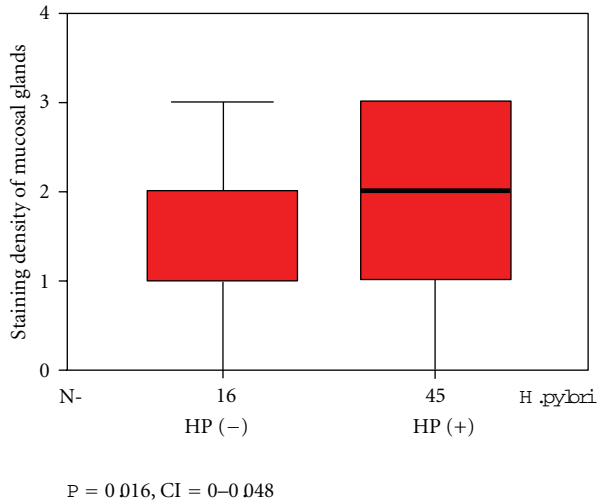


FIGURE 2: Staining density of antral mucosal glands by Hp-positive and -negative cases.

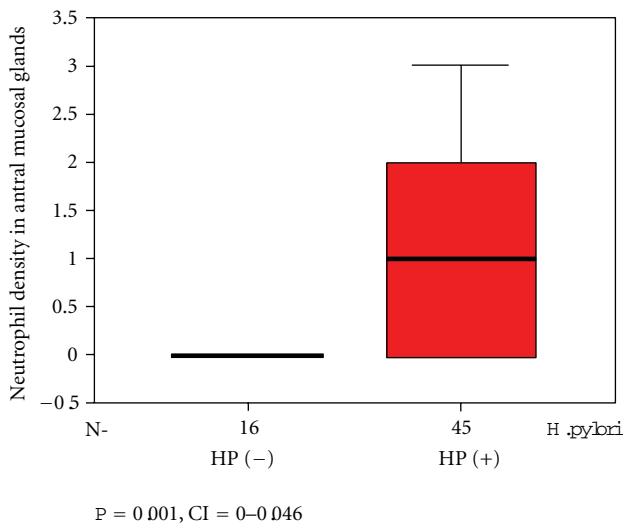


FIGURE 3: Neutrophil density in antral mucosal glands by Hp-positive and -negative cases.

absorption may decrease as a result [20]. Contrary to current theory, it has been proposed that Lf secreted from Hp-activated neutrophils in the stomach transfers iron to the outer cell wall receptor of Hp and that an IDA then results [6, 7]. Though not many studies support this theory, Nakao et al. [21] reported that there is a significant increase in Lf in the gastric fluids and mucosal tissue samples in Hp-infected patients.

Lonnerdal and Iyer [22] reported that the main cause of this Lf increase in gastric tissue was the increase in the inflammatory mediator interleukin-8 causing attraction of neutrophils and monocytes which then secrete Lf. A different study by Nakao et al. [23] also reported a marked relationship between interleukin levels in the gastric mucosa and Lf increase.

Choe et al. [24] reported a study on 101 patients with unexplained epigastric pain and/or iron deficiency, which found markedly high Lf levels in the Hp-positive and anemia group, and Lf levels in the Hp-positive group were found to be significantly raised relative to the control group and anemia-only group. In the same study, control endoscopy 8 weeks after Hp treatment of 12 of the Hp-positive cases with anemia measured Lf and hemoglobin levels in the gastric tissue biopsies. They reported a decrease in tissue Lf and a marked increase in hemoglobin compared to pretreatment.

In this study, staining percentage of antral gland cells of Hp-positive cases and staining density of cells were significantly higher compared to Hp-negative cases ($P = 0.001$, $P = 0.016$). Moreover, the percentage of stained neutrophils in Hp-positive cases was markedly higher compared to Hp-negative cases ($P = 0.001$).

The increase in Lf in Hp-positive cases agreed with previously conducted studies, but conversely, hemoglobin, hematocrit, and ferritin levels in these cases did not differ (Table 3). These results did not match the hypothesis that anemia is caused by loss of iron to Hp bacteria via Lf in the gastric tissue of Hp-positive cases.

We can conclude that the increase of Lf in the gastric tissue of Hp-positive cases is dependent upon inflammation. However, this iron does not seem to be transferred to Hp, as overall iron levels did not decrease in these patients and so we cannot say that the increase in Lf is connected with the subsequent development of anemia.

References

- [1] J. Valle, M. Kekki, P. Sipponen, T. Ihämäki, and M. Siurala, "Long-term course and consequences of *Helicobacter pylori* gastritis: results of a 32-year follow-up study," *Scandinavian Journal of Gastroenterology*, vol. 31, no. 6, pp. 546–550, 1996.
- [2] A. C. Wotherspoon, C. Ortiz-Hidalgo, M. R. Falzon, and P. G. Isaacson, "*Helicobacter pylori*-associated gastritis and primary B-cell gastric lymphoma," *The Lancet*, vol. 338, no. 8776, pp. 1175–1176, 1991.
- [3] J. Carnicer, R. Badfa, and J. Argemf, "*Helicobacter pylori* gastritis and sideropenic refractory anemia," *Journal of Pediatric Gastroenterology and Nutrition*, vol. 25, no. 4, p. 441, 1997.
- [4] M. Marignani, S. Angeletti, C. Bordi et al., "Reversal of long-standing iron deficiency anaemia after eradication of *Helicobacter pylori* infection," *Scandinavian Journal of Gastroenterology*, vol. 32, no. 6, pp. 617–622, 1997.
- [5] C. Hershko, A. Lahad, and D. Kereth, "Gastropathic sideropenia," *Best Practice and Research*, vol. 18, no. 2, pp. 363–380, 2005.
- [6] A. Barabino, C. Dufour, C. E. Marino, F. Claudiani, and A. De Alessandri, "Unexplained refractory iron-deficiency anemia associated with *Helicobacter pylori* gastric infection in children: further clinical evidence," *Journal of Pediatric Gastroenterology and Nutrition*, vol. 28, no. 1, pp. 116–119, 1999.
- [7] A. Barabino, "*Helicobacter pylori*-related iron deficiency anemia: a review," *Helicobacter*, vol. 7, no. 2, pp. 71–75, 2002.
- [8] L. E. Bravo, R. Mera, J. C. Reina et al., "Impact of *Helicobacter pylori* infection on growth of children: a prospective cohort study," *Journal of Pediatric Gastroenterology and Nutrition*, vol. 37, no. 5, pp. 614–619, 2003.

- [9] J. W. Choi, "Does *Helicobacter pylori* infection relate to iron deficiency anaemia in prepubescent children under 12 years of age?" *Acta Paediatrica*, vol. 92, no. 8, pp. 970–972, 2003.
- [10] B. Annibale, M. Marignani, B. Monarca et al., "Reversal of iron deficiency anemia after *Helicobacter pylori* eradication in patients with asymptomatic gastritis," *Annals of Internal Medicine*, vol. 131, no. 9, pp. 668–672, 1999.
- [11] G. Baysoy, D. Ertem, E. Ademoğlu, E. Kotiloğlu, S. Keskin, and E. Pehlivanoglu, "Gastric histopathology, iron status and iron deficiency anemia in children with *Helicobacter pylori* infection," *Journal of Pediatric Gastroenterology and Nutrition*, vol. 38, no. 2, pp. 146–151, 2004.
- [12] Y. H. Choe, S. K. Kim, and Y. C. Hong, "*Helicobacter pylori* infection with iron deficiency anaemia and subnormal growth at puberty," *Archives of Disease in Childhood*, vol. 82, no. 2, pp. 136–140, 2000.
- [13] Y. H. Choe, S. K. Kim, and Y. C. Hong, "The relationship between *Helicobacter pylori* infection and iron deficiency: seroprevalence study in 937 pubescent children," *Archives of Disease in Childhood*, vol. 88, no. 2, p. 178, 2003.
- [14] S. J. Czinn, "*Helicobacter pylori* infection: detection, investigation, and management," *Journal of Pediatrics*, vol. 146, no. 3, pp. S21–S26, 2005.
- [15] Y. H. Choe, S. K. Kim, B. K. Son, D. H. Lee, Y. C. Hong, and S. H. Pai, "Randomized placebo-controlled trial of *Helicobacter pylori* eradication for iron-deficiency anemia in preadolescent children and adolescents," *Helicobacter*, vol. 4, no. 2, pp. 135–139, 1999.
- [16] J. A. Collett, M. J. Burt, C. M. A. Frampton et al., "Seroprevalence of *Helicobacter pylori* in the adult population of Christchurch: risk factors and relationship to dyspeptic symptoms and iron studies," *New Zealand Medical Journal*, vol. 112, no. 1093, pp. 292–295, 1999.
- [17] E. J. Bini, "*Helicobacter pylori* and iron deficiency anemia: guilty as charged?" *American Journal of Medicine*, vol. 111, no. 6, pp. 495–497, 2001.
- [18] B. Annibale, G. Capurso, E. Lahner et al., "Concomitant alterations in intragastric pH and ascorbic acid concentration in patients with *Helicobacter pylori* gastritis and associated iron deficiency anaemia," *Gut*, vol. 52, no. 4, pp. 496–501, 2003.
- [19] R. Yip, P. J. Limburg, D. A. Ahlquist et al., "Pervasive occult gastrointestinal bleeding in an Alaska native population with prevalent iron deficiency: role of *Helicobacter pylori* gastritis," *Journal of the American Medical Association*, vol. 277, no. 14, pp. 1135–1139, 1997.
- [20] B. Annibale, M. Marignani, C. Azzoni et al., "Atrophic body gastritis: distinct features associated with *Helicobacter pylori* infection," *Helicobacter*, vol. 2, no. 2, pp. 57–64, 1997.
- [21] K. Nakao, I. Imoto, E. C. Gabazza et al., "Gastric juice levels of Lactoferrin and *Helicobacter pylori* infection," *Scandinavian Journal of Gastroenterology*, vol. 32, no. 6, pp. 530–534, 1997.
- [22] B. Lonnerdal and S. Iyer, "Lactoferrin: molecular structure and biological function," *Annual Review of Nutrition*, vol. 15, pp. 93–110, 1995.
- [23] K. Nakao, I. Imoto, N. Ikemura et al., "Relation of lactoferrin levels in gastric mucosa with *Helicobacter pylori* infection and with the degree of gastric inflammation," *American Journal of Gastroenterology*, vol. 92, no. 6, pp. 1005–1011, 1997.
- [24] Y. H. Choe, Y. J. Oh, N. G. Lee et al., "Lactoferrin sequestration and its contribution to iron-deficiency anemia in *Helicobacter pylori*-infected gastric mucosa," *Journal of Gastroenterology and Hepatology*, vol. 18, no. 8, pp. 980–985, 2003.

Research Article

Zerumbone Attenuates the Severity of Acute Necrotizing Pancreatitis and Pancreatitis-Induced Hepatic Injury

Deng Wenhong,¹ Yu Jia,¹ Wang Weixing,¹ Chen Xiaoyan,¹ Chen Chen,¹
Xu Sheng,² and Jin Hao¹

¹ Department of General Surgery, Renmin Hospital of Wuhan University, Hubei 430060, China

² Department of General Surgery, People's Hospital of Guangxi Zhuang Autonomous Region, Nanning 530000, China

Correspondence should be addressed to Wang Weixing, sate.llite@163.com

Received 12 August 2011; Revised 11 November 2011; Accepted 10 December 2011

Academic Editor: Rwei-Fen S. Huang

Copyright © 2012 Deng Wenhong et al. This is an open access article distributed under the Creative Commons Attribution License, which permits unrestricted use, distribution, and reproduction in any medium, provided the original work is properly cited.

This paper investigated the potential effects of zerumbone pretreatment on an acute necrotizing pancreatitis rat model induced by sodium taurocholate. The pancreatitis injury was evaluated by serum AMY, sPLA2, and pancreatic pathological score. Pancreatitis-induced hepatic injury was measured by ALT, AST, and hepatic histopathology. The expression of I- κ B α and NF- κ B protein was evaluated by western blot and immunohistochemistry assay while ICAM-1 and IL-1 β mRNA were examined by RT-PCR. The results showed that AMY, sPLA2, ALT, and AST levels and histopathological assay of pancreatic and hepatic tissues were significantly reduced following administration of zerumbone. Applying zerumbone also has been shown to inhibit NF- κ B protein and downregulation of ICAM-1 and IL-1 β mRNA. The present paper suggests that treatment of zerumbone on rat attenuates the severity of acute necrotizing pancreatitis and pancreatitis-induced hepatic injury, via inhibiting NF- κ B activation and downregulating the expression of ICAM-1 and IL-1 β .

1. Introduction

Acute necrotizing pancreatitis (ANP) is an acute abdomen-characterized disease, and it is characterized by elevated pancreatic enzyme levels. Published data has indicated that ANP is an inflammatory disease with a systemic inflammatory response syndrome and a multiple organ dysfunction [1, 2], and hepatic injury is a manifestation of systemic inflammatory response during ANP [3]. Hepatic microcirculatory dysfunction, tissue hypoxia, and inflammatory cytokines also induce hepatic injury by resident macrophages during the progress of pancreatitis [4–6]. Therefore, an effective pharmacological amelioration of hepatic injury could improve the quality of life in ANP patients.

Zerumbone (2,6,9,9-tetramethylcycloundeca-2,6,10-trien-1-one), as the main component of the essential oil of Zingiber zerumbet, is a monocyclic sesquiterpene containing a cross-conjugated dienone system [7]. It has been shown to have antineoplasms and anti-inflammatory properties in animal models. Some studies reported that zerumbone had

the ability to suppress the proliferation of cancer cells and inhibit the invasion of tumor in breast, pancreas, colon, lung, and skin [8–11]. The anti-inflammation effect of zerumbone was evaluated by the suppression of proinflammatory gene and the antioxidant response of element-dependent detoxification pathway [12–17]. Moreover, Annamaria et al. indicated that zerumbone exerted a beneficial effect on inflammatory parameters following experimental pancreatitis [18]. However, there is little available information on how zerumbone regulates pancreatitis-induced hepatic injury. This work places emphasis on the effect of zerumbone on hepatic injury following ANP, suggesting that zerumbone could be a good candidate to attenuate the severity of acute necrotizing pancreatitis and pancreatitis-induced hepatic injury.

2. Materials and Methods

2.1. Animals and Reagents. Male SPF Wistar rats, weighing 200 to 250 g, were obtained from the Center of Experimental

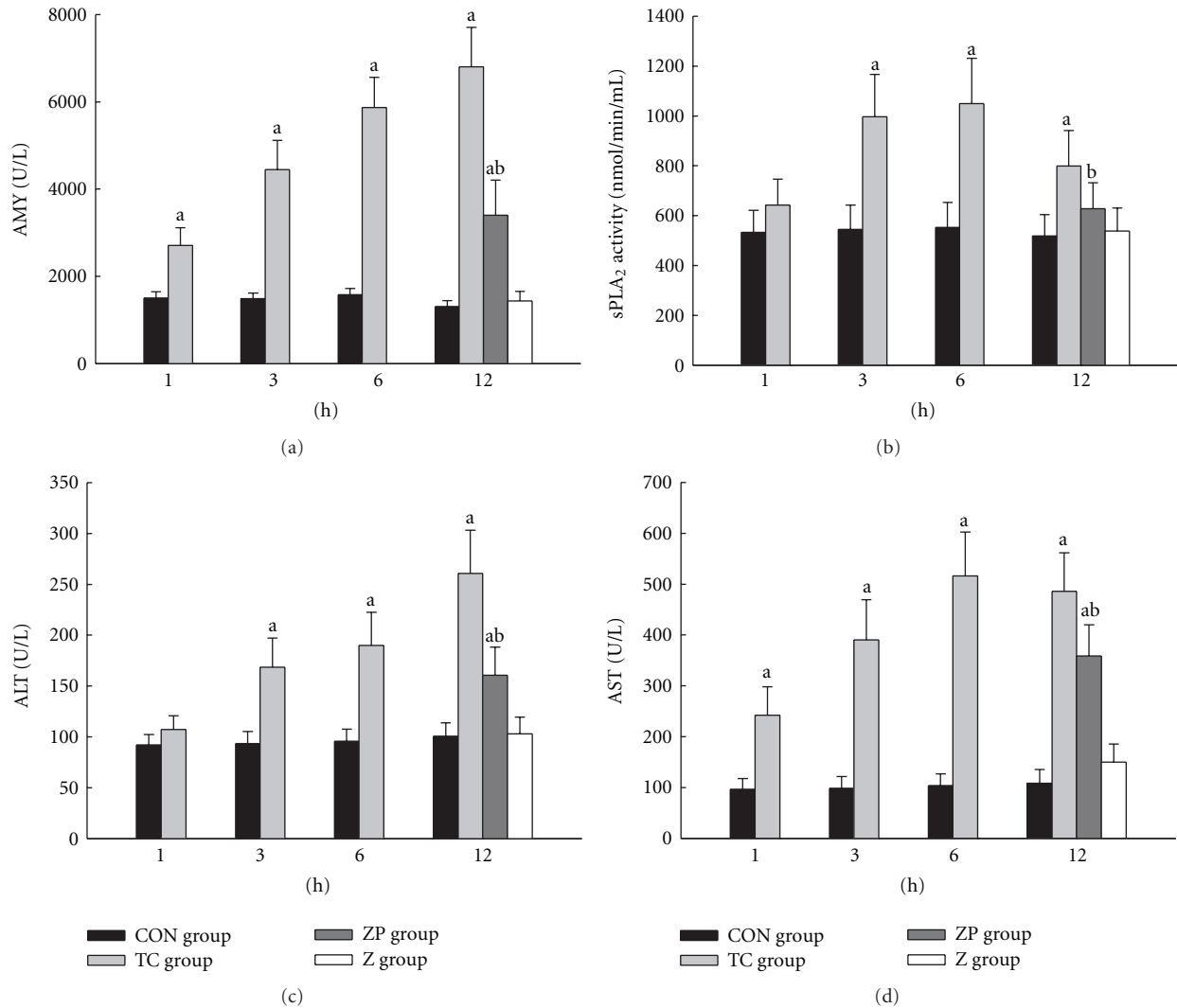


FIGURE 1: (a) Levels of serum amylase (AMY), (c) alanine aminotransferase (ALT), and (d) glutamic oxalacetic transaminase (AST) were measured by an automatic biochemistry analyzer with standard techniques (Olympus Optical Ltd., Japan); (b) serum secretory phospholipase A₂ (sPLA₂) activity was measured by sPLA₂ Assay Kit according to the manufacturer's instructions. ^a $P < 0.05$ versus CON group. ^b $P < 0.05$ versus TC group.

Animals of Hubei Academy of Medical Sciences, Wuhan, China. The animals were kept at room temperature and 12 h light-dark cycles, and with free access to water. Rats in this study were maintained in accordance with the principles of the 1983 Declaration of Helsinki by the Ethics Committee of Wuhan University. Zerumbone (purity > 99%) was obtained from Kingherb's company (Hainan, China). Sodium taurocholate and dimethyl sulfoxide (DMSO) were purchased from Sigma Aldrich Company (St. Louis, MO). Primers were designed and synthesized by Invitrogen Corporation (Carlsbad, CA).

2.2. Induction of Acute Necrotizing Pancreatitis. Rats were fasted overnight and given fresh tap water ad libitum. Anesthesia was administered by intraperitoneal injection of 10% chloralhydrat (3 mL/kg). The pancreatic bile duct was cannulated through the duodenum. Acute necrotizing pancreatitis

was induced by a standardized retrograde infusion of a freshly prepared 5% sodium taurocholate solution (1 mg/kg) into the biliary-pancreatic duct. Isotonic saline solution (20 mL/kg) was injected into the back to compensate for fluid loss.

2.3. Experimental Design. The primary objective of a preliminary study was to obtain the optimal dose of zerumbone for preventing pancreatitis-induced hepatic injury. The second study was a formal study, which was to explore the effect of zerumbone on hepatic injury following ANP. Zerumbone was dissolved in vehicle (10% DMSO v/v) in this study.

In the preliminary study, rats were randomly divided into sham-operated group, acute necrotizing pancreatitis group, and zerumbone-pretreated subgroups ($n = 8$ per group) (Table 1). Zerumbone was injected via femoral vein at various doses (5, 10, 20, and 40 mg/kg) in zerumbone

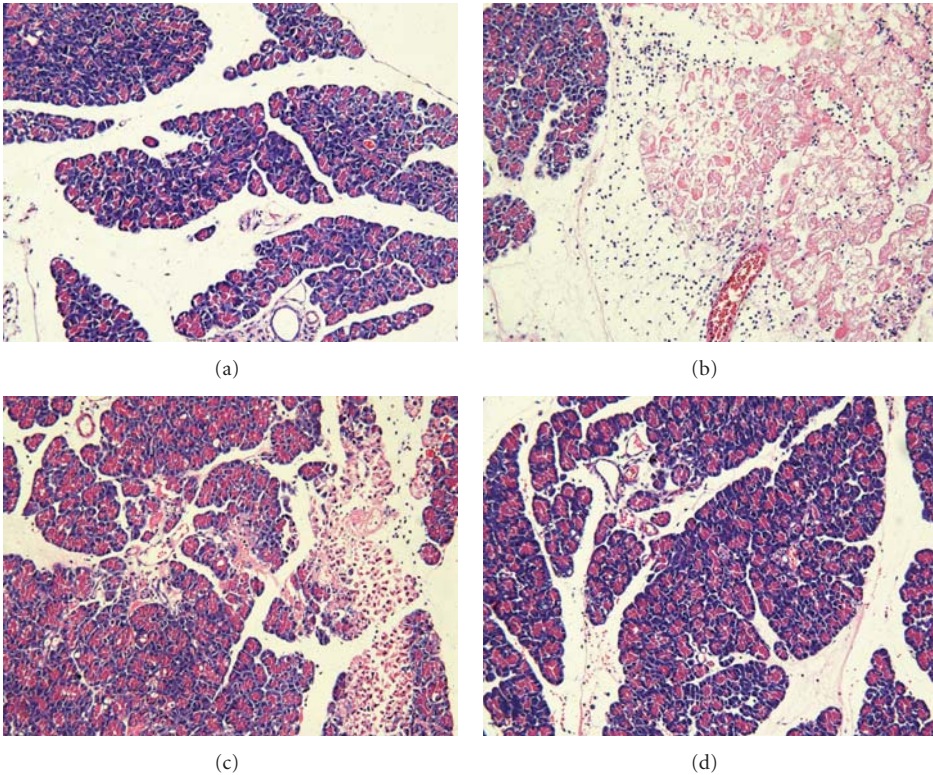


FIGURE 2: Morphologic changes in pancreatic tissue at 12 h. Representative hematoxylin/eosin-stained sections were examined by light microscopy (original magnification: 200x). (a) The CON group, (b) The TC group, (c) The ZP group, and (d) The Z group.

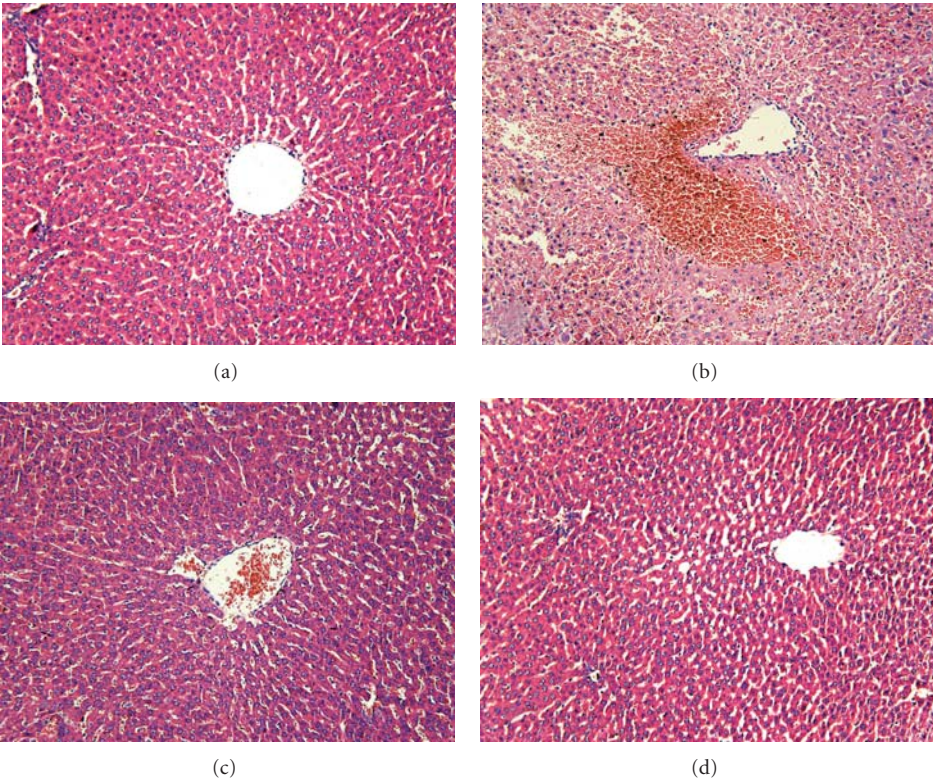


FIGURE 3: Morphologic changes in hepatic injury at 12 h. Representative hematoxylin/eosin-stained sections were examined by light microscopy (original magnification: 200x). (a) The CON group, (b) The TC group, (c) The ZP group, and (d) The Z group.

TABLE 1: Experimental design of the preliminary research.

Group	n	Time		
		−0.5 h	0 h	12 h
Sham-operated group	8	Vehicle (10% DMSO)	Saline	Sacrifice
Acute necrotizing pancreatitis group	8	Vehicle (10% DMSO)	Taurocholate	Sacrifice
Zerumbone pretreated group 5 mg/kg	8	Zerumbone 5 mg/kg	Taurocholate	Sacrifice
Zerumbone pretreated group 10 mg/kg	8	Zerumbone 10 mg/kg	Taurocholate	Sacrifice
Zerumbone pretreated group 20 mg/kg	8	Zerumbone 20 mg/kg	Taurocholate	Sacrifice
Zerumbone pretreated group 40 mg/kg	8	Zerumbone 40 mg/kg	Taurocholate	Sacrifice

In acute necrotizing pancreatitis group, rats received the vehicle (10% DMSO, 2 mL/kg) administered via femoral vein half an hour prior to retrograde infusion of a freshly prepared 5% sodium taurocholate solution (1 mg/kg). In sham-operated group, rats received the vehicle administered via femoral vein and after half an hour, the rats were retrograde infused isotonic saline solution (1 mL/kg). In zerumbone pretreated group, rats received 5, 10, 20, and 40 mg/kg zerumbone dissolved in vehicle (10% DMSO v/v) administered via femoral vein half an hour prior to infusion 5% sodium taurocholate solution (1 mg/kg).

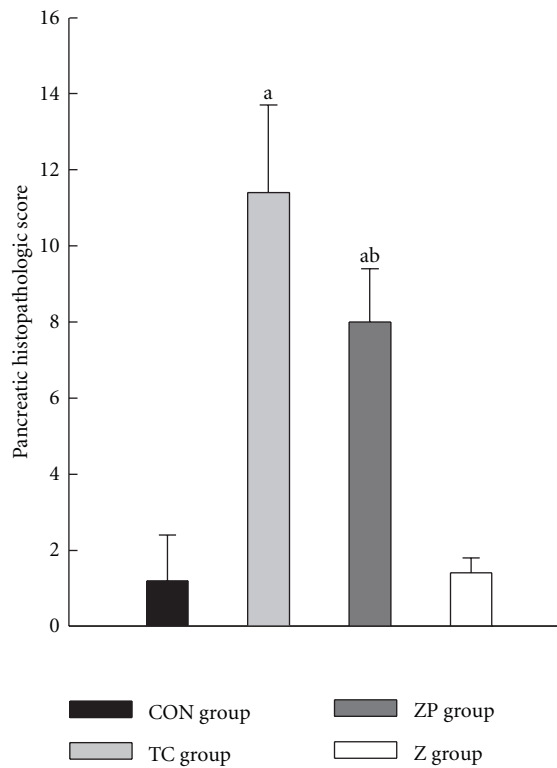


FIGURE 4: Pancreatic histopathological scores in all groups. The pancreatic tissue was with hematoxylin-eosin staining. The sections were evaluated by two independent pathologists who were blinded to this research. Time course changes of the pancreatic histological assessment were scored based on edema, inflammation, hemorrhage, and necrosis according to the scale described by Schmidt et al. [19]. ^a $P < 0.05$ versus CON group. ^b $P < 0.05$ versus TC group.

pretreated group rats. After half an hour of injecting, acute necrotizing pancreatitis was induced by retrograde infusion 5% sodium taurocholate solution. In sham-operated group, infusion isotonic saline solution instead of taurocholate. All rats were sacrificed at 12 h after induction of pancreatitis because intrapancreatic damage reached a peak [20]. The effect of zerumbone was evaluated by the levels of serum amylase (AMY), secretory phospholipase A₂ (sPLA₂), and

alanine aminotransferase (ALT), which had been described before [18].

In the formal study, 10 mg/kg zerumbone was adopted as the optimal dose. 160 male Wistar rats were randomly divided into four groups: (1) taurocholate + vehicle group (TC group, $n = 64$); (2) saline + vehicle as the control group (CON group, $n = 64$); (3) taurocholate + zerumbone group (ZP group, $n = 16$); (4) saline + zerumbone group (Z group, $n = 16$). In the TC group, rats received vehicle (10% DMSO, 2 mL/kg) via femoral vein, half an hour prior to 5% sodium taurocholate infusion. In the CON group, rats only received the vehicle. In the ZP group, rats received 10 mg/kg zerumbone dissolved in the vehicle (10% DMSO v/v). In the Z group, rats received the zerumbone and saline (Table 2). In the ZP and Z groups, rats were only at the time point of 12 h ($n = 16$). Furthermore, in the TC and CON groups, rats were subdivided into subgroups of 1, 3, 6, and 12 h ($n = 16$) (Table 2).

For each group of the two studies, rats were sacrificed by taking blood via heart puncture. Blood samples were collected for centrifuging, and serum was stored at -20°C . After sacrifice, the head of the pancreatic tissue and the right lobe of hepatic tissue were harvested and fixed in 4% PBS-buffered formaldehyde for histopathology observation. The remaining part of the pancreatic and hepatic tissues were immediately snap frozen in liquid nitrogen and stored at -80°C for assay.

2.4. Enzyme Assay. Plasma amylase (AMY), alanine aminotransferase (ALT), and aspartate transaminase (AST) were measured by an automatic biochemistry analyzer with standard techniques (Olympus Optical Ltd., Japan). Serum sPLA₂ activity was measured by sPLA₂ Assay Kit according to the manufacturer's instructions (Ann Arbor, MI).

2.5. Histopathological Examination. Pancreatic and hepatic tissues were fixed, subjected to conventional processing and sectioning, followed by hematoxylin-eosin (H&E) staining. The sections were evaluated by two pathologists who were blinded to this study. Pancreatic histological assessment was determined by edema, inflammation, hemorrhage, and necrosis according to the scale described by Schmidt et al. [19].

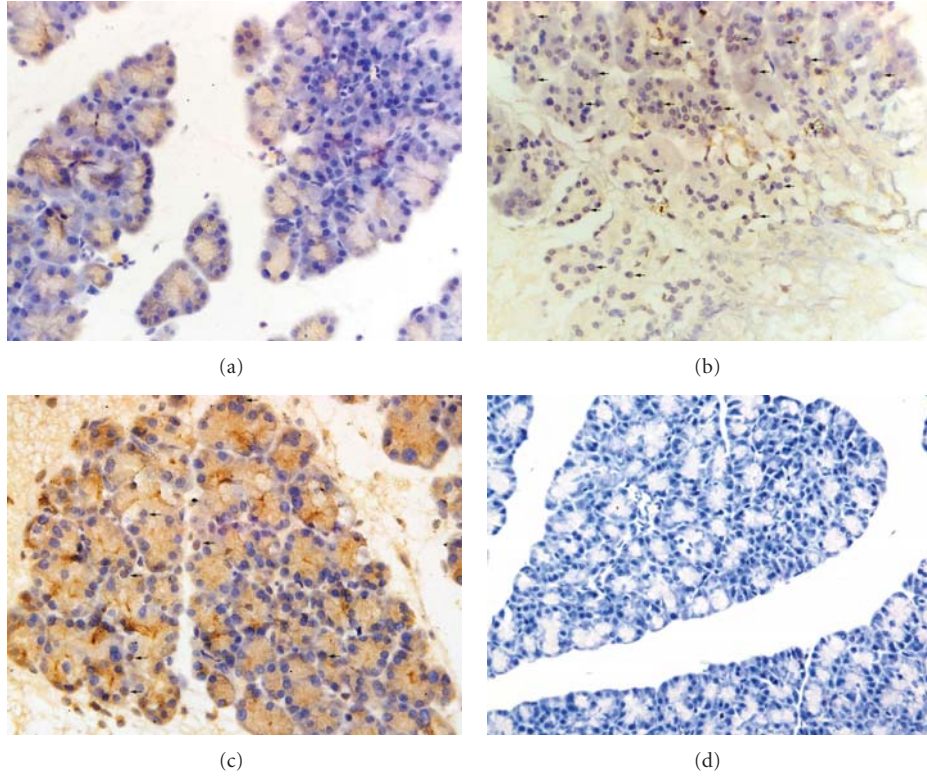


FIGURE 5: Cellular localization of NF- κ B p65 protein in pancreas in different groups (original magnification: 400x). (a) In the CON group, weak immunoreactivity mainly in the cytoplasm. (b) In the TC group, intense immunoreactivity in the nucleus. (c) In the ZP group, low immunoreactivity in the nucleus. (d) Negative control.

TABLE 2: Experimental design of the formal study.

Group	Time					
	-0.5 h	0 h	1 h	3 h	6 h	12 h
CON	Vehicle (10% DMSO)	Saline	Sacrifice ($n = 16$)	Sacrifice ($n = 16$)	Sacrifice ($n = 16$)	Sacrifice ($n = 16$)
TC	Vehicle (10% DMSO)	Taurocholate	Sacrifice ($n = 16$)	Sacrifice ($n = 16$)	Sacrifice ($n = 16$)	Sacrifice ($n = 16$)
ZP	Zerumbone 10 mg/kg	Taurocholate				Sacrifice ($n = 16$)
Z	Zerumbone 10 mg/kg	Saline				Sacrifice ($n = 16$)

In the TC group, rats received the vehicle (10% DMSO, 2 mL/kg) administered via femoral vein half an hour prior to retrograde infusion of a freshly prepared 5% sodium taurocholate solution (1 mg/kg). In the CON group, rats received the vehicle administered via femoral vein. After half an hour, the rats were retrograde infused isotonic saline solution (1 mL/kg). In the ZP group, rats received 10 mg/kg zerumbone dissolved in vehicle (10% DMSO v/v) administered via femoral vein half an hour prior to infusion 5% sodium taurocholate solution (1 mg/kg). In the Z group, rats received the same as ZP group except infusion isotonic saline solution instead of taurocholate.

The severity of hepatic injury was determined by a point-counting method description by Camargo et al. [21].

2.6. Immunohistochemistry Assay. Pancreatic-tissue sections (4 μ m) were obtained from paraffin-embedded tissues. Under deparaffinization, 0.3% (v/v) hydrogen peroxide was used to inactivate endogenous peroxidase activity. The sections underwent a blocking step with 5% normal goat serum diluted in PBS. Endogenous biotin and avidin binding sites were blocked by avidin and biotin, respectively. Sections were incubated with rabbit polyclonal anti-rat NF- κ B p65 antibody (1 : 200, Sigma, St. Louis, MO) in a moisture chamber. Sections were then counterstained with hematoxylin.

Negative control studies were performed in which PBS was used instead of primary antibody.

2.7. Western Blot. Proteins (including cytoplasmic and nuclear proteins) were extracted by the Nuclear-Cytosol Extraction Kit (Applygen Technologies Inc., Beijing, China), followed by manufacturer's instructions. Proteins were evaluated by the Bradford method with bovine serum albumin as a standard. 40 mg protein samples were electrophoresed in 8% sodium dodecylsulphate polyacrylamide (SDS-PAGE) gels and transferred to nitrocellulose membranes. Membranes were blocked with blocking buffer (TBS containing 5% non-fat dry milk, 0.1% Tween-20) for 2 h at room temperature.

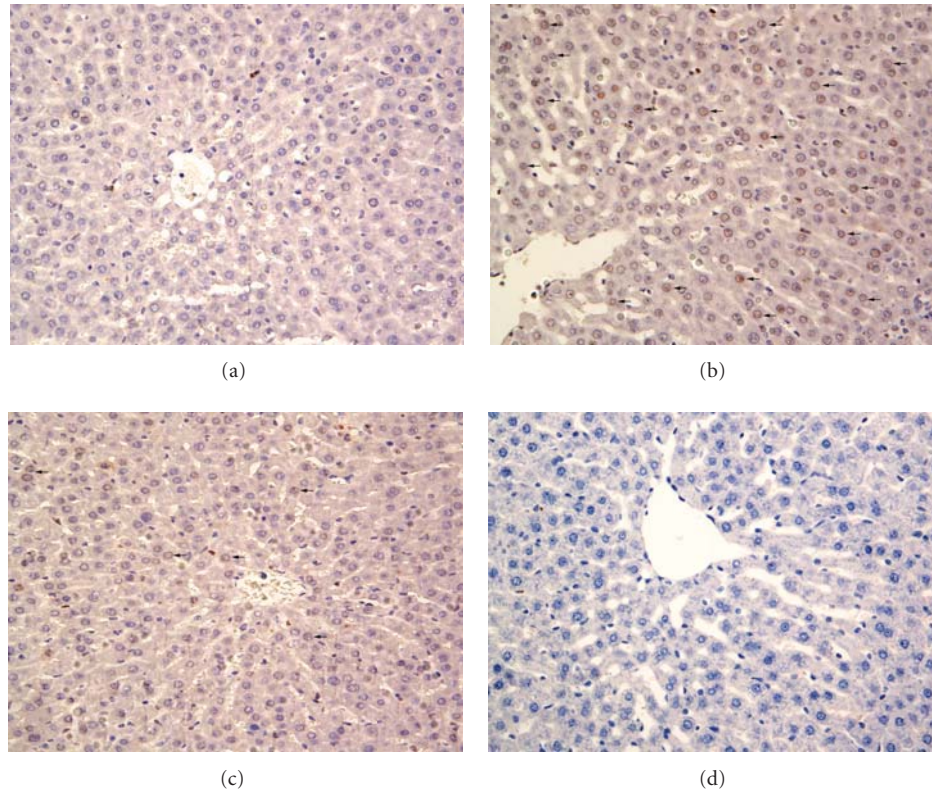


FIGURE 6: Cellular localization of NF- κ B p65 protein in hepatic tissue in different groups (original magnification: 400x). (a) In the CON group, weak immunoreactivity mainly in the cytoplasm. (b) In the TC group, intense immunoreactivity in the nucleus. (c) In the ZP group, low immunoreactivity in the nucleus. (d) Negative control.

The cytoplasmic proteins were incubated with primary antibodies of rabbit polyclonal anti-rat I- κ B α antibody (1:1000, Santa Cruz, CA), actin antibody (1:2000, Santa Cruz, CA). Meanwhile, the nuclear proteins were incubated with rabbit polyclonal anti-rat NF- κ B p65 antibody (1:2000, Sigma, St. Louis, MO) and actin antibody (1:2000, Santa Cruz, CA) overnight at 4°C. The membrane was washed with TBST (TBS containing 0.05% Tween-20) and then incubated with horseradish peroxidase-conjugated goat anti-rabbit secondary antibodies (1:5000, Pierce Biotechnology, Rockford, IL) for 1 h at room temperature. After repeated washings with TBST, the antibody-antigen complexes were detected by ECL reagent (Immobilon Western HRP Substrate, Millipore Corporation, Bedford, MA).

2.8. Reverse Transcriptase Polymerase Chain Reaction (RT-PCR). Total RNA was extracted from one hundred milligram frozen pancreatic and hepatic tissues. RNA was reverse-transcribed to complementary DNA according to the manufacturer's instructions of Revert Aid First Strand cDNA Synthesis Kit (Fermentas, Hanover, MD). Polymerase chain reaction was performed with the primers for intercellular adhesion molecule-1 (ICAM-1) (F: CGGTAG-ACACAAGCAAGAGA; R: GCAGGGATTGACCATAATTT; 517 bp; NM-012967); interleukin-1 β (IL-1 β) (F: CCAGGAT-GAGGACCCAAGCA; R: TCCCGACCATTTGCTGTTTCC; 519 bp; NM-031512); glyceraldehyde-3-phosphate dehydro-

genase (GAPDH) (F: TCATGAAGTGTGACGTGGACATC; R: CAGGAGGAGCAATGATCTTGATCT; 309 bp; NM-017008). PCR was performed by using a Gene Cyclyer (Bio-Rad, Hercules, CA). Amplification steps were ICAM-1 (initial denaturation 94°C 5 min, then denaturation 94°C 30 sec, annealing 56°C 30 sec, extension 72°C 1 min for 35 cycles, final extension 72°C 7 min); IL-1 β (initial denaturation 94°C 5 min, then denaturation 95°C 30 sec, annealing 63°C 45 sec, extension 72°C 35 sec for 35 cycles, final extension 72°C 7 min); GAPDH (initial denaturation 94°C 5 min, then denaturation 94°C 30 sec, annealing 55°C 30 sec, extension 72°C 80 sec for 35 cycles, final extension 72°C 7 min). PCR products were electrophoresed in 2% agarose gel containing ethidium bromide (0.5 mg/mL). Gels were under UV light and then photographed. Band intensity was determined by optical density with PCR product/GAPDH ratios.

2.9. Statistical Analysis. All data were expressed as means \pm standard deviation values. Data were compared between all groups by one-way analysis of variance (ANOVA) except hepatic histopathological examination, which was analyzed by Kruskal-Wallis nonparametric test, followed by Mann-Whitney test. Statistical analysis was performed with the SPSS statistical package (SPSS 13.0 for Windows; SPSS Inc., Chicago, IL). A value of $P < 0.05$ was regarded as a significant difference.

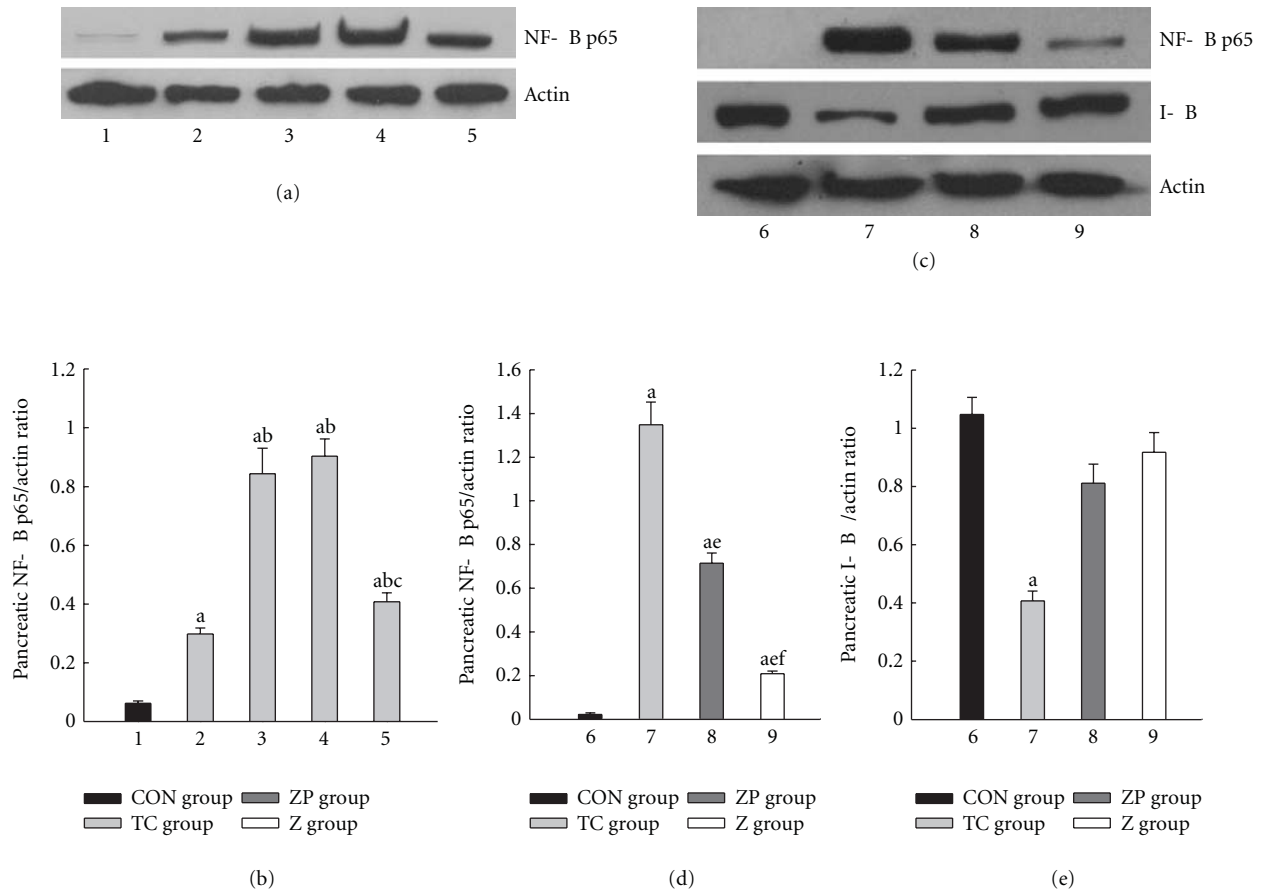


FIGURE 7: Expression of NF-κB p65 and I-κBα in pancreatic tissue. 1, 6 CON group; 2, TC group 1 h; 3, TC group 3 h; 4, TC group 6 h; 5, 7 TC group 12 h; 8, ZP group; 9, Z group. ^a $P < 0.05$ versus CON group. ^b $P < 0.05$ versus TC group 1 h. ^c $P < 0.05$ versus TC group 3 h. ^d $P < 0.05$ versus TC group 6 h. ^e $P < 0.05$ versus TC group 12 h. ^f $P < 0.05$ versus ZP group.

3. Results

3.1. Preliminary Study Results. The results indicated that neither 5 mg/kg nor 40 mg/kg zerumbone improve serum sPLA₂ and ALT levels. Compared to 20 mg/kg, concentration of 10 mg/kg has already shown significant reduction of sPLA₂ and ALT levels ($P < 0.05$) (Table 3).

3.2. Analysis of Serum AMY, sPLA₂, ALT, and AST. Compared with the CON group, the TC group had significant increased serum AMY, sPLA₂, ALT, and AST levels from 1 h to 12 h ($P < 0.05$) except for 1 h sPLA₂ and ALT. In the ZP group, pretreatment with zerumbone significantly reduced serum enzyme levels compared with the TC group ($P < 0.05$). In Z group, all serum enzyme levels were not significant compared with the CON group (Figures 1(a)–1(d)).

3.3. Histopathological Assay. Representative pathological changes in pancreatic tissue were shown in Figures 2(a)–2(d). Injuries were estimated by Schmidt's description including edema, inflammation, hemorrhage, and necrosis [19]. The pancreatic microscopy was similar among the CON subgroups exhibiting no hemorrhage or necrosis. In the TC group, 5% sodium taurocholate promoted the destruction

of acinar cell. However, pretreatment with zerumbone decreased the pancreatic histopathological score clearly in the ZP group (Figure 4).

The change in hepatic sections was determined by Camargo's description [21]. There were four grades: grade 0: minimal or no evidence of injury; grade I: mild injury consisting in cytoplasmic vacuolation and focal nuclear pyknosis; grade II: moderate to severe injury with extensive nuclear pyknosis, cytoplasmic hypereosinophilia, and loss of intercellular borders; grade III: severe necrosis with disintegration of hepatic cords, hemorrhage, and neutrophil infiltration. Pathological changes in hepatic tissue were shown in Figures 3(a)–3(d). In the TC group, 5% sodium taurocholate had destroyed most of the liver cells and caused obvious bleeding. However, the hepatic pathological grade reduced to a much lower level by pretreatment with zerumbone in the ZP group (Table 4).

3.4. Immunohistochemistry Analysis. In performing the localization of NF-κB expression, immunohistochemical assay was used. There were no significant changes in the immunoreactivity of NF-κB in the CON group. NF-κB expression was expressed mainly in the cytoplasm in pancreatic or hepatic tissue (Figures 5(a), 6(a)). Following pancreatitis, NF-κB

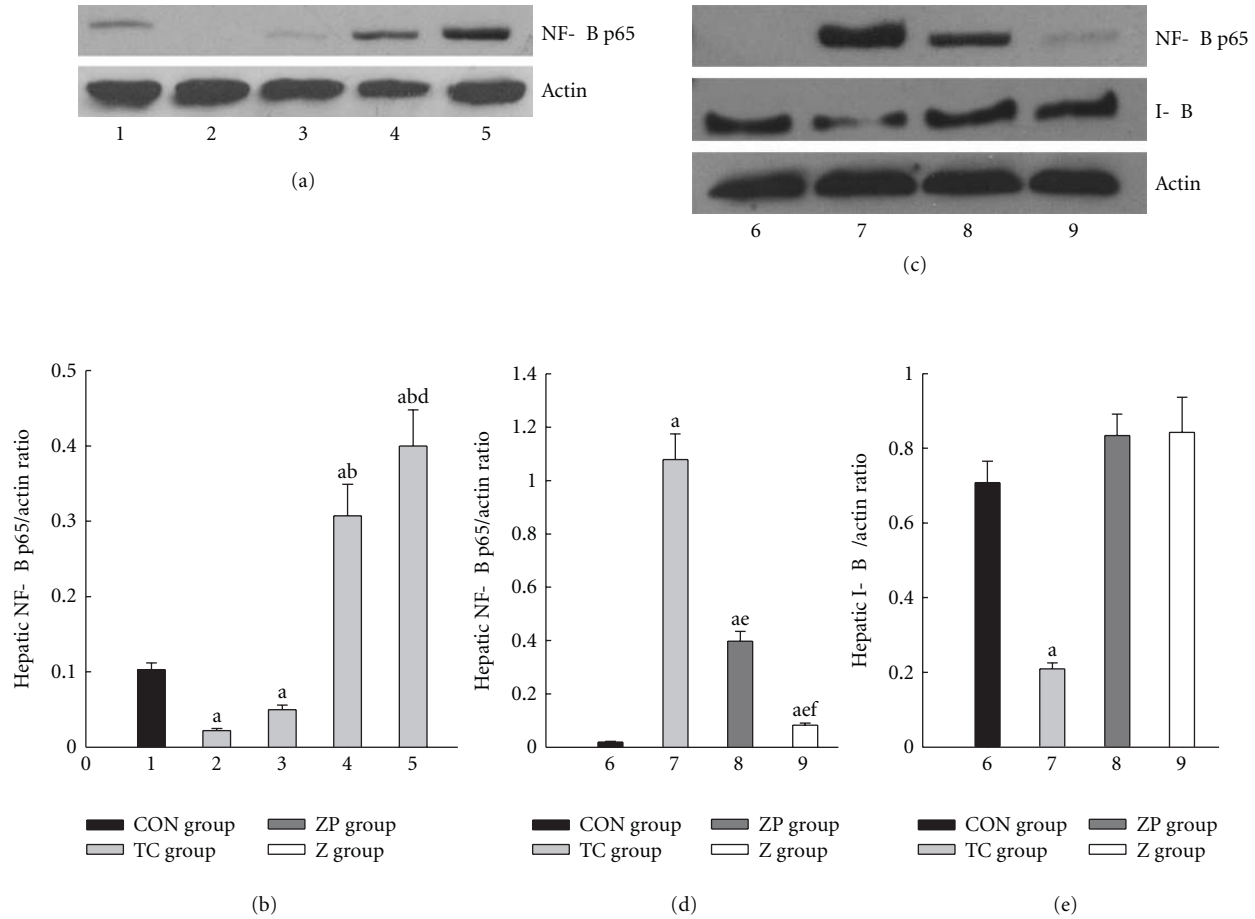


FIGURE 8: Expression of NF- κ B p65 and I- κ B α in hepatic tissue. 1, 6 CON group; 2, TC group 1 h; 3, TC group 3 h; 4, TC group 6 h; 5, 7 TC group 12 h; 8, ZP group; 9, Z group. ^a $P < 0.05$ versus CON group. ^b $P < 0.05$ versus TC group 1 h. ^c $P < 0.05$ versus TC group 3 h. ^d $P < 0.05$ versus TC group 6 h. ^e $P < 0.05$ versus TC group 12 h. ^f $P < 0.05$ versus ZP group.

TABLE 3: Preliminary study results of different doses of zerumbone.

Group	<i>n</i>	AMY (U/L)	sPLA ₂ (U/L)	ALT (U/L)
Sham-operated group	8	1304.8 ± 114.7	519.7 ± 63.9	95.7 ± 7.9
Acute necrotizing pancreatitis group	8	6774.8 ± 739.0 ^a	789.0 ± 124.2 ^a	257.6 ± 41.7 ^a
Zerumbone pretreated group 5 mg/kg	8	5279.5 ± 857.4 ^{a,b}	775.5 ± 160.9 ^a	230.1 ± 50.4 ^a
Zerumbone pretreated group 10 mg/kg	8	3342.6 ± 542.4 ^{a,b,c}	621.7 ± 73.8	157.5 ± 31.2 ^{a,b}
Zerumbone pretreated group 20 mg/kg	8	3440.9 ± 575.9 ^{a,b,c}	625.9 ± 108.9	181.7 ± 30.3 ^{a,b}
Zerumbone pretreated group 40 mg/kg	8	3073.7 ± 461.5 ^{a,b,c}	667.0 ± 108.2 ^a	245.8 ± 30.5 ^a

Rats from different groups were ended at 12 h after sodium taurocholate infusion. The serum amylase (AMY), secretory phospholipase A₂ (sPLA₂), and alanine aminotransferase (ALT) in serum was measured by an automatic biochemistry analyzer with standard techniques (Olympus Optical Ltd., Japan). Data were expressed as means ± standard error values. ^a $P < 0.05$ versus sham-operated group. ^b $P < 0.05$ versus acute necrotizing pancreatitis group. ^c $P < 0.05$ versus zerumbone pretreated group 5 mg/kg.

immunoreactivity highly expressed in nucleus (Figures 5(b), 6(b)). However, a marked decrease in NF- κ B staining was found in the nucleus with the zerumbone pretreatment (Figures 5(c), 6(c)), but increase in the cytoplasm. Moreover, negative control showed no immunoreactivity (Figures 5(d), 6(d)).

3.5. NF- κ B p65 and I- κ B α Expression. Figures 7(a)-7(b) showed peak expression of NF- κ B p65 protein in pancreas

occurred at 3 h, duration to 6 h, decreased at 12 h in the TC group, which was higher than in the CON group. In the ZP group, the NF- κ B p65 expression declined to a much lower level than in the TC group ($P < 0.05$) (Figures 7(c)-7(d)). Moreover, only TC group showed a significant decrease of I- κ B α expression (Figure 7(e)).

Hepatic NF- κ B expression increased gradually after induction of pancreatitis in the TC group and the peak expression occurred at 12 h (Figures 8(a)- 8(b)). Figures 8(c)-8(d)

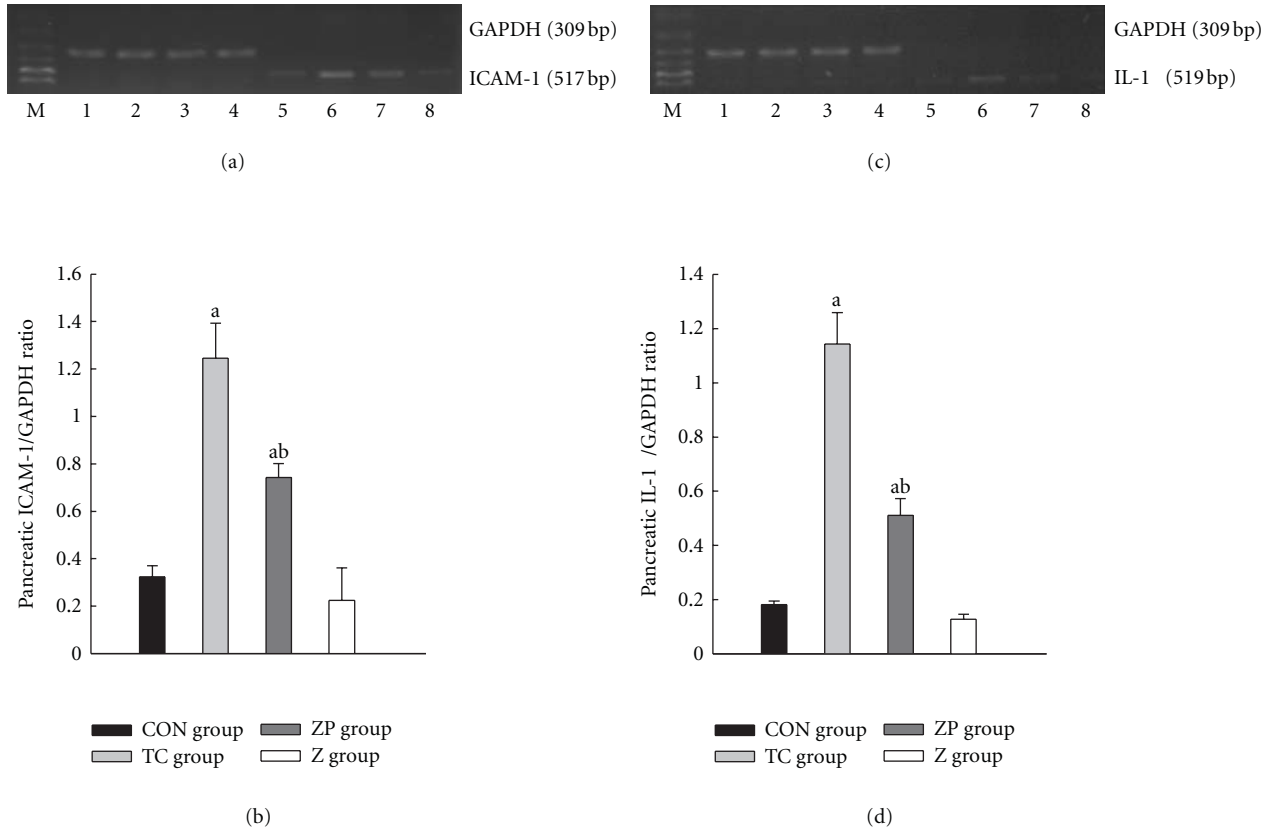


FIGURE 9: Expression of ICAM-1 and IL-1 β mRNA in pancreatic tissue by RT-PCR analysis. 1–4 GAPDH; 5, CON group; 6, TC group 12 h; 7, ZP group; 8, Z group. ^a $P < 0.05$ versus CON group. ^b $P < 0.05$ versus TC group 12 h.

TABLE 4: Hepatic pathological grades with sodium taurocholate-induced pancreatitis.

Group	<i>n</i>	Grade				Mean rank
		0	1	2	3	
CON group	12	12	0	0	0	10.5
TC group	12	0	1	1	10	40.7 ^a
ZP group	12	0	4	6	2	31.5 ^{ab}
Z group	12	8	3	1	0	15.8

Rats from different groups were ended at 12 h after sodium taurocholate infusion. The sections were evaluated by two independent pathologists who were blinded to this research. The change of hepatic sections was detected by Camargo's description [21]. Each value is the number of animals with grading changes. ^a $P < 0.05$ versus CON group. ^b $P < 0.05$ versus TC group.

showed that the expression of NF- κ B p65 protein in the ZP group was lower than in the TC group. Furthermore, only TC group showed a significant decrease of hepatic I- κ B α expression (Figure 8(e)).

3.6. ICAM-1 and IL-1 β mRNA Expression. In this study, expressions of ICAM-1 and IL-1 β in pancreas were found to be much higher than in the CON group ($P < 0.05$) (Figures 9(a)–9(d)). However, these mRNA expressions were much lower in the ZP group than in the TC group ($P < 0.05$) (Figures 9(a)–9(d)). The tendencies of these mRNA

expressions in hepatic tissue (Figures 10(a)–10(d)) were the same as in pancreas.

4. Discussion

Zerumbone, as a component of a wild ginger, was first isolated and structurally elucidated forty years ago [22]. It has been widely used in experiments by virtue of its anti-neoplasms and anti-inflammatory properties [13, 15]. This study was to discuss the alleviating effect of zerumbone on hepatic injury following acute necrotizing pancreatitis.

In the preliminary study, the 12 h time point was chosen after pancreatitis was induced when intrapancreatic damage had already peaked during pancreatitis [20, 23]. It indicated that all concentrations of zerumbone injected via femoral vein had the ability to attenuate serum AMY. However, only 10 and 20 mg/kg zerumbone could decrease serum sPLA2 and ALT. Therefore, the minimum effective dose (optimal dose) was 10 mg/kg. It had been reported that doses of 0.1, 1, 10, 20, and 100 mg/kg zerumbone were tested on Wistar rats via intraperitoneal injection following cholecystokinin octapeptide-induced pancreatitis. The dose of 20 mg/kg zerumbone was the optimal dose [18]. Another study used male ICR mice, receiving intraperitoneal injection of zerumbone (5, 10, 50, and 100 mg/kg) to estimate the effect of zerumbone on paw edema, granuloma, and toxicity

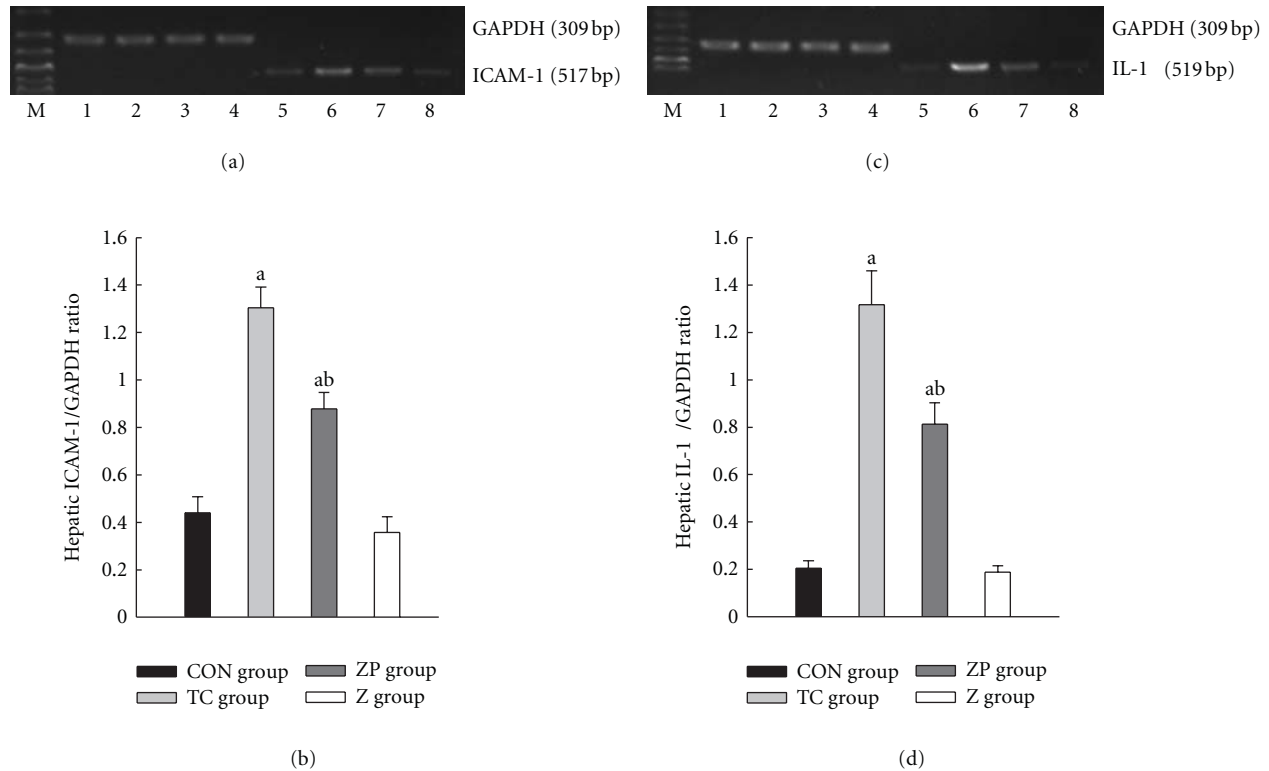


FIGURE 10: Expression of ICAM-1 and IL-1 β mRNA in hepatic tissue by RT-PCR analysis. 1–4 GAPDH; 5, CON group; 6, TC group 12 h; 7, ZP group; 8, Z group. ^a $P < 0.05$ versus CON group. ^b $P < 0.05$ versus TC group 12 h.

test. It was demonstrated that all zerumbone doses could suppress granulomatous tissue formation in cotton pellet-induced granuloma test [24].

The increased AMY and sPLA₂ levels in the TC group and the elevated histopathological score of pancreas [25] indicated that pancreas injury deteriorated gradually following ANP. Moreover, the increased AMY and sPLA₂ levels advocated the theory of autodigestion of pancreas. [26]. In the TC group, increased ALT and AST levels and hepatic histological examination also showed the damage of hepatic injury from bad to worse [27]. Is there any relationship between the changes in pancreatic and hepatic tissues?

Previous researches showed that the active RelA/p65 NF- κ B subunit played an essential role in systemic inflammatory response in pancreatitis [28–30]. Cytoplasmic I κ B proteins were primary regulators interacting with NF- κ B subunits in the cytoplasm of normal cells [31–33]. Upon stimulation, these I κ B proteins were rapidly degraded, allowing NF- κ B translocate into nucleus and activate the transcription of related genes: ICAM-1 and IL-1 β [34–36]. Other studies showed that downregulation of NF- κ B not only inhibited ICAM-1 and IL-1 β expression, but also attenuated pancreatic and hepatic injury in pancreatitis [35–37].

The result of immunohistochemistry assay indicated that NF- κ B has been shown to translocate from the cytoplasm into the nucleus upon activation in pancreatic or hepatic tissues during pancreatitis. The western blot results showed that the I- κ B α protein expression was much lower during

pancreatitis because of rapidly degradation. Pancreatic NF- κ B expression elevated from 1 h, peaked at 3 h and continued to 6 h following ANP. It is accordance with published data [38]. The peaking expression of NF- κ B in hepatic tissue was lagged behind up to 12 h following ANP. These results supported that the early phase of NF- κ B activation started from pancreas by translocating into the nucleus. Up to 12 h in ANP, the NF- κ B expression in hepatic tissue was strong due to the inflammatory cascade. The multiple organ dysfunction syndromes may occur relying on the NF- κ B inflammatory cascade, if longer or more organs were applied. However, the peaking expression of NF- κ B in hepatic tissue lagged behind in pancreas, thus the period from 3 h to 12 h following ANP was defined as “window period,” which was the potential period for hepatic protection.

It was reported that zerumbone exerted a beneficial effect on inflammation but failed to improve histology [18]. Furthermore, published data indicated that administration of zerumbone could decrease NF- κ B p65 expression [14, 39–41]. Triptolide as well as zerumbone, was a crude plant extract and could attenuate hepatic injury and inhibit NF- κ B activation [42]. Western blot and immunohistochemistry assay in this study showed that zerumbone inhibited NF- κ B activation and decreased ICAM-1 and IL-1 β mRNA expression. The serum assay and the changes in histopathological examination indicated that zerumbone attenuated the severity of acute necrotizing pancreatitis and pancreatitis-induced hepatic injury.

In summary, this work suggests that zerumbone attenuates the severity of acute necrotizing pancreatitis and pancreatitis-induced hepatic injury, through inhibiting NF- κ B activation and downregulation of intercellular adhesion molecule-1 and Interleukin-1 β . However, its complete molecular mechanism still remains unclear. These works can serve as a basis for further studies on the therapeutic potential of zerumbone in acute necrotizing pancreatitis.

Authors' Contributions

D. Wenhong and Y. Jia contributed equally to this paper.

Acknowledgments

This paper is supported by NSFC (no. 81070368), Program Foundation for the Basic Research and Operating of Central institutions (no. 4104003), and Scientific and Technological Project of Wuhan city (no. 201060938363-01). The authors completed the work at the Laboratory Animal Center, the Institute for Gastroenterology and Hepatology, and the Central Laboratory, Renmin Hospital of Wuhan University. They are grateful to Mr. Hong Xia and Ms. Qing He for their technical support and great help during their study.

References

- [1] R. M. S. Mitchell, M. F. Byrne, and J. Baillie, "Pancreatitis," *The Lancet*, vol. 361, no. 9367, pp. 1447–1455, 2003.
- [2] E. Vaquero, I. Gukovsky, V. Zaninovic, A. S. Gukovskaya, and S. J. Pandol, "Localized pancreatic NF- κ B activation and inflammatory response in taurocholate-induced pancreatitis," *American Journal of Physiology*, vol. 280, no. 6, pp. G1197–G1208, 2001.
- [3] R. Yang, A. L. Shaufl, M. E. Killeen, and M. P. Fink, "Ethyl pyruvate ameliorates liver injury secondary to severe acute pancreatitis," *Journal of Surgical Research*, vol. 153, no. 2, pp. 302–309, 2009.
- [4] Y. Hori, Y. Takeyama, T. Ueda, M. Shinkai, K. Takase, and Y. Kuroda, "Macrophage-derived transforming growth factor- β 1 induces hepatocellular injury via apoptosis in rat severe acute pancreatitis," *Surgery*, vol. 127, no. 6, pp. 641–649, 2000.
- [5] M. Dobosz, S. Hac, L. Mionskowska, D. Dymecki, S. Dobrowolski, and Z. Wajda, "Organ microcirculatory disturbances in experimental acute pancreatitis. A role of nitric oxide," *Physiological Research*, vol. 54, no. 4, pp. 363–368, 2005.
- [6] Y. Shen, N. Cui, B. Miao, and E. Zhao, "Immune dysregulation in patients with severe acute pancreatitis," *Inflammation*, vol. 34, no. 1, pp. 36–42, 2011.
- [7] T. Kitayama, R. Nagao, T. Masuda et al., "The chemistry of zerumbone IV: asymmetric synthesis of Zerumbol," *Journal of Molecular Catalysis B*, vol. 17, no. 2, pp. 75–79, 2002.
- [8] B. Sung, S. Jhurani, K. S. Ahn et al., "Zerumbone down-regulates chemokine receptor CXCR4 expression leading to inhibition of CXCL12-induced invasion of breast and pancreatic tumor cells," *Cancer Research*, vol. 68, no. 21, pp. 8938–8944, 2008.
- [9] M. Kim, S. Miyamoto, Y. Yasui, T. Oyama, A. Murakami, and T. Tanaka, "Zerumbone, a tropical ginger sesquiterpene, inhibits colon and lung carcinogenesis in mice," *International Journal of Cancer*, vol. 124, no. 2, pp. 264–271, 2009.
- [10] A. Murakami, M. Miyamoto, and H. Ohigashi, "Zerumbone, an anti-inflammatory phytochemical, induces expression of proinflammatory cytokine genes in human colon adenocarcinoma cell lines," *Biofactors*, vol. 21, no. 1–4, pp. 95–101, 2004.
- [11] A. Murakami, T. Tanaka, J. Y. Lee et al., "Zerumbone, a sesquiterpene in subtropical ginger, suppresses skin tumor initiation and promotion stages in ICR mice," *International Journal of Cancer*, vol. 110, no. 4, pp. 481–490, 2004.
- [12] Y. Nakamura, C. Yoshida, A. Murakami, H. Ohigashi, T. Osawa, and K. Uchida, "Zerumbone, a tropical ginger sesquiterpene, activates phase II drug metabolizing enzymes," *FEBS Letters*, vol. 572, no. 1–3, pp. 245–250, 2004.
- [13] A. Murakami, R. Hayashi, T. Tanaka, K. H. Kwon, H. Ohigashi, and R. Safitri, "Erratum: suppression of dextran sodium sulfate-induced colitis in mice by zerumbone, a subtropical ginger sesquiterpene, and nimesulide: separately and in combination," *Biochemical Pharmacology*, vol. 67, no. 2, p. 395, 2004.
- [14] A. Murakami, K. Matsumoto, K. Koshimizu, and H. Ohigashi, "Effects of selected food factors with chemopreventive properties on combined lipopolysaccharide- and interferon- γ -induced I κ B degradation in RAW264.7 macrophages," *Cancer Letters*, vol. 195, no. 1, pp. 17–25, 2003.
- [15] T. Y. Chien, L. G. Chen, C. J. Lee, F. Y. Lee, and C. C. Wang, "Anti-inflammatory constituents of Zingiber zerumbet," *Food Chemistry*, vol. 110, no. 3, pp. 584–589, 2008.
- [16] A. Murakami, D. Takahashi, K. Koshimizu, and H. Ohigashi, "Synergistic suppression of superoxide and nitric oxide generation from inflammatory cells by combined food factors," *Mutation Research*, vol. 523–524, pp. 151–161, 2003.
- [17] A. Murakami, D. Takahashi, T. Kinoshita et al., "Zerumbone, a Southeast Asian ginger sesquiterpene, markedly suppresses free radical generation, proinflammatory protein production, and cancer cell proliferation accompanied by apoptosis: The α,β -unsaturated carbonyl group is a prerequisite," *Carcinogenesis*, vol. 23, no. 5, pp. 795–802, 2002.
- [18] S. Annamaria, T. Laszlo, K. Jozsef et al., "Zerumbone exerts a beneficial effect on inflammatory parameters of cholecystokinin octapeptide-induced experimental pancreatitis but fails to improve histology," *Pancreas*, vol. 35, no. 3, pp. 249–255, 2007.
- [19] J. Schmidt, D. W. Rattner, K. Lewandrowski et al., "A better model of acute pancreatitis for evaluating therapy," *Annals of Surgery*, vol. 215, no. 1, pp. 44–56, 1992.
- [20] A. S. Paszkowski, B. Rau, J. M. Mayer, P. Moller, and H. G. Beger, "Therapeutic application of caspase 1/interleukin-1 β -converting enzyme inhibitor decreases the death rate in severe acute experimental pancreatitis," *Annals of Surgery*, vol. 235, no. 1, pp. 68–76, 2002.
- [21] C. A. Camargo Jr., J. F. Madden, W. Gao, R. S. Selvan, and P. A. Clavien, "Interleukin-6 protects liver against warm ischemia/reperfusion injury and promotes hepatocyte proliferation in the rodent," *Hepatology*, vol. 26, no. 6, pp. 1513–1520, 1997.
- [22] T. Kitayama, T. Okamoto, R. K. Hill et al., "Chemistry of zerumbone—1. Simplified isolation, conjugate addition reactions, and a unique ring contracting transannular reaction of its dibromide," *Journal of Organic Chemistry*, vol. 64, no. 8, pp. 2667–2672, 1999.
- [23] S. H. Xia, D. C. Fang, C. X. Hu, H. Y. Bi, Y. Z. Yang, and Y. Di, "Effect of BN52021 on NF κ -Bp65 expression in pancreatic tissues of rats with severe acute pancreatitis," *World Journal of Gastroenterology*, vol. 13, no. 6, pp. 882–888, 2007.

- [24] M. R. Sulaiman, E. K. Perimal, M. N. Akhtar et al., "Anti-inflammatory effect of zerumbone on acute and chronic inflammation models in mice," *Fitoterapia*, vol. 81, no. 7, pp. 855–858, 2010.
- [25] S. Xu, C. Chen, W. X. Wang, S. R. Huang, J. Yu, and X. Y. Chen, "Crucial role of group IIA phospholipase A2 in pancreatitis-associated adrenal injury in acute necrotizing pancreatitis," *Pathology Research and Practice*, vol. 206, no. 2, pp. 73–82, 2010.
- [26] M. L. Kylanpaa, H. Repo, and P. A. Puolakkainen, "Inflammation and immunosuppression in severe acute pancreatitis," *World Journal of Gastroenterology*, vol. 16, no. 23, pp. 2867–2872, 2010.
- [27] X. P. Zhang, L. Zhang, Y. Wang et al., "Study of the protective effects of dexamethasone on multiple organ injury in rats with severe acute pancreatitis," *Journal of the Pancreas*, vol. 8, no. 4, pp. 400–412, 2007.
- [28] G. Telek, R. Ducroc, J. Y. Scazecz, C. Pasquier, G. Feldmann, and C. Roze, "Differential upregulation of cellular adhesion molecules at the sites of oxidative stress in experimental acute pancreatitis," *Journal of Surgical Research*, vol. 96, no. 1, pp. 56–67, 2001.
- [29] X. Chen, B. Ji, B. Han, S. A. Ernst, D. Simeone, and C. D. Logsdon, "NF- κ B activation in pancreas induces pancreatic and systemic inflammatory response," *Gastroenterology*, vol. 122, no. 2, pp. 448–457, 2002.
- [30] Y. Peng, S. F. Gallagher, K. Haines, K. Baksh, and M. M. Murr, "Nuclear factor- κ B mediates Kupffer cell apoptosis through transcriptional activation of Fas/FasL," *Journal of Surgical Research*, vol. 130, no. 1, pp. 58–65, 2006.
- [31] J. Ding, D. Song, X. Ye, and S. F. Liu, "A pivotal role of endothelial-specific NF- κ B signaling in the pathogenesis of septic shock and septic vascular dysfunction," *Journal of Immunology*, vol. 183, no. 6, pp. 4031–4038, 2009.
- [32] H. J. Lee, H. J. Lim, D. Y. Lee et al., "Carabrol suppresses LPS-induced nitric oxide synthase expression by inactivation of p38 and JNK via inhibition of I- κ B α degradation in RAW 264.7 cells," *Biochemical and Biophysical Research Communications*, vol. 391, no. 3, pp. 1400–1404, 2010.
- [33] H. Xu, X. Ye, H. Steinberg, and S. F. Liu, "Selective blockade of endothelial NF- κ B pathway differentially affects systemic inflammation and multiple organ dysfunction and injury in septic mice," *Journal of Pathology*, vol. 220, no. 4, pp. 490–498, 2010.
- [34] B. Manavalan, S. Basith, Y. M. Choi, G. Lee, and S. Choi, "Structure-function relationship of cytoplasmic and nuclear I κ B proteins: an in silico analysis," *PLoS ONE*, vol. 5, no. 12, Article ID e15782, 2010.
- [35] Z. Xiping, W. Dijiong, L. Jianfeng et al., "Effects of salvia miltiorrhizae on ICAM-1, TLR4, NF- κ B and bax proteins expression in multiple organs of rats with severe acute pancreatitis or obstructive jaundice," *Inflammation*, vol. 32, no. 4, pp. 218–232, 2009.
- [36] M. Q. Xu, X. R. Shuai, M. L. Yan, M. M. Zhang, and L. N. Yan, "Nuclear factor- κ B decoy oligodeoxynucleotides attenuates ischemia/reperfusion injury in rat liver graft," *World Journal of Gastroenterology*, vol. 11, no. 44, pp. 6960–6967, 2005.
- [37] Y. Y. Li, X. L. Li, C. X. Yang, H. Zhong, H. Yao, and L. Zhu, "Effects of tetrandrine and QYT on ICAM-1 and SOD gene expression in pancreas and liver of rats with acute pancreatitis," *World Journal of Gastroenterology*, vol. 9, no. 1, pp. 155–159, 2003.
- [38] I. Gukovsky, A. S. Gukovskaya, T. A. Blinman, V. Zaninovic, and S. J. Pandol, "Early NF- κ B activation is associated with hormone-induced pancreatitis," *American Journal of Physiology*, vol. 275, no. 6, pp. G1402–G1414, 1998.
- [39] B. Sung, A. Murakami, B. O. Oyajobi, and B. B. Aggarwal, "Zerumbone abolishes RaNKL-induced NF- κ B activation, inhibits osteoclastogenesis, and suppresses human breast cancer-induced bone loss in athymic nude mice," *Cancer Research*, vol. 69, no. 4, pp. 1477–1484, 2009.
- [40] Y. Takada, A. Murakami, and B. B. Aggarwal, "Zerumbone abolishes NF- κ B and I κ B α kinase activation leading to suppression of antiapoptotic and metastatic gene expression, up-regulation of apoptosis, and downregulation of invasion," *Oncogene*, vol. 24, no. 46, pp. 6957–6969, 2005.
- [41] B. B. Aggarwal, A. B. Kunnumakkara, K. B. Harikumar, S. T. Tharakan, B. Sung, and P. Anand, "Potential of spice-derived phytochemicals for cancer prevention," *Planta Medica*, vol. 74, no. 13, pp. 1560–1569, 2008.
- [42] Y. F. Zhao, W. L. Zhai, S. J. Zhang, and X. P. Chen, "Protection effect of triplolide to liver injury in rats with severe acute pancreatitis," *Hepatobiliary and Pancreatic Diseases International*, vol. 4, no. 4, pp. 604–608, 2005.

Research Article

Effect of Magnolol on the Function of Osteoblastic MC3T3-E1 Cells

Eun Jung Kwak,¹ Young Soon Lee,² and Eun Mi Choi²

¹ Department of Food Science Technology, Yeungnam University, Gyeongsan 712-749, Republic of Korea

² Department of Food & Nutrition, Kyung Hee University, 1 Hoegi-dong, Dongdaemun-gu, Seoul 130-701, Republic of Korea

Correspondence should be addressed to Eun Mi Choi, cheunmi@hanmail.net

Received 24 August 2011; Accepted 6 November 2011

Academic Editor: Rwei-Fen S. Huang

Copyright © 2012 Eun Jung Kwak et al. This is an open access article distributed under the Creative Commons Attribution License, which permits unrestricted use, distribution, and reproduction in any medium, provided the original work is properly cited.

Objectives. In the present study, the ability of magnolol, a hydroxylated biphenyl compound isolated from *Magnolia officinalis*, to stimulate osteoblast function and inhibit the release of bone-resorbing mediators was investigated in osteoblastic MC3T3-E1 cells. **Methods.** Osteoblast function was measured by cell growth, alkaline phosphatase activity, collagen synthesis, and mineralization. Glutathione content was also measured in the cells. Bone-resorbing cytokines, receptor activator of nuclear factor- κ B ligand (RANKL), TNF- α , and IL-6 were measured with an enzyme immunoassay system. **Results.** Magnolol caused a significant elevation of cell growth, alkaline phosphatase activity, collagen synthesis, mineralization, and glutathione content in the cells ($P < 0.05$). Skeletal turnover is orchestrated by a complex network of regulatory factors. Among cytokines, RANKL, TNF- α , and IL-6 were found to be key osteoclastogenetic molecules produced by osteoblasts. Magnolol significantly ($P < 0.05$) decreased the production of osteoclast differentiation inducing factors such as RANKL, TNF- α , and IL-6 in the presence of antimycin A, which inhibits mitochondrial electron transport and has been used as an ROS generator. **Conclusion.** Magnolol might be a candidate as an agent for the prevention of bone disorders such as osteoporosis.

1. Introduction

Bone tissue is continuously replaced through bone formation by osteoblasts and bone resorption by osteoclasts [1]. Both systemic factors and factors produced in the bone microenvironment are involved in the complex network regulating bone metabolism. Some of the locally produced factors involved in prevention of imbalances between bone formation and bone resorption also play prominent roles in diseases characterized by inflammation and increased bone resorption activity. TNF- α and IL-6 are proinflammatory cytokines produced by osteoblasts/stromal cells and well-known stimulator of bone resorption [2]. As a result, the number of osteoclasts is increased, leading to bone resorption, and osteoblast activity is repressed, leading to decreased mineralization. Receptor activator of nuclear factor- κ B ligand (RANKL) is a member of the tumor necrosis factor superfamily that is expressed in osteoblasts. RANKL, secreted mainly by osteoblastic stromal cells, is necessary for osteoclast formation from its committed precursors,

which bear its receptor RANK. Activation of RANK leads to activation of downstream signaling pathways including NF- κ B, p38 kinase, and c-Jun N-terminal kinase (JNK) [3]. The RANKL: RANK signaling pathway could be a major target of antiresorptive agents.

Magnolia officinalis (Magnoliaceae) has long been used for the treatment of fever, headache, anxiety, diarrhea, asthma, and stroke and possesses potent anti-inflammatory effects [4]. It has been reported that magnolol, a compound purified from *Magnolia officinalis*, relaxes rat vascular smooth muscle [5], scavenges hydroxyl radicals [6], inhibits neutrophil aggregation and superoxide anion generation [7, 8], suppresses the expression of vascular cell adhesion molecule-1 in endothelial cells [9], and inhibits nitric oxide (NO) production in lipopolysaccharide- (LPS-) activated macrophages [10]. Previous studies showed that magnolol could attenuate peroxidative damage and improve the survival of rats after surgically induced sepsis [11] or sepsis-induced haemorrhagic shock [12]. Since magnolol has been reported to have antioxidant effect [13], it seems to have

an effect on age-related osteoporosis. In the previous study, it was demonstrated that apocynin, a naturally occurring methoxy-substituted catechol, caused a significant elevation of osteoblast differentiation and decreased the production of ROS and osteoclast differentiation inducing factors in MC3T3-E1 cells [14].

The preosteoblastic MC3T3-E1 cell undergoes a temporal pattern of osteoblast development similar to *in vivo* bone formation. Thus, this cell is a well-accepted model of osteogenesis *in vitro* [15]. During the proliferative phase, this cell undergoes DNA synthesis and cell division, resulting in a rapid increase in cell number until confluence. At this juncture, proliferation is arrested, and there is an increase in the sequential expression of mature osteoblastic characteristics including alkaline phosphatase (ALP) production, conversion of procollagen to collagen, and the deposition of extracellular matrix on the substrate, which is subsequently mineralized [16]. In this study, to clarify the role of magnolol in bone formation and growth, the effects of magnolol on the proliferation and differentiation of osteoblastic cell lines were investigated using MC3T3-E1 *in vitro*. We also investigated whether magnolol inhibits the induction of bone resorbing mediators by antimycin A, which inhibits mitochondrial electron transport and has been used as an ROS generator.

2. Experimental Methods

2.1. Materials. Magnolol isolated from *Magnolia officinalis* was purchased from ChromaDex Inc. (Irvine, CA, USA) and antimycin A was purchased from Sigma Chemical (St. Louis, MO, USA). These were dissolved in dimethylsulfoxide (DMSO) and then diluted with the medium (final DMSO concentration $\leq 0.05\%$ (v/v)). α -Modified minimal essential medium (α -MEM) and fetal bovine serum (FBS) were purchased from Gibco BRL (Grand Island, NY, USA). Other reagents were of the highest commercial grade available and purchased from Sigma Chemical (St. Louis, MO, USA).

2.2. Cell Culture. MC3T3-E1 cells (RCB1126, an osteoblast-like cell line from C57BL/6 mouse calvaria) were obtained from the RIKEN Cell Bank (Tsukuba, Japan). MC3T3-E1 cells were cultured at 37°C in 5% CO₂ atmosphere in α -modified minimal essential medium (α -MEM; GIBCO). Unless otherwise specified, the medium contained 10% heat-inactivated fetal bovine serum (FBS), 100 U/mL penicillin, and 100 mg/mL streptomycin.

2.3. Cell Growth. The cells were suspended in medium and plated at a density of 10⁴ cells/well into a 24-well culture dish (Costar, Cambridge, MA, USA). After 48 h, the medium was replaced with serum-free media containing 0.3% bovine serum albumin supplemented with magnolol. After 2 days of culture, cell growth was measured by MTT assay. This assay is based on the ability of viable cells to convert soluble 3-(4,5-dimethyl-thiazol-2-yl)-2,5-diphenyl tetrazolium bromide (MTT) into an insoluble dark blue formazan reaction product. MTT 20 μ L in 7.2 mM phosphate buffer solution, pH 6.5 (5 mg/mL), was added to each well, and the plates

were incubated for an additional 2 h. After the removal of solutions in the well, dimethyl sulfoxide was added to dissolve formazan products, and the plates were shaken for 5 min. The absorbance of each well was recorded on a microplate spectrophotometer at 570 nm.

2.4. Collagen Content. The cells were treated, at confluence, with culture medium containing 10 mM β -glycerophosphate and 50 μ g/mL ascorbic acid (differentiation medium) to initiate differentiation. After 6 days, the cells were incubated with magnolol for 48 h. Collagen content was quantified by Sirius Red-based colorimetric assay. Cultured osteoblasts were washed with PBS, followed by fixation with Bouin's fluid for 1 h. After fixation, the fixation fluid was removed and the culture dishes were washed by immersion in running tap water for 15 min. The culture dishes were air dried and stained by Sirius Red dye reagent for 1 h under mild shaking on a shaker. Thereafter, the solution was removed, and the cultures were washed with 0.01 N HCl to remove nonbound dye. The stained material was dissolved in 0.1 N NaOH, and absorbance was measured at 550 nm.

2.5. Alkaline Phosphatase Activity. The cells were treated, at confluence, with differentiation medium to initiate differentiation. After 6 days, the cells were incubated with magnolol for 48 h. The cells were lysed with 0.2% Triton X-100, with the lysate centrifuged at 14,000 \times g for 5 min. The clear supernatant was used to measure the ALP activity, which was determined using an ALP activity assay kit (Asan Co. Korea). Protein concentrations were determined using the BioRad protein assay reagent.

2.6. Calcium Deposition Assay. The cells were treated, at confluence, with differentiation medium. After 14 days, the cells were cultured with medium containing magnolol for 2 days. On harvesting, the cells were fixed with 70% ethanol for 1 h and then stained with 40 mM Alizarin Red S for 10 min with gentle shaking. To quantify the bound dye, the stain was solubilized with 10% cetylpyridinium chloride by shaking for 15 min. The absorbance of the solubilized stain was measured at 561 nm.

2.7. Intracellular Glutathione Measurement. The cells were treated, at confluence, with differentiation medium to initiate differentiation. After 6 days, the cells were incubated with magnolol for 48 h. Cells were lysed by homogenization in 1–2 mL of cold buffer containing 50 mM MES or phosphate (pH 6–7) and 1 mM EDTA. After centrifugation at 10,000 g for 15 min at 4°C, supernatant was used for assay. Glutathione was measured by use of the Glutathione Assay Kit (BioAssay Systems, Hayward, CA, USA) according to manufacturer's instructions. Determination of glutathione is based on the reaction of 5, 5'-dithiobis-2-nitrobenzoic acid (DTNB) with glutathione which yield a yellow-colored chromophore, 5-thionitrobenzoic acid (TNB) with a maximum absorbance at 412 nm. Concentrations of glutathione were determined from a freshly prepared standard curve of glutathione.

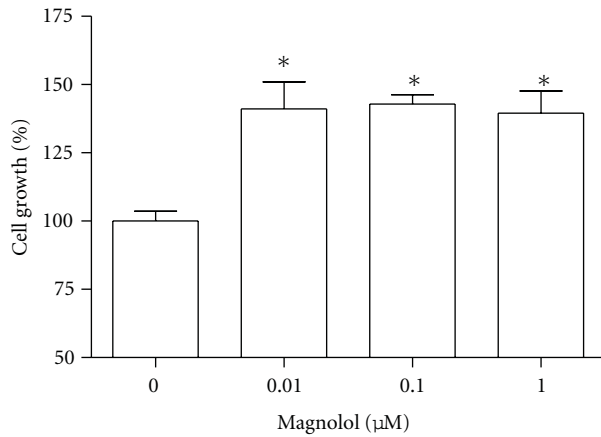


FIGURE 1: Effect of magnolol on the growth of MC3T3-E1 cells. Data were expressed as a percentage of control. * $P < 0.05$ compared with control.

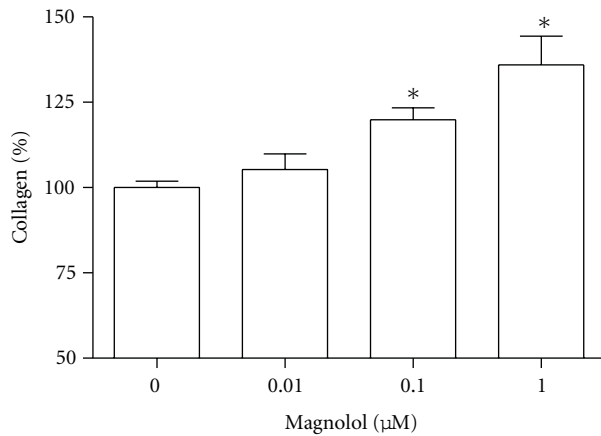


FIGURE 2: Effect of magnolol on the collagen synthesis of MC3T3-E1 cells. Data were expressed as a percentage of control. The control value for collagen content was $23.45 \pm 0.659 \mu\text{g}/10^6$ cells. * $P < 0.05$ compared with control.

2.8. Measurement of RANKL, TNF- α , and IL-6. The cells were treated, at confluence, with differentiation medium to initiate differentiation. After 6 days, the cells were pre-incubated with magnolol for 1 h before treatment with antimycin A for 48 h. RANKL, TNF- α , and IL-6 contents in the medium were measured with an enzyme immunoassay system (R&D system Inc., Minneapolis, MN, USA) according to the manufacturer's recommendation.

2.9. Statistical Analysis. All experiments were carried out in triplicate, and all results are expressed as mean \pm SEM of at least 3 independent experiments. Statistical significance was determined by analysis of variance and subsequently applying Dunnett's t -test ($P < 0.05$).

3. Results

3.1. Effect of Magnolol on the Growth and Differentiation of MC3T3-E1 Cells. MC3T3-E1 cells were incubated with

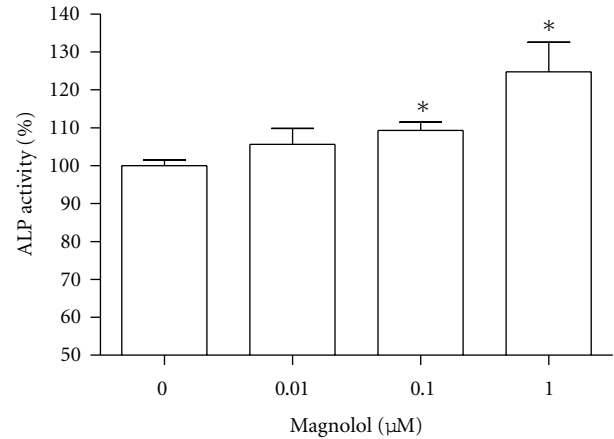


FIGURE 3: Effect of magnolol on the alkaline phosphatase activity of MC3T3-E1 cells. Data were expressed as a percentage of control. The control value for ALP activity was 0.871 ± 0.016 Unit/mg. * $P < 0.05$ compared with control.

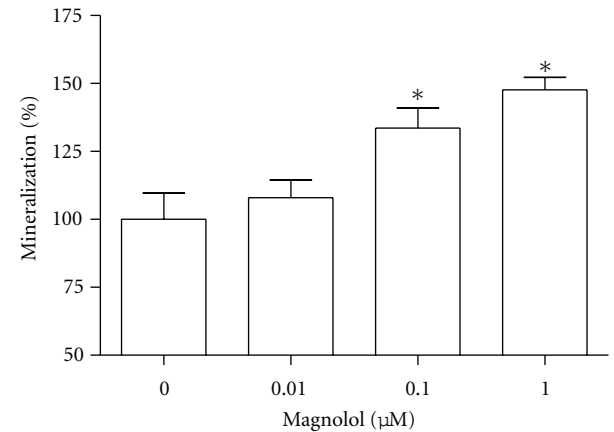


FIGURE 4: Effect of magnolol on the mineralization of osteoblastic MC3T3-E1 cells. Data were expressed as a percentage of control. The control value for mineralization was 0.504 ± 0.006 OD/ 10^6 cells. * $P < 0.05$ compared with control.

magnolol and cell growth was measured. Cell populations cultured in basal or magnolol-treated media appeared as Figure 1. MC3T3-E1 cell growth was promoted by stimulation with magnolol ($0.1 \sim 1 \mu\text{M}$) significantly compared with control cells. The effect of magnolol on collagen synthesis in osteoblastic MC3T3-E1 cells is shown in Figure 2. The collagen synthesis of MC3T3-E1 cells was significantly increased by the addition of $0.1 \sim 1 \mu\text{M}$ magnolol. ALP activity was measured to study the effect of magnolol on the osteoblastic differentiation in MC3T3-E1 cells. The cultured cells in the presence of magnolol (0.1 and $1 \mu\text{M}$) caused a significant increase in the ALP activity of osteoblastic cells (Figure 3). The MC3T3-E1 cells were treated with various concentrations of magnolol, and the mineralization of osteoblasts was measured. The increase of mineralization was significant at magnolol concentrations of 0.1 and $1 \mu\text{M}$ in MC3T3-E1 cell culture (Figure 4).

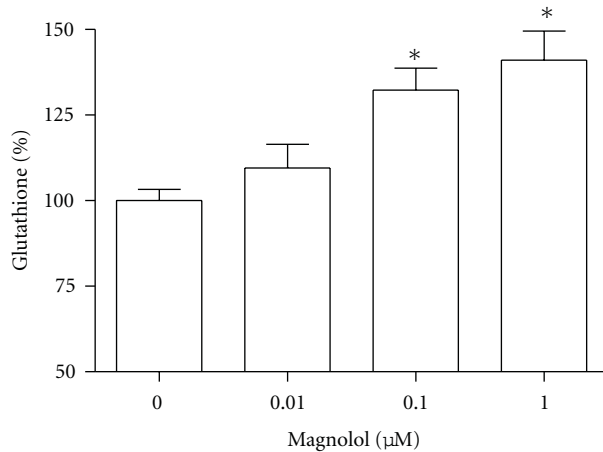


FIGURE 5: Effect of magnolol on the glutathione content of MC3T3-E1 cells. Data were expressed as a percentage of control. The control value for collagen content was 12.8 ± 0.305 nmole/mg. * $P < 0.05$ compared with control.

3.2. Effect of Magnolol on the Intracellular Glutathione Content of MC3T3-E1 Cells. Glutathione content reflects the amount of substrate available to act as antioxidant. The level of glutathione after magnolol exposure for 48 h was significantly increased at the concentration of 0.1 and 1 μ M as compared with control, indicating that magnolol-induced enhancements of osteoblast function are associated with an increase in glutathione (Figure 5).

3.3. Effect of Magnolol on RANKL Production of MC3T3-E1 Cells in the Presence of Antimycin A. In order to further determine the regulator of osteoclast differentiation in osteoblasts, we examined the production of RANKL in the osteoblastic MC3T3-E1 cells. When 70 μ M antimycin A was added to cells, the production of RANKL increased significantly (Figure 6). However, antimycin A-induced RANKL production was significantly inhibited by treatment of magnolol (0.01–1 μ M).

3.4. Effect of Magnolol on Antimycin A-Induced TNF- α and IL-6 Production in MC3T3-E1 Cells. TNF- α and IL-6 have been demonstrated to increase osteoclastic activity. Thus, we also investigated whether magnolol modulates antimycin A-induced production of TNF- α and IL-6 (Figure 7). When 70 μ M antimycin A was added to cells, production of TNF- α and IL-6 increased significantly. However, antimycin A-induced TNF- α and IL-6 productions were significantly inhibited by treatment of magnolol at 0.01–1 μ M and 0.1–1 μ M, respectively.

4. Discussion

The osteoblast phenotypes are acquired in two stages. In the first stage, the matrix matures and specific proteins associated with the bone cell phenotype, such as collagen and ALP, are detected. In the second stage, matrix becomes mineralized by calcium deposition. As a result, layers of

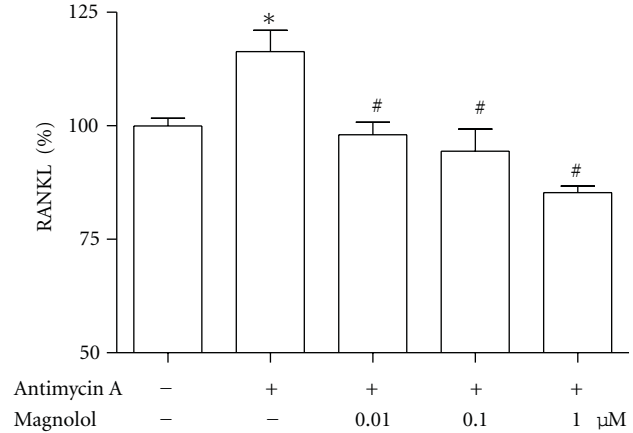


FIGURE 6: Effect of magnolol on antimycin A-induced RANKL production of MC3T3-E1 cells. Effect of magnolol on the production of RANKL in the presence of antimycin A. Osteoblasts were pre-incubated with magnolol before treatment with 70 μ M antimycin A for 48 h. Data were expressed as a percentage of control. The control value for RANKL was 3.378 ± 0.074 ng/mg. * $P < 0.05$, control versus antimycin A; # $P < 0.05$, antimycin A versus magnolol.

spongy bone are formed around the original cartilage. Later in development, spaces among the spongy bone are filled with bone matrix and become compact bone [17]. Hence, collagen content and ALP activity, an early differentiation marker, and cellular calcium content, a late marker of differentiation, were examined to investigate the effects of magnolol on the differentiation of osteoblast cells. In this study, it was found that magnolol markedly increased osteoblast growth and differentiation in osteoblastic MC3T3-E1 cells. The findings of the present study supported our hypothesis that magnolol increases the osteogenic effect in osteoblastic MC3T3-E1 cells and these stimulated osteogenic effects are mediated by increasing osteoblast proliferation and differentiation. Findings from this study show that magnolol increased osteoblast proliferation during the early osteoblast proliferation phase. During the early proliferation period, osteoblasts synthesize and secrete cell-growth proteins such as TGF- β or IGF [18] and collagen, which is the most abundant protein in extracellular matrix accounting for matrix maturation [19]. Therefore, we suggest that increased osteoblast proliferation by magnolol indicates an anabolic effect on the bone matrix formation by stimulating osteoblast cell growth rate and by increasing collagenous protein synthesis which is a critical factor for matrix maturation.

Oxidative stress [20] and changes in the bone microenvironment composition with aging [21] may play an important role in the pathogenesis of postmenopausal osteoporosis by impairing osteoprogenitor cell recruitment and differentiation. Jiang et al. [22] studied *in vitro* the characteristics of alveolar osteoblasts from elderly women and revealed differences in proliferative capacity and bone formation functions, which dropped with aging. In this context, an important correlation has been shown between oxidative stress and postmenopausal bone loss occurrence during aging. Maggio et al. [23] reported that antioxidant

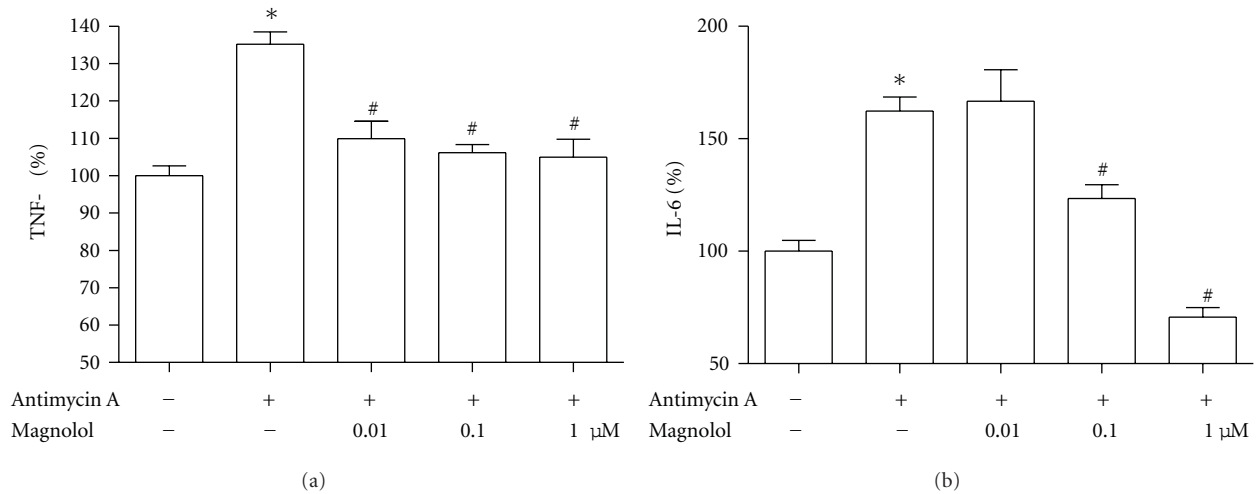


FIGURE 7: Effect of magnolol on antimycin A-induced cytokines production of MC3T3-E1 cells. Osteoblasts were preincubated with magnolol before treatment with 70 μM antimycin A for 48 h. Data were expressed as a percentage of control. The control values for TNF-α (a) and IL-6 (b) were 0.228 ± 0.006 ng/mg and 0.655 ± 0.033 ng/mg, respectively. * $P < 0.05$, control versus antimycin A; # $P < 0.05$, antimycin A versus magnolol.

defenses are markedly decreased in plasma of osteoporotic women. In agreement, Altindag et al. [24] associated this imbalance between oxidant and antioxidant status in postmenopausal osteoporosis with increase of osteoclastic activity and decreased osteoblastic activity. Reduced glutathione is considered one of the most important intracellular reducer agents. This tripeptide is involved in the protection against cytotoxicity electrophilic agents and metabolites, and it is also involved with the regulation of the effects of oxidative stress on the cells, maintaining, in this way, the intracellular redox balance [25]. Glutathione is considered to be responsible for reactivation of some proteins after suffering oxidative stress [26]. In the presence of glutathione, the sulfenic derivative can be converted in a more stable product, preventing further oxidation [27]. In the present study, the level of glutathione after magnolol exposure was significantly increased. Our result shows that the enhancement of antioxidants by magnolol may be related with the increased function of osteoblasts.

Apart from having an effect on bone formation, osteoblasts are also coupled with osteoclasts through the release of various cytokines, including RANKL [28]. Most proosteoclastogenic cytokines act primarily through osteoblasts to alter levels of RANKL. RANKL is a protein expressed on the osteoblast cell membrane that binds to its cognate receptor RANK, which is present on the osteoclast progenitor membrane. The binding of RANKL to RANK activates nuclear factor-κB and c-jun N-terminal protein kinase, which is associated with osteoclastic differentiation and activation [29]. Oxidative stress plays an important role in the destruction of bone cells during the development of osteoporosis. Impaired mitochondrial function can lead to increased ROS generation and may increase oxidative stress if the antioxidant defense mechanisms of the cells are overwhelmed [30]. Increased oxidative stress caused by mitochondrial dysfunction is considered the causal link

between elevated ROS and the major biochemical pathways postulated to be involved in the pathogenesis of senile disorders [31]. Antimycin A is an inhibitor of mitochondrial electron transport via its binding to complex III [32]. In this study, magnolol inhibited the production of RANKL induced by antimycin A in osteoblastic cells. Dong et al. [33] reported that 3,3'-diindolmethane, one of the natural compounds formed during the autolysis of glucobrassicin, effectively inhibited the expression of RANKL in osteoblastic cells, leading to the blockade of osteoclastogenesis and consequently an alleviation of experimental arthritis. Because RANKL is also known to induce actin ring formation in mature osteoclasts, magnolol-induced inhibition of RANKL release in osteoblastic cells could result in disruption of actin tings in osteoclasts.

Several family members are produced by bone cells and have been implicated to be involved in regulation of bone metabolism. In the present paper, we show that TNF-α and IL-6 releases induced by antimycin A were decreased by magnolol. The inhibitory effect on TNF-α and IL-6 production by magnolol may contribute to the bone antiresorbing effect of magnolol and possibly also play a role in the reduction of bone loss seen in the vicinity of inflammatory processes such as rheumatoid arthritis and periodontal disease. Although the precise and detailed mechanism of magnolol inhibition remains to be scrutinized, we propose that magnolol might be useful as a potential therapeutic medication for attenuating osteoclast formation and function in the prevention and treatment of bone diseases such as osteoporosis. That TNF-α can inhibit osteoblast differentiation, and bone formation is well known. Using two models of osteoblast differentiation, Gilbert et al. [34] found that TNF-α inhibited cell differentiation by downregulating the transcription of Runx2, which regulates the expression of bone matrix proteins. RUNX2 protein stability has also been shown to be destabilized by TNF-α

[35]. Hughes and Howells [36] treated osteoblasts derived from fetal rat calvaria with recombinant human IL-6 and showed that bone nodule formation was inhibited. Fang and Hahn [37] examined the effects of IL-6 in UMR-106-01 cells, a rat osteoblastic osteosarcoma line, and observed that it suppressed collagen synthesis. IL-6 may have a role in the osteopenia associated with inflammation *in vivo*. Patients with inflammatory diseases in whom IL-6 levels are highest may be at increased risk for osteopenia.

In summary, magnolol increased the proliferation of osteoblasts and stimulated ALP activity and bone matrix proteins, such as collagen, and these increases trigger osteoblastic differentiation (e.g., mineralized nodule formation). Moreover, our data indicate that magnolol suppresses the production of the bone-resorbing factors in the presence of antimycin A, a mitochondrial inhibitor that increases the generation of ROS. Thus, magnolol may be a good candidate for the protection of osteoblast dysfunction. These results may aid in the development of a therapeutic approach of magnolol in the prevention of osteoporosis.

Authors' Contributions

These authors contributed equally to this study.

Acknowledgments

This research was supported by the Basic Science Research Program through the National Research Foundation of Korea (NRF) funded by the Ministry of Education, Science and Technology (20110005020).

References

- [1] G. Karsenty and E. F. Wagner, "Reaching a genetic and molecular understanding of skeletal development," *Developmental Cell*, vol. 2, no. 4, pp. 389–406, 2002.
- [2] S. C. Manolagas, "The role of IL-6 type cytokines and their receptors in bone a," *Annals of the New York Academy of Sciences*, vol. 840, pp. 194–204, 1998.
- [3] S. L. Teitelbaum, "Bone resorption by osteoclasts," *Science*, vol. 289, no. 5484, pp. 1504–1508, 2000.
- [4] J. P. Wang, M. F. Hsu, S. L. Raung, C. C. Chen, J. S. Kuo, and C. M. Teng, "Anti-inflammatory and analgesic effects of magnolol," *Naunyn-Schmiedeberg's Archives of Pharmacology*, vol. 346, no. 6, pp. 707–712, 1992.
- [5] C. M. Teng, S. M. Yu, C. C. Chen, Y. L. Huang, and T. F. Huang, "EDRF-release and Ca^{2+} -channel blockade by magnolol, an antiplatelet agent isolated from Chinese herb *Magnolia officinalis*, in rat thoracic aorta," *Life Sciences*, vol. 47, no. 13, pp. 1153–1161, 1990.
- [6] S. Fujita and J. Taira, "Biphenyl compounds are hydroxyl radical scavengers: their effective inhibition for UV-induced mutation in *Salmonella typhimurium* TA102," *Free Radical Biology and Medicine*, vol. 17, no. 3, pp. 273–277, 1994.
- [7] J. P. Wang, P. L. Lin, M. F. Hsu, and C. C. Chen, "Possible involvement of protein kinase C inhibition in the reduction of phorbol ester-induced neutrophil aggregation by magnolol in the rat," *Journal of Pharmacy and Pharmacology*, vol. 50, no. 10, pp. 1167–1172, 1998.
- [8] J. P. Wang, M. F. Hsu, S. L. Raung et al., "Inhibition by magnolol of formylmethionyl-leucyl-phenyl alanine-induced respiratory burst in rat neutrophils," *Journal of Pharmacy and Pharmacology*, vol. 51, no. 3, pp. 285–294, 1999.
- [9] Y. H. Chen, S. J. Lin, J. W. Chen, H. H. Ku, and Y. L. Chen, "Magnolol attenuates VCAM-1 expression in vitro in TNF- α -treated human aortic endothelial cells and in vivo in the aorta of cholesterol-fed rabbits," *British Journal of Pharmacology*, vol. 135, no. 1, pp. 37–47, 2002.
- [10] H. Matsuda, T. Kageura, M. Oda, T. Morikawa, Y. Sakamoto, and M. Yoshikawa, "Effects of constituents from the bark of *Magnolia obovata* on nitric oxide production in lipopolysaccharide-activated macrophages," *Chemical and Pharmaceutical Bulletin*, vol. 49, no. 6, pp. 716–720, 2001.
- [11] C. W. Kong, K. Tsai, J. H. Chin, W. L. Chan, and C. Y. Hong, "Magnolol attenuates peroxidative damage and improves survival of rats with sepsis," *Shock*, vol. 13, no. 1, pp. 24–28, 2000.
- [12] H. C. Shih, Y. H. Wei, and C. H. Lee, "Magnolol alters the course of endotoxin tolerance and provides early protection against endotoxin challenge following sublethal hemorrhage in rats," *Shock*, vol. 22, no. 4, pp. 358–363, 2004.
- [13] H. C. Ou, F. P. Chou, W. H. H. Sheu, S. L. Hsu, and W. J. Lee, "Protective effects of magnolol against oxidized LDL-induced apoptosis in endothelial cells," *Archives of Toxicology*, vol. 81, no. 6, pp. 421–432, 2007.
- [14] Y. S. Lee and E. M. Choi, "Apocynin stimulates osteoblast differentiation and inhibits bone-resorbing mediators in MC3T3-E1 cells," *Cellular Immunology*, vol. 270, no. 2, pp. 224–229, 2011.
- [15] L. D. Quarles, D. A. Yohay, L. W. Lever, R. Caton, and R. J. Wenstrup, "Distinct proliferative and differentiated stages of murine MC3T3-E1 cells in culture: an in vitro model of osteoblast development," *Journal of Bone and Mineral Research*, vol. 7, no. 6, pp. 683–692, 1992.
- [16] C. G. Bellows, J. E. Aubin, and J. N. M. Heersche, "Initiation and progression of mineralization of bone nodules formed in vitro: the role of alkaline phosphatase and organic phosphate," *Bone and Mineral*, vol. 14, no. 1, pp. 27–40, 1991.
- [17] R. A. Logan, "The role of osteoblasts and osteoclasts in osteogenesis," *American Journal of Orthodontics and Oral Surgery*, vol. 28, no. 9, pp. 561–566, 1942.
- [18] M. S. Burnstone, "Histochemical observations on enzymatic processes in bones and teeth," *Annals of the New York Academy of Sciences*, vol. 85, pp. 431–444, 1960.
- [19] J. B. Lian and G. S. Stein, "Concepts of osteoblast growth and differentiation: basis for modulation of bone cell development and tissue formation," *Critical Reviews in Oral Biology and Medicine*, vol. 3, no. 3, pp. 269–305, 1992.
- [20] O. F. Sendur, Y. Turan, E. Tastaban, and M. Serter, "Antioxidant status in patients with osteoporosis: a controlled study," *Joint Bone Spine*, vol. 76, no. 5, pp. 514–518, 2009.
- [21] B. M. Abdallah, M. Haack-Sørensen, T. Fink, and M. Kassem, "Inhibition of osteoblast differentiation but not adipocyte differentiation of mesenchymal stem cells by sera obtained from aged females," *Bone*, vol. 39, no. 1, pp. 181–188, 2006.
- [22] S. Y. Jiang, R. Shu, Y. F. Xie, and S. Y. Zhang, "Age-related changes in biological characteristics of human alveolar osteoblasts," *Cell Proliferation*, vol. 43, no. 5, pp. 464–470, 2010.
- [23] D. Maggio, M. Barabani, M. Pierandrei et al., "Marked decrease in plasma antioxidants in aged osteoporotic women: results of a cross-sectional study," *Journal of Clinical Endocrinology and Metabolism*, vol. 88, no. 4, pp. 1523–1527, 2003.

- [24] O. Altindag, O. Erel, N. Soran, H. Celik, and S. Selek, "Total oxidative/anti-oxidative status and relation to bone mineral density in osteoporosis," *Rheumatology International*, vol. 28, no. 4, pp. 317–321, 2008.
- [25] J. Ning and M. H. Grant, "The role of reduced glutathione and glutathione reductase in the cytotoxicity of chromium (VI) in osteoblasts," *Toxicology in Vitro*, vol. 14, no. 4, pp. 329–335, 2000.
- [26] P. Chiarugi, M. L. Taddei, N. Schiavone et al., "LMW-PTP is a positive regulator of tumor onset and growth," *Oncogene*, vol. 23, no. 22, pp. 3905–3914, 2004.
- [27] P. Chiarugi, T. Fiaschi, M. L. Taddei et al., "Two vicinal cysteines confer a peculiar redox regulation to low molecular weight protein tyrosine phosphatase in response to platelet-derived growth factor receptor stimulation," *Journal of Biological Chemistry*, vol. 276, no. 36, pp. 33478–33487, 2001.
- [28] D. L. Lacey, E. Timms, H. L. Tan et al., "Osteoprotegerin ligand is a cytokine that regulates osteoclast differentiation and activation," *Cell*, vol. 93, no. 2, pp. 165–176, 1998.
- [29] E. Jimi, S. Akiyama, T. Tsurukai et al., "Osteoclast differentiation factor acts as a multifunctional regulator in murine osteoclast differentiation and function," *Journal of Immunology*, vol. 163, no. 1, pp. 434–442, 1999.
- [30] P. Jezek and L. Hlavata, "Mitochondria in homeostasis of reactive oxygen species in cell, tissues, and organism," *International Journal of Biochemistry and Cell Biology*, vol. 37, no. 12, pp. 2478–2503, 2005.
- [31] T. Nishikawa and E. Araki, "Impact of mitochondrial ROS production in the pathogenesis of diabetes mellitus and its complications," *Antioxidants and Redox Signaling*, vol. 9, no. 3, pp. 343–353, 2007.
- [32] Y. H. Han and W. H. Park, "Growth inhibition in antimycin A treated-lung cancer Calu-6 cells via inducing a G1 phase arrest and apoptosis," *Lung Cancer*, vol. 65, no. 2, pp. 150–160, 2009.
- [33] L. Dong, S. Xia, F. Gao, D. Zhang, J. Chen, and J. Zhang, "3,3'-Diindolylmethane attenuates experimental arthritis and osteoclastogenesis," *Biochemical Pharmacology*, vol. 79, no. 5, pp. 715–721, 2010.
- [34] L. Gilbert, X. He, P. Farmer et al., "Expression of the osteoblast differentiation factor RUNX2 (Cbfa1/AML3/PeBP2 α) is inhibited by tumor necrosis factor- α ," *Journal of Biological Chemistry*, vol. 277, no. 4, pp. 2695–2701, 2002.
- [35] H. Kaneki, R. Guo, D. Chen et al., "Tumor necrosis factor promotes Runx2 degradation through up-regulation of Smurf1 and Smurf2 in osteoblasts," *Journal of Biological Chemistry*, vol. 281, no. 7, pp. 4326–4333, 2006.
- [36] F. J. Hughes and G. L. Howells, "Interleukin-6 inhibits bone formation in vitro," *Bone and Mineral*, vol. 21, no. 1, pp. 21–28, 1993.
- [37] M. A. Fang and T. J. Hahn, "Effects of interleukin-6 on cellular function in UMR-106-01 osteoblastlike cells," *Journal of Bone and Mineral Research*, vol. 6, no. 2, pp. 133–139, 1991.

Research Article

Pegylated Arginine Deiminase Downregulates Colitis in Murine Models

Helieh S. Oz,^{1,2} Jian Zhong,^{2,3} and Willem J. S. de Villiers^{2,3}

¹ Department of Physiology, College of Medicine, University of Kentucky Medical Center, Lexington, KY 40515-0298, USA

² Department of Internal Medicine, College of Medicine, University of Kentucky Medical Center, Lexington, KY 40515-0298, USA

³ Division of Digestive Diseases and Nutrition, Department of Internal Medicine, College of Medicine, University of Kentucky Medical Center, Lexington, KY 40515-0298, USA

Correspondence should be addressed to Helieh S. Oz, hoz2@email.uky.edu

Received 21 September 2011; Accepted 11 October 2011

Academic Editor: Sung-Ling Yeh

Copyright © 2012 Helieh S. Oz et al. This is an open access article distributed under the Creative Commons Attribution License, which permits unrestricted use, distribution, and reproduction in any medium, provided the original work is properly cited.

Arginine deiminase (ADI), an arginine-metabolizing enzyme involved in cell signaling, is dysregulated in multiple inflammatory diseases and cancers. We hypothesized that pegylated ADI (ADI-PEG) provide protection against colitis. *Methods.* Dextran sodium sulfate colitis was induced in IL-10-deficient and BALB/c (WT) mice. ADI-PEG was administered *i.p.*, and inflammatory mediators and pathology were evaluated. *Results.* Acute colitis in mice was manifested by increases in inflammatory biomarkers, such as serum amyloid A (SAA, $P < 0.001$), IL-12 p40, and disease index (3-Fold). In contrast, ADI-PEG significantly decreased clinical disease index, SAA levels, and inflammatory cytokines in blood as well as in colonic explants. Animals developed moderate (2.2 ± 0.3 WT) to severe (3.6 ± 0.5 IL-10 deficient) colonic pathology; and ADI-PEG treatment significantly improved the severity of colitis ($P < 0.05$). Marked infiltration of CD68⁺ macrophages and iNOS expression were detected in colonic submucosa in colitic animals but not detected in ADI-PEG-treated animals. *Conclusion.* ADI-PEG attenuated inflammatory responses by suppression of macrophage infiltration and iNOS expression in colitic animals. ADI-PEG can serve as a potential therapeutic value in IBD.

1. Introduction

Arginine deiminase (ADI) plays important role in cell signaling pathways, including apoptosis, differentiation, and transcriptional regulation [1, 2]. ADI is an arginine-degrading enzyme that catalyzes the hydrolysis of peptidylarginine to form peptidylcitrulline. ADI activity is dysregulated in multiple human diseases including rheumatoid arthritis (RA), inflammatory bowel disease (IBD), and cancer. Since, tumor cell lines require arginine for growth, selective elimination of arginine from the circulation has been suggested as a potential cancer treatment modality and currently in use in human trials [3]. Conversely, ADI inhibition with cl-amidine has been shown to reduce disease severity in the collagen-induced arthritis model of RA [4, 5].

Nitric oxide (NO) is known to be elevated in the colonic tissues of patients with active IBD and increased NO production and nitric oxide synthase (NOS) activity are detected in cultured mucosal explants from patients with active IBD,

both ulcerative colitis and Crohn's disease [6–9]. Immunohistochemical analysis has identified inducible nitric oxide synthase (iNOS), a key inflammatory mediator, responsible for generation of NO and as the NOS isoform elevated in IBD [10, 11]. This increase-associated iNOS is localized to macrophages and epithelial cells, particularly in luminal epithelia that expose colonic tissue [11].

Additionally, the expression of iNOS in circulating monocytes and the percentage of iNOS-positive monocytes are increased in patients with active IBD as compared to healthy controls [12]. Arginine metabolism is likely to be another factor with regard to the roles of NOS in colitis. In addition to serving as a NOS substrate, arginine is a mediator for the enzyme arginase, which synthesizes ornithine, an intermediate in polyamine biosynthesis. Polyamines have been suggested to protect against colitis, possibly by stimulating reepithelialization and increasing arginase activity associated with healing following experimental colonic anastomosis [13, 14]. Arginine, is a nonessential amino acid,

synthesized in normal cells and tissues from citrulline in a 2-step process using the urea cycle enzymes argininosuccinate synthase and argininosuccinate lyase. As an arginine metabolizing enzyme, ADI (Scheme 1), has major properties with respect to the issues of harmful and helpful NO and alternative arginine metabolism with preventing harmful NO generation [15].

In fact, the native ADI is very immunogenic with a short circulating lifespan of only 5 h. ADI covalently binds to polyethylene glycol (PEG) with molecular weight of 20 kDa and forms ADI-PEG. ADI-PEG is less antigenic with a significant increased circulating life span of about 5 days and reported to be safe in mice as well as humans [3, 16].

Although, ADI plays an important role in regulating cell signaling, the mechanism by which the enzyme's activity is regulated under physiological as well as pathological conditions leading to IBD is not fully discovered. Here we hypothesized the potential protective action of a microbial enzyme, ADI-PEG treatment against acute colitis.

2. Methods

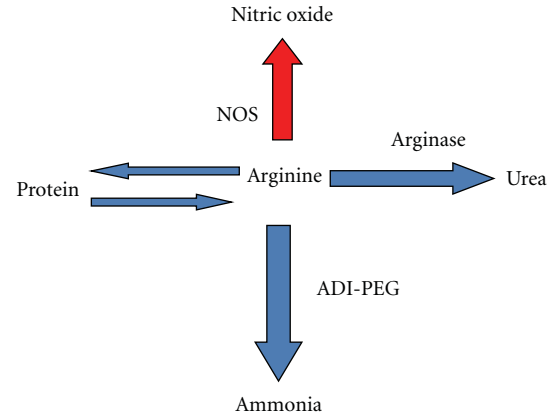
Pegylated arginine deiminase (ADI-PEG) was prepared and provided by Dr. Steiner (University of KY; USA). Briefly, nonmammalian ADI gene from *Mycoplasma hominis* was expressed in *E. coli* and purified by anion-exchange chromatography with a POROS HQ resin column. The recombinant ADI was then pegylated according to the manufacture recommendation, and the enzyme activity was measured [16].

2.1. Animals. This study was approved and performed in accordance with the guidelines for the care and use of laboratory animals at the accredited University of Kentucky and Veterans Administration (VA) Medical Center in Lexington, KY, USA. IL-10-deficient mice were bred in animal facility at VA Medical Center and UK Medical Center. Male pups were weaned and at 5 weeks of age enrolled in this study.

In addition, five-week-old male BALB/c wildtype mice were purchased from Harlan Laboratories (Indianapolis, IN) and acclimatized for 10 days prior to the experiment. The IL-10-deficient mice were cohoused with wildtype mice (WT) in conventional condition, in microisolator cages, with free access to water and food (Harlan Teklad Laboratory Diet, Madison, WI) and kept in a room with a 12 h light/dark cycle.

2.2. Colitis Induction. Colitis was induced in IL-10-deficient and WT mice by oral ingestion of 3% dextran sodium sulfate (DSS) for 7 days and assessed by clinical disease index, inflammatory mediators, and histological grading scores. ADI-PEG low dose (5 IU) and high dose (10 IU) were chosen based on the safe and effective doses detected in previous cell culture studies. ADI-PEG was administered *i.p.* on day 0 and day 5 to the treated groups as ADI-PEG has a 1/2 lifespan of about 5-6 days.

2.3. The Clinical Disease Index. The clinical disease activity score was determined by the mean measurement of animal survival, extent of weight loss, stool consistency, presence of



SCHEME 1: Arginine metabolism.

blood in the stool, anemia as expressed by the hematocrit, colonic weight and length, and prolapse collectively which were scored from 0, to present normal up to 10, the most severe case.

2.4. Colonic Histopathology. Colonic tissues were flushed with ice-cold phosphate-buffered saline (PBS pH 7.2) and cut longitudinally in half. One portion of each colon was Swiss-rolled and fixed in 10% formalin for histological examination. The remainder was snap-frozen in liquid nitrogen and stored at -80°C . The formalin fixed sections were processed and stained with hematoxylin and eosin (H and E) and evaluated under light microscopy. Severity of colitis was assessed with a histological semiquantitative grading score [17] and in a blinded manner. The scores were based on histological features with a numeric value (0 to 4) assigned according to the tissue involvement and severity of lesions that corresponded to either of the following criteria:

- grade (0): No detectable lesions, no inflammatory cells, and normal mucosal appearance,
- grade (1): Focal inflammatory infiltrate in the mucosa (25% involved),
- grade (2): Mild multi-focal inflammation with moderate expansion to the mucosa (50% involved),
- grade (3): Moderate multifocal inflammation with moderate expansion of the mucosa (75% involved),
- grade (4): Severe diffuse inflammation with crypt epithelium disruption and ulceration (over 75% involved).

2.5. Plasma Analysis for Inflammatory Biomarkers Concentrations. Blood was collected via right heart ventricle puncture in lightly heparinized syringes and kept on ice. Sera were separated by 5 min centrifugation at $5000 \times g$ and stored at -80°C prior to the analysis.

2.6. Colonic Explant Production of Cytokines. Proximal sections of cleansed colonic cuffs from each mouse were weighted and washed with sterile PBS and the RPMI 1640 culture medium. Each explant was then plated in 24-well

plates and cultured in 1 mL of complete RPMI 1640 medium supplemented with 5% fetal bovine serum (FBS, BioWhittaker, Walkersville, MD, USA) for 24 h at 37°C. LPS (10 ng/mL) was added into duplicate wells to stimulate the cells. Culture supernatant was collected with centrifugation, and aliquots were stored at -80°C until analyzed for inflammatory markers.

2.7. Inflammatory Biomarkers. Cytokines were measured by ELISA kits and assayed according to the manufacturer's recommendation. The concentrations of IL-6, IL-12p40, and TNF α were measured by ELISA kits obtained from R and D (Minneapolis, MN, USA), and SAA was analyzed by Kits from BioSource (Camarillo, CA, USA).

2.8. Immunohistochemical Assay (IHC). Paraffin-embedded sections were cut, deparaffinized with hexane, rehydrated in alcohol baths, washed in PBS, microwaved in antigen retrieval solution (high pH; DAKO, Carpinteria, CA, USA) for 5 min, washed with PBS, incubated in 0.3% H₂O₂-methanol for 10 min, and then rinsed with water. Slides were incubated at room temperature for 1.5 h in a blocking solution consisting of normal serum, rinsed with PBS, and then incubated with primary antibody at 4°C overnight. Rabbit polyclonal IgG against CD68 and iNOS was obtained from Zymed-Invitrogen. Invitrogen (Carlsbad, CA, USA) and Millipore (Billerica, MA, USA) respectively. The "Elite ABC" kit was used with biotinylated secondary antibodies and biotin-conjugated horseradish peroxidase and then developed using a 3-3'-diaminobenzidine solution per manufacturer's instructions. The slides were subsequently counterstained with Methyl Green (Dako, Carpinteria, CA, USA). The CD68 (the macrophage specific-marker) staining for the quantification of macrophages and anti-iNOS (iNOS positive macrophage) for the assessment of iNOS expression was performed to evaluate macrophage infiltration and activation in colonic tissue [18].

2.9. Nitric Oxide (NO) Analysis. NO was assessed indirectly by the measurement of its breakdown products, nitrite plus nitrate [19], in a microtiter plate assay. Briefly, nitrate was reduced into nitrite by incubation with nitrate reductase, untreated NADPH was oxidized, and then total nitrite was colorimetrically measured following incubation with the Griess reagent. Griess reagent: 1% (w/v) ammonium chloride was adjusted to pH 8.0 with sodium borate, 1:1 solution of 0.1% (w/v) *N*-(1-naphthyl) ethylenediamine dihydrochloride, and 1% (w/v) sulfanilamide, in 5% (v/v) phosphoric acid.

2.10. Statistical Analysis. Results are expressed as the mean \pm SEM unless otherwise stated. Data was analyzed with ANOVA followed by appropriate post hoc test (Tukey compared all pairs) using GraphPad Instat version 3 for Windows (San Diego, CA, USA). Statistical significance was set at $P < 0.05$.

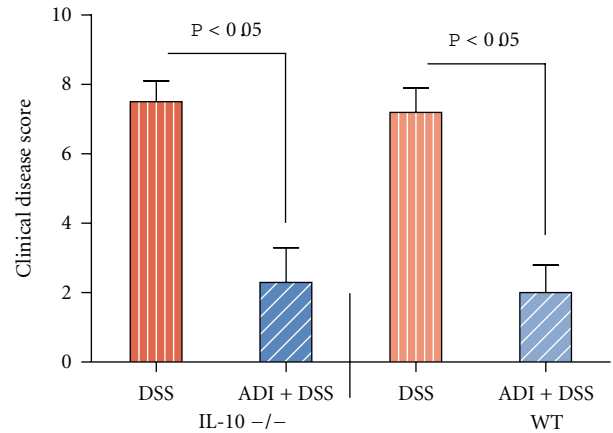


FIGURE 1: Effects of ADI-PEG therapy on the clinical disease index in DSS-induced acute colitis. ADI-PEG was administered *i.p.* on day 0 and day 5. Clinical disease index was determined by parameters as means for extent of weight loss, presence of diarrhea, rectal bleeding, prolapse, and anemia ($n = 6$ /group). ADI-PEG markedly decreased the clinical disease index in WT and IL-10-deficient colitic mice.

3. Results

Colitis was induced in WT and IL-10-deficient mice by oral ingestion of DSS in daily drinking water for 7 days. ADI-PEG was administered *i.p.* on day 0 and day 5 to the treated groups (ADI-PEG circulating 1/2 life is 5 days). Clinical disease index was determined by using parameters such as survival, extent of weight loss, the presence or absence of diarrhea, rectal bleeding, anemia, and prolapse.

DSS-exposed IL-10-deficient and WT animals all lost weight and developed anemia due to blood loss. In contrast, ADI-PEG treatment significantly protected DSS-exposed mice from weight loss and rectal bleeding compared to untreated DSS colitic animals (data shown collectively as disease index Figure 1). Over 80% of animals in both IL-10-deficient and WT groups developed diarrhea and occult blood, whereas only IL-10-deficient colitic animals progressed to prolapse. In contrast, ADI-PEG treatment significantly protected WT as well as IL-10-deficient animals against diarrhea, occult blood, and prolapse (Figure 1). Colitic animals developed significant increases at the levels of inflammatory cytokines including plasma concentrations of IL-6 and IL-12p40 (Tables 1 and 2). Additionally, marked increases in the production of TNF α (Figure 2), IL-6, and IL-12p40 were noted in the stimulated colonic explants (Tables 1 and 2) corresponding to inflammatory response in colitic mice both IL-10 deficient and WTs. In contrast, ADI-PEG-treated animals had a significant reduction of these inflammatory cytokines ($P < 0.05$) in their stimulated colonic explants (Tables 1 and 2).

Acute inflammatory biomarker, serum amyloid A (SAA), was significantly increased in the colitic IL-10-deficient (400-fold) and WT (30-fold) animals, while, ADI-PEG-treated animals exhibited significant reduction at the levels of SAA biomarker compared to untreated colitic animals (Tables 1 and 2). In addition, there was a significant increase at the

TABLE 1: IL-10 deficient-mice: comparison of inflammatory markers in plasma and colonic explants in IL-10-deficient (IL-10^{-/-}) mice treated with DSS and ADI-PEG versus sham controls. * $P < 0.05$, ** $P < 0.01$, and *** $P < 0.001$.

Inflammatory markers	Plasma				Colonic explant + LPS	
	IL-6 (pg/mL)	IL-12p40 (pg/mL)	SAA (μ g/mL)	NO (μ M)	IL-6 (ng/mL)	IL-12p40 (pg/mL)
Control	24 \pm 3	233 \pm 18	3 \pm 1	80 \pm 5	126 \pm 54	170 \pm 56
ADI	25 \pm 4	297 \pm 13	38 \pm 31	50 \pm 5	179 \pm 83	199 \pm 113
DSS	202 \pm 28**	319 \pm 20	1591 \pm 550***	205 \pm 39*	1768 \pm 629***	1194 \pm 130**
DSS + ADI-PEG (low dose)	49 \pm 15	292 \pm 23	276 \pm 130**	60 \pm 2	257 \pm 73*	255 \pm 28*
DSS + ADI-PEG (high dose)	126 \pm 20*	295 \pm 7	1105 \pm 662*	90 \pm 20	108 \pm 41**	313 \pm 85

TABLE 2: WT mice: comparison of inflammatory markers in plasma and colonic explants in BALB/c (WT) mice treated with DSS and ADI-PEG versus sham controls. * $P < 0.05$, ** $P < 0.01$, and *** $P < 0.001$.

Inflammatory markers	Plasma			Colonic explant + LPS
	IL-6 (pg/mL)	SAA (μ g/mL)	NO (μ M)	IL-12p40 (pg/mL)
Control	45 \pm 14	12 \pm 1	24 \pm 1	550 \pm 25
ADI	27 \pm 5	48 \pm 37	27 \pm 2.5	650 \pm 50
DSS	182 \pm 27*	427 \pm 121**	36 \pm 3	875 \pm 150*
DSS + ADI-PEG (Low dose)	55 \pm 9	24 \pm 12*	24 \pm 3	475 \pm 50

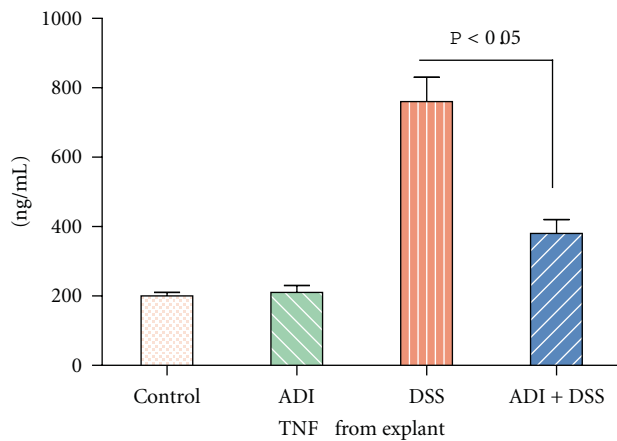


FIGURE 2: ADI-PEG treatment significantly decreased inflammatory response to LPS-stimulated TNF α production by colonic explants ($P < 0.05$).

plasma levels of NO production presumably released mainly from activated macrophages/monocytes. NO production was measured as the concentration of NO breakdown products (nitrate + nitrite) and was increased 2-fold in the colitic IL-10-deficient animals as compared to normal controls. Contrary to IL-10-deficient animals, the excess NO release did not reach statistical significance in WT animals as colitis was less severe in WT mice compared to IL-10-deficient counterparts. ADI-PEG treatment significantly ameliorated the NO release in colitic animals (Tables 1 and 2).

3.1. Colonic Histopathology. DSS administration induced moderate colitis (2.2 ± 0.3) in WT mice to severe cases (3.6 ± 0.5) in IL-10-deficient mice (Figure 3) possibly due to more severe immune reaction to overgrowth of gut microbial due to the lack of protective IL-10 and overactivation of macrophages and inflammatory cells. This was in accordance

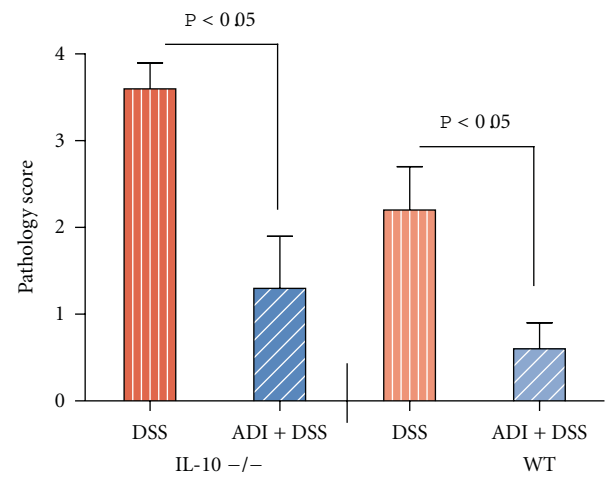


FIGURE 3: Effect of ADI-PEG on histopathology scores (0–4) according to the severity of lesions in DSS-colitic animals. Histopathological assessment revealed that ADI-PEG markedly attenuated DSS-induced colitis in WT as well as IL-10 deficient mice. ($n = 6/\text{group}$).

with pathological manifestations including shortening of crypts, loss of brush boarder epithelial cells, thickening of submucosa, and ulcer formation in colitic animals as confirmed in histological sections (Figure 3). In general, the H and E histological damage scores were consistent with infiltration of inflammatory cells, extensive macrophage proliferation, followed by shortening of colonic length, and increased disease index in the colitic WT as well as IL-10-deficient animals. Furthermore, marked CD68⁺ macrophage infiltration in the submucosa of the colonic tissue was confirmed by immunohistochemical analysis in WT and IL-10-deficient colitic animals. Similar to CD68⁺ specific macrophage infiltration, the expression of macrophage derived iNOS was upregulated in the colonic macrophages

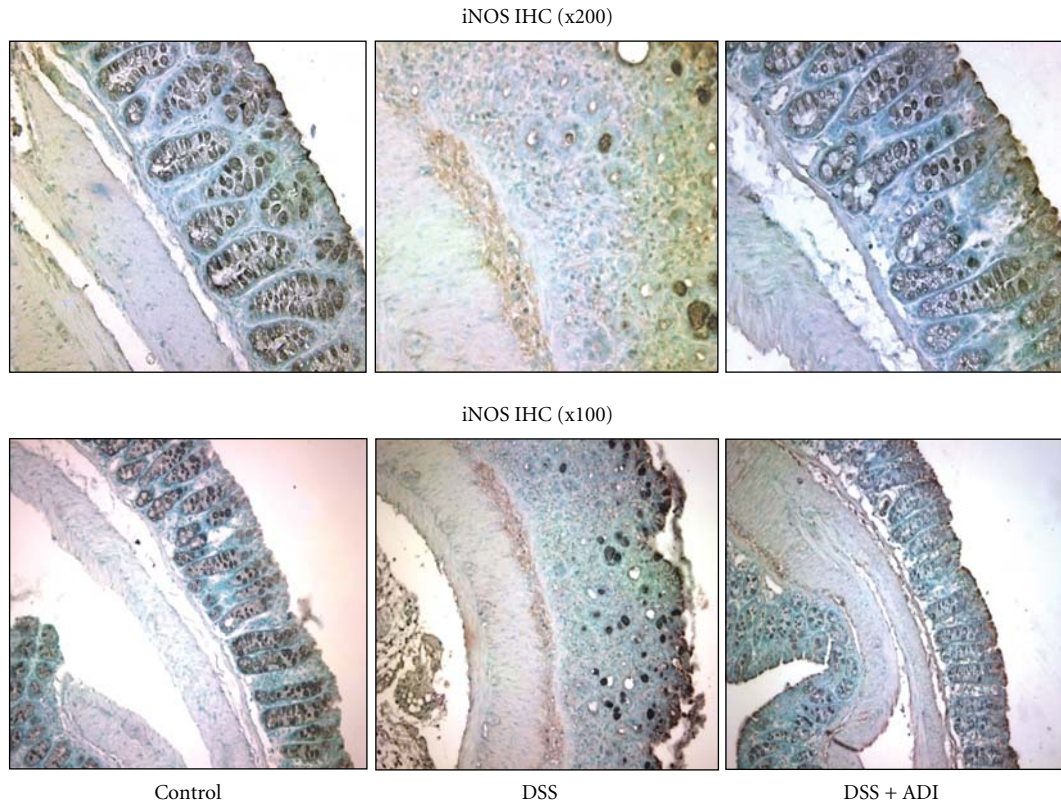


FIGURE 4: Effect of ADI-PEG on macrophage infiltration in colonic tissue from colitic IL-10-deficient mice. ADI-PEG markedly decreased submucosal macrophage infiltration and iNOS expression in DSS-induced colitic IL-10-deficient as well as WT mice (not shown). ($n = 6/\text{group}$).

(Figure 4) as well as local gut epithelia, supporting the notion that ADI-PEG provides protection against colitis by preventing CD68⁺ macrophage proliferation and iNOS activation in colonic tissues from IL-10 deficient and to a lesser extent in WT animals (data not shown).

Therefore, ADI-PEG-treated animals developed significantly less severe colitis as manifested by improved disease index (survival and increased body weight), decreased levels of inflammatory biomarkers, and decreased distal and proximal colonic histological damage scores. Colonic explants from ADI-PEG-treated mice released significantly less inflammatory cytokines compared with untreated DSS-colitic mice. Collectively, ADI-PEG was better tolerated in low dose and was more effective in normalizing SAA, plasma IL-6, and NO compared to high dose against colitis in animals (Table 1).

4. Discussion

These data demonstrate that ADI formulated with polyethylene glycol (ADI-PEG) effectively attenuated colonic inflammatory response induced in 2 phenotypic distinct IBD murine models. As anticipated in DSS-induced colitis model, the levels of the acute phase protein, SAA, are significantly elevated due to inflammatory cascade as occurs in colitic animals [17, 18, 20]. ADI-PEG markedly ameliorated the elevated levels of inflammatory mediators including SAA,

IL-6, and IL-12p40, in sera as well as in colonic explants' supernatants from treated animals. IL-12p40 is specifically released by the activated macrophages involved in Th-1 mediated immune responses.

Macrophage infiltration and activation are one of the major potential mechanisms of DSS-induced colitis in animals presumably due to the overgrowth of gram-negative bacteria and are regulated by the luminal microbiota [21]. As CD68⁺-macrophage-specific marker and the iNOS activity in the colonic tissues were significantly elevated following inflammatory cascades by infiltration and activation of macrophages in both WT as well as IL-10-deficient colitic animals. Our data indicate that pegylated ADI effectively attenuates intestinal inflammation induced in colitis and diminishes macrophage proliferation and activation in these colitic animals.

The luminal NO level is shown to be increased in IBD patients [7, 8], and the plasma NO is elevated in active ulcerative colitis and Crohn's disease versus inactive state or normal controls [9]. Additionally, gene expression (mRNA) of inducible nitric oxide synthase, iNOS, is elevated in Crohn's and ulcerative colitis patients [22]. In addition, 2-fold increases at the plasma levels of NO production were presumably released from activated macrophages/monocytes in the colitic IL-10-deficient animals as compared to the normal controls. In contrast, the excess NO release did not reach statistical significance in WT animals, as colitis was less

severe in WT mice compared to IL-10-deficient counterparts. In this study, the reduction in the colonic inflammation is possibly associated with decreased macrophage-derived NO release by ADI-PEG, as demonstrated by a significant decrease in macrophage infiltration and iNOS expression in WTs as well as IL-10 deficient mice. Further, nNOS appears to protect against DSS-induced colitis, since disease is more severe in nNOS^{-/-} mice as compared to WT animals [23]. These findings indicate that ADI-PEG is a promising agent for the elucidation of the role of arginine-related events in the pathogenesis of colitis.

However, there is controversy with regard to the role of NO in IBD since NO has been shown to have some protective role, indicating reduction in double IL-10/iNOS^{-/-} mice [24] and some beneficial effect with an NO donor [25]. Dissimilarity in experimental design may contribute to some of these variations [26]. Also, that NO may play dual function, both deleterious and protective function in the gut [27]. It is anticipated that inflammation-related NO synthesized by macrophage iNOS is highly pathogenic, while intestinal epithelial iNOS may synthesize protective NO in nature and function in healing and reepithelialization [28, 29]. In addition, increased arginase activity is observed in IBD [30]. Arginine metabolism is likely to be another factor with regard to the roles of NOS in colitis. Macrophage arginase expression is stimulated by lipopolysaccharides, LPS, IL-10, alone or in combination to (LPS + IL-10), a protective cytokine in IBD, which synergizes with respect to increased arginine expression [31]. Indeed, as proposed previously “more global” considerations of arginine metabolism, particularly arginase and NOS, might be the key elements to reveal the roles of NO in IBD [32] and further the potential mechanism of ADI-PEG on the development of IBD.

In the current study, the microbial enzyme, *Mycoplasma hominis* ADI gene was cloned and expressed in *Escherichia coli* and then conjugated with PEG to increase the circulating half-life from 5 h to 5 days and to drastically decrease the immunogenicity of the recombinant enzyme [16]. Generally, ADI converts plasma arginine into citrulline, a metabolite which is taken up and converted back into arginine only by normal cells and tissues but not by tumor cells such as hepatocellular carcinoma [33]. The reduction in the intestinal inflammation is related to decreased inflammatory cytokines as well as decreased macrophage-derived NO levels by ADI-PEG, as shown by reduced macrophage infiltration and colonic iNOS expression.

Overall, DSS-induced colitis was more severe in IL-10 deficient mice than in WT animals as IL-10 cytokine plays an important role as an anti-inflammatory element with a protective action against colitis [20]. Also, that ADI-PEG acts through the inhibition of macrophage activation and proliferation.

Overall, ADI-PEG significantly ameliorated colitic symptoms and pathology in treated animals by blocking infiltration/proliferation of these inflammatory cells in tissues. Therefore, ADI-PEG is a possible promising agent against colitis as well as for the elucidation of the role of arginine-related events in the pathogenesis of colitis.

5. Conclusion

ADI-PEG treatment protects against colitis in 2 distinct phenotypic animal models, BALB/c wildtypes as well as IL-10 deficient mice, presumably due to the attenuation of inflammatory markers such as SAA, suppression of macrophage infiltration, and iNOS expression in colonic tissues. As such, ADI-PEG can serve as a potential therapeutic value in IBD.

Abbreviations

ADI:	Arginine deiminase
CD:	Crohn's disease
DSS:	Dextran sodium sulfate
IBD:	Inflammatory bowel disease
IHA:	Immunohistochemistry
iNOS:	Inducible nitric oxide synthase
IU:	International unit.
LPS:	Lipopolysaccharide
MΦ:	Macrophage
PEG:	Polyethylene glycol
SAA:	Serum amyloid A
TNFα:	Tumor necrotic factor
UC:	Ulcerative colitis
WT:	Wildtype
IL-10:	Interleukin 10.

Conflict of Interests

The authors declare that they have no conflict of interests.

Acknowledgments

ADI-PEG was kindly provided by Dr. Steiner at the University of KY. This research was partially supported by the National Institutes of Health Grants: NCCAM-AT1490 and NIDCR-DE19177 (HO).

References

- [1] J. E. Jones, C. P. Causey, B. Knuckley, J. L. Slack-Noyes, and P. R. Thompson, “Protein arginine deiminase 4 (PAD4): current understanding and future therapeutic potential,” *Current Opinion in Drug Discovery and Development*, vol. 12, no. 5, pp. 616–627, 2009.
- [2] J. L. Slack, L. E. Jones, M. M. Bhatia, and P. R. Thompson, “Autodeimination of protein arginine deiminase 4 alters protein-protein interactions but not activity,” *Biochemistry*, vol. 50, no. 19, pp. 3997–4010, 2011.
- [3] E. S. Glazer, M. Piccirillo, V. Albino et al., “Phase II study of pegylated arginine deiminase for nonresectable and metastatic hepatocellular carcinoma,” *Journal of Clinical Oncology*, vol. 28, no. 13, pp. 2220–2226, 2010.
- [4] V. C. Willis, A. M. Gizinski, N. K. Banda et al., “N-α-benzoyl-N5-(2-chloro-1-iminoethyl)-L-ornithine amide, a protein arginine deiminase inhibitor, reduces the severity of murine collagen-induced arthritis,” *The Journal of Immunology*, vol. 186, no. 7, pp. 4396–4404, 2011.

- [5] B. A. Kidd, P. P. Ho, O. Sharpe et al., "Epitope spreading to citrullinated antigens in mouse models of autoimmune arthritis and demyelination," *Arthritis Research and Therapy*, vol. 10, no. 5, article no. 119, 2008.
- [6] D. Rachmilewitz, J. S. Stampler, D. Bachwich, F. Karmeli, Z. Ackerman, and D. K. Podolsky, "Enhanced colonic nitric oxide generation and nitric oxide synthase activity in ulcerative colitis and Crohn's disease," *Gut*, vol. 36, no. 5, pp. 718–723, 1995.
- [7] J. O. N. Lundberg, P. M. Hellstrom, J. M. Lundberg, and K. Alving, "Greatly increased luminal nitric oxide in ulcerative colitis," *The Lancet*, vol. 344, no. 8938, pp. 1673–1674, 1994.
- [8] T. Ljung, E. Beijer, M. Herulf et al., "Increased rectal nitric oxide in children with active inflammatory bowel disease," *Journal of Pediatric Gastroenterology and Nutrition*, vol. 34, no. 3, pp. 302–306, 2002.
- [9] M. Oudkerk Pool, G. Bouma, J. J. Visser et al., "Serum nitrate levels in ulcerative colitis and Crohn's disease," *Scandinavian Journal of Gastroenterology*, vol. 30, no. 8, pp. 784–788, 1995.
- [10] I. Ikeda, "Distribution of inducible nitric oxide synthase in ulcerative colitis," *American Journal of Gastroenterology*, vol. 92, no. 8, pp. 1339–1341, 1997.
- [11] G. Dijkstra, H. Moshage, H. M. van Dullemen et al., "Expression of nitric oxide synthases and formation of nitrotyrosine and reactive oxygen species in inflammatory bowel disease," *Journal of Pathology*, vol. 186, no. 4, pp. 416–421, 1998.
- [12] G. Dijkstra, A. J. H. Zandvoort, A. C. Muller Kobold et al., "Increased expression of inducible nitric oxide synthase in circulating monocytes from patients with active inflammatory bowel disease," *Scandinavian Journal of Gastroenterology*, vol. 37, no. 5, pp. 546–554, 2002.
- [13] D. M. Mosser, "The many faces of macrophage activation," *Journal of Leukocyte Biology*, vol. 73, no. 2, pp. 209–212, 2003.
- [14] M. B. Witte, N. Vogt, C. Stuelten, T. Gotoh, M. Mori, and H. D. Becker, "Arginase acts as an alternative pathway of L-Arginine metabolism in experimental colon anastomosis," *Journal of Gastrointestinal Surgery*, vol. 7, no. 3, pp. 378–385, 2003.
- [15] D. N. D. Riccia, F. Bizzini, M. G. Perilli et al., "Anti-inflammatory effects of *Lactobacillus brevis* (CD2) on periodontal disease," *Oral Diseases*, vol. 13, no. 4, pp. 376–385, 2007.
- [16] F. W. Holtsberg, C. M. Ensor, M. R. Steiner, J. S. Bomalaski, and M. A. Clark, "Poly(ethylene glycol) (PEG) conjugated arginine deiminase: effects of PEG formulations on its pharmacological properties," *Journal of Controlled Release*, vol. 80, no. 1–3, pp. 259–271, 2002.
- [17] H. S. Oz, J. Zhong, and W. J. S. de Villiers, "Pattern recognition scavenger receptors, SR-A and CD36, have an additive role in the development of colitis in mice," *Digestive Diseases and Sciences*, vol. 54, no. 12, pp. 2561–2567, 2009.
- [18] H. S. Oz, T. S. Chen, and H. Nagasawa, "Comparative efficacies of 2 cysteine prodrugs and a glutathione delivery agent in a colitis model," *Translational Research*, vol. 150, no. 2, pp. 122–129, 2007.
- [19] M. B. Grisham, G. G. Johnson, and J. R. Lancaster, "Quantitation of nitrate and nitrite in extracellular fluids," *Methods in Enzymology*, vol. 268, pp. 237–246, 1996.
- [20] H. S. Oz, M. Ray, T. S. Chen, and C. J. McClain, "Efficacy of a transforming growth factor β 2 containing nutritional support formula in a murine model of inflammatory bowel disease," *Journal of the American College of Nutrition*, vol. 23, no. 3, pp. 220–226, 2004.
- [21] H. C. Rath, M. Schultz, R. Freitag et al., "Different subsets of enteric bacteria induce and perpetuate experimental colitis in rats and mice," *Infection and Immunity*, vol. 69, no. 4, pp. 2277–2285, 2001.
- [22] A. J. León, E. Gómez, J. A. Garrote et al., "High levels of proinflammatory cytokines, but not markers of tissue injury, in unaffected intestinal areas from patients with IBD," *Mediators of Inflammation*, vol. 2009, Article ID 580450, 10 pages, 2009.
- [23] S. M. Cohn, S. Schloemann, T. Tessner, K. Seibert, and W. F. Stenson, "Crypt stem cell survival in the mouse intestinal epithelium is regulated by prostaglandins synthesized through cyclooxygenase-1," *Journal of Clinical Investigation*, vol. 99, no. 6, pp. 1367–1379, 1997.
- [24] D. M. McCafferty, E. Sihota, M. Muscara, J. L. Wallace, K. A. Sharkey, and P. Kubes, "Spontaneously developing chronic colitis in IL-10/iNOS double-deficient mice," *American Journal of Physiology*, vol. 279, no. 1, pp. G90–G99, 2000.
- [25] K. Ohtake, M. Koga, H. Uchida et al., "Oral nitrite ameliorates dextran sulfate sodium-induced acute experimental colitis in mice," *Nitric Oxide*, vol. 23, no. 1, pp. 65–73, 2010.
- [26] K. P. Pavlick, F. S. Laroux, J. Fuseler et al., "Role of reactive metabolites of oxygen and nitrogen in inflammatory bowel disease," *Free Radical Biology and Medicine*, vol. 33, no. 3, pp. 311–322, 2002.
- [27] P. Kubes, "Inducible nitric oxide synthase: a little bit of good in all of us," *Gut*, vol. 47, no. 1, pp. 6–9, 2000.
- [28] J. MacMicking, Q. W. Xie, and C. Nathan, "Nitric oxide and macrophage function," *Annual Review of Immunology*, vol. 15, pp. 323–350, 1997.
- [29] J. L. Gookin, J. M. Rhoads, and R. A. Argenzio, "Inducible nitric oxide synthase mediates early epithelial repair of porcine ileum," *American Journal of Physiology*, vol. 283, no. 1, pp. G157–G168, 2002.
- [30] R. Lang, D. Patel, J. J. Morris, R. L. Rutschman, and P. J. Murray, "Shaping gene expression in activated and resting primary macrophages by IL-10," *The Journal of Immunology*, vol. 169, no. 5, pp. 2253–2263, 2002.
- [31] P. Kocna, P. Fric, M. Zavoral, and T. Pelech, "Arginase activity determination a marker of large bowel mucosa proliferation," *European Journal of Clinical Chemistry and Clinical Biochemistry*, vol. 34, no. 8, pp. 619–623, 1996.
- [32] R. K. Cross and K. T. Wilson, "Nitric oxide in inflammatory bowel disease," *Inflammatory Bowel Diseases*, vol. 9, no. 3, pp. 179–189, 2003.
- [33] T. S. Yang, S. N. Lu, Y. Chao et al., "A randomised phase II study of pegylated arginine deiminase (ADI-PEG 20) in Asian advanced hepatocellular carcinoma patients," *British Journal of Cancer*, vol. 103, no. 7, pp. 954–960, 2010.